Overview of physiological, biochemical, and regulatory aspects of nitrogen fixation in *Azotobacter vinelandii*

Julia S. Martin del Campo[a], Jack Rigsbee[b], Marcelo Bueno Batista[c], Florence Mus[d], Luis M. Rubio[e], Oliver Einsle[f], John W. Peters[d], Ray Dixon[c], Dennis R. Dean[a]*, Patricia C. Dos Santos[b]*

[a]Department of Biochemistry, Virginia Tech, Blacksburg, USA; [b]Department of Chemistry, Wake Forest University, Winston-Salem, USA; [c]Department of Mol Microbiol, John Innes Centre, Norwich, UK, [d]Institute of Biological Chemistry, Washington State University Pullman, USA; [e] Centro de Biotecnología y Genómica de Plantas, Universidad Politécnica de Madrid (UPM) - Instituto Nacional de Investigación y Tecnología Agraria y Alimentaria (INIA), Pozuelo de Alarcón, Spain; [f]Department of Biochemistry, University of Freiburg, Freiburg, Germany

* Patricia C. Dos Santos, Department of Chemistry, Wake Downtown, 455 Vine St. Winston-Salem, NC, USA, 27101. Email: dossanpc@wfu.edu

* Dennis R. Dean, Department of Biochemistry, Virginia Tech, West Campus Dr., Blacksburg, VA, USA, 24060. Email: deandr@vt.edu

ORCID ID: Julia S. Martin del Campos (0000-0001-8914-2504), Florence Mus (0000-0002-1655-1267), Marcelo Bueno Batista (0000-0002-6642-6624), Luis M. Rubio (0000-0003-1596-2475), Oliver Einsle (0000-0001-8722-2893), John W. Peters (0000-0001-9117-9568), Ray Dixon (0000-0002-6348-639X), Dennis R. Dean (0000-0001-8960-6196), Patricia C. Dos Santos (0000-0002-3364-0931)

other trafficking proteins with their cognate client proteins is not known, but the occurrence of proteins displaying tethered domains separately involved in cluster binding and target client specificity could be a general feature of Fe-S cluster trafficking.

There are no clear phenotypes associated with the inactivation of NifX, NifY, or NafY, suggesting functional redundancy or functional crosstalk among the different cluster trafficking species in *A. vinelandii* (Rubio et al., 2002). For example, there is already evidence that NifY might functionally replace NafY because both proteins have the capacity to bind apo-MoFe protein (Jimenez-Vicente et al., 2018). The C-terminal domain of NifB provides another example of potential functional redundancy within the NifX family. Like NifU, *A. vinelandii* NifB has a modular structure. The N-terminal domain of NifB contains the NifB-co assembly site; whereas its C-terminal contains a NifX-like domain (**Figure 22**) (Moreno-Vivian et al., 1989) that is not required for NifB-co assembly but could be involved in the transfer of NifB-co to other catalytic cofactor assembly sites (Arragain et al., 2017). Based on genomic context (**Figure 5**), it is likely that NifX, NifY, NafY, and NafX are specifically associated with the Mo-dependent nitrogenase, and VnfX and VnfY are associated with V-dependent nitrogenase. Although there is no obvious phenotype associated with the inactivation of VnfX, a strain inactivated for VnfY exhibits slow diazotrophic growth and a lower level of VFe protein replete with FeV-cofactor (Ruttimann-Johnson et al., 2003; Yang et al., 2021). Thus, in the case of VFe protein maturation, there is both physiological and biochemical evidence that VnfY serves as an FeV-cofactor trafficking protein.

Based on deduced primary structures, there are no obvious members of the NifX family of proteins located within the *anf* gene cluster. The apparent absence of intermediate carrier proteins specifically associated with FeFe-cofactor trafficking is consistent with evidence that a

terminal assembly node is not required for FeFe-cofactor formation. However, AnfO can be considered a member of the NifX family based on the predicted fold of a domain located within its N-terminal region (**Figure 22**). The gene encoding AnfO is located immediately downstream of the Fe-only nitrogenase structural gene cluster *anfHDGK*. Genetic and biochemical studies revealed that AnfO inactivation results in the accumulation of a form of FeFe-protein-containing FeV-cofactor instead of FeFe-cofactor (Pérez-González et al., 2022). Thus, certain members of the NifX family could be involved not only in trafficking catalytic cofactors and their associated intermediates to appropriate client sites but might also assist the fidelity of cluster insertion by preventing the misincorporation of the incorrect cluster. This aspect could be an important fine-tuning mechanism given the topological similarity of all three catalytic clusters and their common assembly intermediate NifB-co.

8: Regulation of Mo-dependent Nitrogenase Gene Expression.

A. vinelandii tightly regulates the expression of genes associated with Mo-dependent nitrogen fixation in response to a variety of environmental signals, including the levels of O_2 and the availability of fixed nitrogen and carbon sources. Such expression is primarily controlled by NifA, a bacterial enhancer-binding protein that activates transcription at σ^{54} dependent promoters (Bush and Dixon, 2012). Similar to other members of this family, NifA binds to upstream activator sequences (indicated by blue dots on the gene organization shown in **Figure 5)** and contacts σ^{54}-RNA polymerase bound at the promoter via DNA looping. NifA is co-transcribed with its anti-activator protein NifL. The *nifLA* transcription unit is in the genomic neighborhood of the *rnfABCDEFG* genes (**Figure 5**), and this genomic organization could ensure coordination of the expression of the *rnf* genes to allow efficient electron flow in support of nitrogen fixation

(Bueno Batista and Dixon, 2019). The function of the Rnf complex is discussed in more detail in section 10.

Expression of the *A. vinelandii nifLA* transcription unit is constitutive and apparently not subjected to nitrogen regulation. This feature is distinct from the expression of these genes in other diazotrophs encoding a NifL-NifA system (*e.g*., *Klebsiella oxytoca* (Dixon et al., 1980; Dixon, 1984)*, Pseudomonas stutzeri* (Desnoues et al., 2003; Yan et al., 2008), and *Azoarcus olearius* (Egener et al., 2002), where the role of the nitrogen regulatory protein NtrC in controlling the expression of the *nifLA* operon from a σ^{54} dependent promoter is well established. Thus, the nature of regulation of this operon in *A. vinelandii* remains the subject of debate. Studies reported in the 1990's (Bali et al., 1992; Blanco et al., 1993; Raina, Bageshwar, and Das, 1993) suggested the *nifLA* promoter in *A. vinelandii* is not controlled by the σ^{54} RNA polymerase, despite the presence of a relatively well-conserved sequence upstream of *nifLA* that resembles a σ^{54} promoter consensus. Conversely, other studies performed in the 2000's (Mitra, Das, and Dixit, 2005; Poza-Carrión et al., 2014) suggested that *nifLA* expression might be autoactivated by NifA. However, more recent studies using engineered strains in which NifA escapes regulation by NifL have provided no evidence to support autoregulated *nifA* expression (Barney et al., 2017; Bueno Batista et al., 2021). Therefore, it appears that the consensus σ^{54} element upstream of *nifLA* is not functional (Blanco et al., 1993), and a different promoter, yet to be identified, might drive constitutive low-level expression *nifLA* transcripts in *A. vinelandii*.

NifL acts as a dedicated anti-activator of NifA. It is a flavoprotein having a domain architecture resembling the cytosolic histidine protein kinase family (**Figure 23A**). However, unlike other representatives of this family, it does not employ phosphorylation to regulate NifA activity because NifA does not have a receiver domain. Instead, NifL regulates NifA activity via

stoichiometric protein-protein interactions (Dixon, 1998; Martinez-Argudo et al., 2004; Martinez-Argudo et al., 2005) controlled by the redox status, ligand binding, and interaction with the P_{II}-like signal transduction protein GlnK. Owing to this unusual mode of action, the NifL-NifA system is considered a non-canonical two-component system.

NifL is a multidomain protein (**Figure 23A**) carrying an N-terminal PAS domain (PAS1) that senses cellular redox status via a flavin adenine dinucleotide (FAD) cofactor (Hill et al., 1996; Macheroux et al., 1998). A second PAS domain (PAS2) appears to play a structural role in relaying the redox changes perceived by the PAS1 domain to the central (H) and C-terminal (GHKL) domains of NifL (Little, Martinez-Argudo, and Dixon, 2006; Little et al., 2007; Slavny et al., 2010). The latter is responsible for ADP binding (Eydmann et al., 1995; Söderbäck et al., 1998), which is probably the site of interaction for the GlnK signal transduction protein (Little et al., 2002; Rudnick et al., 2002) that conveys the nitrogen regulatory signal to NifL-NifA system.

The bacterial enhancer-binding protein NifA is the protein partner of NifL and is the master transcription activator of gene clusters associated with Mo-dependent nitrogenase (**Figure 23B**). The regulatory GAF domain of *A. vinelandii* NifA binds the TCA cycle intermediate 2-oxoglutarate (Little and Dixon, 2003), serving as an important signaling metabolite at the intersection of carbon and nitrogen metabolism (Huergo and Dixon, 2015). A higher-order oligomer is formed when NifA is in its active state. An AAA+ domain within NifA contacts the σ^{54} subunit of RNA polymerase and stimulates the formation of the open complex during transcription initiation in a reaction driven by ATP hydrolysis (Morett and Segovia, 1993; Studholme and Dixon, 2003; Zhang et al., 2016). The helix-turn-helix domain responsible for DNA binding recognizes an upstream activation sequence TGT-N_{10}-ACA (Morett et al., 1988), typically located approximately -80 to -150 base-pairs from the transcriptional start site in σ^{54}

dependent promoters (Bush and Dixon, 2012). σ^{54} -RNA polymerase holoenzyme binds at conserved elements located at positions -24 (GG) and -12 (TGC) from the transcriptional start site. A wider consensus for σ^{54} promoters has been described elsewhere (Morett and Buck, 1989; Barrios et al., 1999). Notably, *A. vinelandii* also encodes a paralog of NifA located elsewhere in the genome, designated as NifA2 (Setubal et al., 2009), although its function is unknown.

NifL has evolved a mechanism to sense redox changes in response to excess O_2, which triggers inhibition of NifA activity via complex formation (**Figure 23C**). This regulatory feature is relevant to the extreme O_2 sensitivity of nitrogenase. NifA-NifL complex formation is controlled by O_2 levels sensed by the reversible oxidation of the FAD cofactor located within the PAS1 domain of NifL. Activation of target promoters by NifA under low O_2 level conditions is also dependent on conditions of low levels of fixed nitrogen, signaled by uridylylated GlnK and sufficient levels of carbon, signaled by 2-oxoglutarate binding to the NifA GAF domain (**Figure 23D**).

Integration of the nitrogen status with NifL-NifA signaling is coordinated by the signal transduction protein GlnK. In *A. vinelandii,* GlnK is required to stimulate the interaction between NifL and NifA (Little et al., 2002; Little et al., 2000; Reyes-Ramirez, Little, and Dixon, 2001). This feature is distinct from interactions observed in *Klebsiella oxytoca* for which both non-uridylylated and uridylylated forms of GlnK are competent to prevent NifL interaction with NifA (Dixon and Kahn, 2004). In *A. vinelandii*, under excess fixed nitrogen conditions, the signal transduction protein GlnK is non-uridylylated and reduced NifL can form a ternary GlnK-NifL-NifA complex to inhibit NifA activity (**Figure 23D,** upper left). Upon a switch to nitrogen limiting conditions, when GlnK is fully uridylylated and provided 2-oxoglutarate is available to bind the NifA GAF domain, the ternary inhibitory complex is released, permitting activation of

NifA (**Figure 23D,** upper right). In some circumstances, as observed in biochemical assays with isolated protein components, non-modified GlnK can still form an inhibitory complex with NifL-NifA even if 2-oxoglutarate is bound to the GAF domain of NifA (**Figure 23D,** bottom left). This suggests that under excess fixed nitrogen, the signaling transmitted by non-uridylylated GlnK comes first in the regulatory hierarchy in relation to the carbon status signaled by 2-oxoglutarate. The carbon status also comes into play under conditions of low fixed nitrogen. Under combined low nitrogen and poor carbon availability, the GAF domain of NifA does not bind 2-oxoglutarate favoring NifL inhibition, even if GlnK is fully uridylylated and unable to interact with NifL to reinforce NifA inhibition (**Figure 23D,** bottom right). For a more detailed review, refer to (Martinez-Argudo et al., 2004; Martinez-Argudo et al., 2005).

GlnK is a small trimeric signal transduction protein that integrates the regulation of both nitrogen fixation and its assimilation (Forchhammer and Lüddecke, 2016; Huergo, Chandra, and Merrick, 2013; Ninfa and Jiang, 2005) (**Figure 24**). GlnK responds to nitrogen status by its reversible uridylylation. This post-translational modification is aided by the bifunctional reversible uridyltransferase, GlnD. The GlnK signaling cascade is integrated into broader nitrogen metabolism since the addition or removal of uridylyl groups to or from each GlnK monomer by the GlnD enzyme, is dependent on the availability of fixed nitrogen signaled by intracellular Glutamine levels. Glutamine and 2-oxoglutarate are important intermediate metabolites in the coupled nitrogen assimilation reaction driven by glutamine synthetase (GS) and glutamate synthase (GOGAT). In this enzymatic scheme, the TCA cycle intermediate 2-oxoglutarate provides the carbon backbone for the reductive transamination of glutamine catalyzed by glutamate synthase, yielding one molecule of glutamate as the net product (van Heeswijk, Westerhoff, and Boogerd, 2013). In *A. vinelandii*, the coupled glutamine synthetase-

glutamate synthase pathway is the main route for ammonia assimilation because glutamate dehydrogenase is not encoded within the genome of this organism (Kleiner and Kleinschmidt, 1976; Kleinschmidt and Kleiner, 1978). In certain other organisms, ammonia can be assimilated by an NADH-dependent condensation of ammonia and 2-oxoglutarate to form glutamate.

In addition to its direct role in controlling NifA activity (see **Figures 24D & 25**), GlnK also indirectly regulates the activity of glutamine synthetase. In this role, GlnK modulates the activity of the bifunctional adenyltransferase GlnE that can either attach or remove adenylyl groups to or from glutamine synthetase (**Figure 24**). Under low ammonia availability, GlnK-UMP activates the adenylyl removal activity of GlnE to activate glutamine synthetase allowing ammonia assimilation (van Heeswijk, Westerhoff, and Boogerd, 2013). In this form, GlnK-UMP is unable to stimulate inhibition of NifL towards NifA via complex formation. In *A. vinelandii*, GlnK-UMP is a key regulatory component linking nitrogen fixation to NH_3 assimilation, thereby ensuring that fixed nitrogen is readily incorporated into biomass and not released into the environment (**Figure 24**). Conversely, under conditions of high ammonia availability, unmodified GlnK can both stimulate inhibition of NifA via the formation of a ternary complex with NifL and inactivate glutamine synthetase by activating the adenylylation function of GlnE. Thus, the dual regulatory role of GlnK avoids potentially wasteful energy consumption in the reactions catalyzed by the glutamine synthetase and nitrogenase enzymes.

The current regulatory model derived from *in vivo* and *in vitro* studies reveals a complicated hierarchy of integrated regulatory signals to control activation of genes associated with Mo-dependent nitrogenase by the NifL-NifA system (**Figures 24 and 25**). Under conditions of excess O_2, the redox status of NifL can override the signals of nitrogen and carbon status. Likewise, excess nitrogen can override the metabolic signal of the carbon status when NifL is

fully reduced under limiting O_2 conditions. Similarly, even if the concentration of O_2 and ammonia are permissive to nitrogen fixation, but carbon is insufficient, NifA can still be inhibited by NifL in the absence of bound 2-oxoglutarate. A variant form of NifA, namely NifA-E356K, can resist inhibition by GlnK bound NifL under conditions of nitrogen excess. Characterization of this variant demonstrated how carbon status signaling can restore some level of control over NifA activity. The altered activity of the variant protein leads to disruption of the original regulatory hierarchy, with carbon signaling overriding the other regulatory components. These findings emphasize the role of 2-oxoglutarate as a master signaling molecule of physiologically available carbon in modulating the NifL-NifA system in *A. vinelandii.* (Bueno Batista et al., 2021). The variant NifA also bypasses inhibition by NifL, leading to elevated expression of genes associated with Mo-dependent nitrogenase, thereby uncoupling nitrogen fixation and ammonia assimilation resulting in the extracellular release of excess ammonia. Interestingly, the regulation of the NifA variant remains dependent upon carbon levels signaled by 2-oxoglutarate, as it is still inhibited by NifL under conditions of poor carbon supply (Bueno Batista et al., 2021).

9: Regulation of alternative nitrogenase gene expression

The ability of *A. vinelandii* to express three nitrogenase isoenzymes having different metal specificities requires sensing mechanisms to detect the availability of Mo, V, and Fe. Relevant regulatory elements include transcriptional factors involved in the expression of Mo-dependent nitrogenase-associated genes, as already discussed, and metal-dependent regulation of the V- and Fe-only nitrogenases, encoded by *vnf*- and *anf*-genes, respectively (**Figure 5**). Transcriptional control of alternative nitrogenase gene expression in response to metal availability involves the

regulation of both the expression and activity of dedicated σ^{54}-dependent activator homologs belonging to the bacterial enhancer-binding protein family having similar domain structures as NifA (**Figure 25**) (Joerger, Jacobson, and Bishop, 1989). VnfA1 is the master transcriptional activator for genes required for the biosynthesis and activity of V-nitrogenase, whereas AnfA is exclusively required to activate genes involved in the assembly and activity of Fe-only nitrogenase. The hierarchical regulatory network associated with these activators ensures that each nitrogenase isoenzyme is selectively expressed according to metal availability and catalytic efficiency (**Figure 26**). As the Mo-dependent enzyme is the most efficient nitrogenase in terms of electron allocation to N_2 reduction, it is the preferred catalyst, but under Mo-deficient conditions, the V-dependent enzyme is preferred if V is available, and in the absence of both Mo and V, the Fe-only system is utilized.

A. vinelandii is renowned for its ability to transport and accumulate Mo. The siderophores, protochelin and azotochelin scavenge molybdate from the environment (Bellenger et al., 2008; McRose et al., 2017), which is transported across the cytoplasmic membrane by high-affinity ABC transporters. Notably, *A. vinelandii* encodes three homologous *modABC* transport systems (**Figure 5**), emphasizing the importance of intracellular Mo accumulation to support nitrogen fixation. Two of these systems, *modA1- modB1-modC1* and *modA3-modB3a-modB3b-modC3* are adjacent on the genome, whereas the *modA2-modB2-modC3* operon is located near the *nif* structural gene cluster (**Figure 5**). The *modG* gene, which is co-transcribed with *modC3*, encodes a trimeric protein that binds 8 atoms of Mo (Pau and Lawson, 2002). Although ModG has been proposed to have an important role in Mo homeostasis, its exact function is unknown (Mouncey, Mitchenall, and Pau, 1995). In addition, the accumulation of Mo in *A. vinelandii* is facilitated by a Mo storage protein encoded by *mosA, mosB* (**Figure 5**) that

utilizes ATP hydrolysis to garner up to 120 Mo atoms per hexamer, resulting in an intracellular Mo concentration of up to 2.5 mM (Fenske et al., 2005; Navarro-Rodríguez, Buesa, and Rubio, 2019). Expression of the *modA1-modB1-modC1* operon is regulated by the adjacent *modE1* gene, encoding a transcriptional regulator that binds to its DNA targets under Mo-replete conditions. The binding of Mo to the Mop domain of ModE1 induces a conformational change that promotes dimerization and increases the affinity of ModE1 for its specific DNA binding sequences (reviewed in Hernandez, George, and Rubio, 2009). As anticipated, non-polar *modE1* mutations result in constitutive expression of the *modA1-modB1-modC1* operon. Surprisingly, however, instead of enhancing high-affinity Mo transport, disruption of *modE1* significantly decreases *A. vinelandii* Mo uptake, suggesting that ModE1 has unknown roles in regulating Mo transport (Mouncey, Mitchenall, and Pau, 1996). This possibility is consistent with the tungsten (W) tolerant phenotype of *modE1* disruptions, implying that W transport is also disfavored in the absence of ModE1 (Pérez-González et al., 2021). W is a powerful inhibitor of Mo-dependent nitrogenase activation and is accumulated using the various Mo acquisition components.

The expression of the master transcriptional regulators for the alternative nitrogenases, *vnfA1* and *anfA,* is highly repressed in the presence of molybdenum (Hamilton et al., 2011). Furthermore, ModE1 inactivation has only relatively minor effects in relieving repression of either the *vnfU-vnfA1* transcription unit or *anfA* transcription in response to Mo availability (Premakumar et al., 1998). Current results suggest that both ModE1 and ModE2 are competent to repress *vnfU-vnfA1* and *anfA* transcription and hence are functionally redundant in terms of preventing expression of the alternative nitrogenase transcriptional activators when Mo is available (**Figure 26**). A similar situation occurs in other diazotrophic proteobacteria, in which two ModE homologs can functionally substitute for each other and independently repress the

expression of the transcriptional activators for alternative nitrogenases in response to Mo availability (Demtröder, Narberhaus, and Masepohl, 2019; Wiethaus et al., 2006).

The two ModE homologs are the only known regulators of the *vnfUA* transcription unit, and under Mo-deficient and nitrogen-limiting conditions, transcription of this operon is enhanced regardless of vanadium availability. Hence, VnfU and VnfA1 are expressed in the presence or absence of V. However, little is known about the regulation of VnfA1 activity itself. Like NifA, both VnfA1 and AnfA contain N-terminal GAF domains postulated to regulate the catalytic activity of their AAA+ domains in driving open promoter complex formation by σ^{54} RNA polymerase (**Figure 25**). In contrast to NifA, the GAF domains of these alternative activators contain conserved cysteine residues indicative of a role in redox or metal sensing. These cysteine residues are critical for the functionality of VnfA1 and AnfA (Nakajima et al., 2010; Premakumar, Loveless, and Bishop, 1994). Cluster reconstitution experiments indicate the presence of a [3Fe-4S] cluster in the GAF domain of VnfA1 when the protein is heterologously expressed and isolated from *E. coli.* However, *in vivo* activity measurements in the heterologous host do not suggest a major role for the GAF domain in regulating activity, except under conditions of oxidative stress (Nakajima et al., 2010; Yoshimitsu et al., 2011). Perhaps, factors required for the appropriate assembly of a metal center or Fe-S cluster in the GAF domain are not present in *E. coli*. For example, VnfU, which is a homolog of the C-terminal domain of NifU could be involved in VnfA1 Fe-S cluster insertion, a possibility supported by the adjacent position and co-transcription of their corresponding genes.

VnfA1 activates transcription of the σ^{54} -dependent promoters for the *vnfHDGK* genes encoding V-nitrogenase catalytic components and the *vnfENX* genes encoding the FeV-co maturation scaffold. It binds to upstream enhancer sites with the consensus GTAC-N_6-GTAC

(purple dots in gene organization scheme shown in **Figure 5**). It is not yet clear if the genes located downstream of *vnfDGK*, which include the *vod* genes involved in V uptake, are part of the same operon or can be expressed independently utilizing a separate promoter. Notably, these downstream genes are more highly expressed under Fe-only conditions than the *vnfDGK* operon, which is significantly downregulated in the absence of V (Hamilton et al., 2011). An additional complication to understanding V-dependent regulation of the alternative nitrogenases arises from the presence of two paralogs of VnfA1 encoded in the *A. vinelandii* genome. The *vnfA2* gene is located close to *modE2,* whereas *vnfA3* is co-expressed in an operon with *vnfZ*, encoding a potential V-binding protein. Both paralogous activator genes are more highly expressed under V- and Fe-only nitrogenase-dependent growth conditions than when grown in the presence of Mo and are expressed from σ^{54} promoters activated by VnfA1 (Appia-Ayme et al 2022). Both VnfA2 and VnfA3 contain conserved cysteines associated with their N-terminal GAF domains at equivalent positions to those in VnfA1 and have highly similar recognition sequences in their DNA binding domains, suggesting that they may recognize the same enhancer sequences (**Figure 25**). Indeed ChIP-Seq analysis has revealed that VnfA1 and VnfA3 bind to exactly the same target sites in the *A.vinelandii* genome and that a subset of promoters require both VnfA1 and VnfA3 to co-activate transcription, potentially through the formation of hetero-hexamers. Co-activation of this promoter subset by VnfA1 in combination with VnfA3 is dependent on the accessory protein VnfZ and occurs in the absence of vanadium, demonstrating the involvement of VnfA paralogs in the regulation of gene expression under Fe-only conditions (Appia-Ayme et al 2022).

In addition to its role in activating genes required for the biosynthesis and function of V-dependent nitrogenase, VnfA1 also plays a role in negative regulation of the structural operons for the Mo-dependent and Fe-only nitrogenases in response to V (Joerger, Jacobson, and Bishop, 1989; Walmsley, Toukdarian, and Kennedy, 1994; Appia-Ayme et al., 2022) (**Figure 26**). Disruption of *vnfA1* results in increased expression of the *nifHDK* operon and increased expression of *anfA*, resulting in the expression of the Fe-only nitrogenase in the presence of V. VnfA1, therefore, represses synthesis of the Fe-only nitrogenase under vanadium replete conditions. The mechanism of VnfA1 repression is not understood as there are no apparent VnfA binding sites in either the *nifH* or the *anfA* promoter regions. Potentially this negative regulation could be indirect or could result from negative control of the activity of the cognate regulators by VnfA1. It is also not understood how V influences the activity of VnfA1 to affect this negative regulation.

Repression of *anfA* gene transcription by ModE1 and ModE2 occurs in the presence of Mo and the negative regulation exerted by VnfA1 on *anf* gene expression explains why the synthesis of Fe-only nitrogenase is prevented in the presence of V. However, another level of control is exerted upon the activity of AnfA itself because transcriptional activation by AnfA requires NifH, the Mo-dependent nitrogenase Fe protein (Joerger, Wolfinger, and Bishop, 1991) (**Figure 26**). The role of NifH in the activation of AnfA is unclear, and it is not yet known if activation by NifH is regulated in response to metal availability. However, a truncated version of AnfA, lacking the N-terminal regulatory GAF domain, relieves NifH dependency in *E. coli*, invoking a model whereby in the absence of NifH, the GAF domain represses the activity of the catalytic AAA+ domain of AnfA (Frise, Green, and Drummond, 1994). According to this model, NifH might provide a reductase function enabling maturation or reduction of a metal cluster in

the GAF domain, resulting in a conformational change that removes intramolecular repression of the catalytic domain to activate AnfA.

Further complexity in the regulation of Fe-only nitrogenase gene expression has been uncovered by the finding that the *anfH* promoter also contains binding sites for VnfA1/VnfA3 and these paralogs, in combination with VnfZ contribute to activation of *anfH* transcription in Fe-only conditions (**Figure 26**). Co-IP analysis in *A.vinelandii* indicates that VnfZ only interacts with VnfA3/VnfA1 in the absence of vanadium and since *anfH* transcription is ablated in a *vnfZ* deletion mutant, it seems likely that VnfZ facilitates co-activation by VnfA3/VnfA1 in Fe only conditions (Appia-Ayme et al 2022). Since VnfZ is a homolog of VodA, the periplasmic binding protein of a putative ABC transporter for vanadate, but lacks the corresponding N-terminal signal sequence, it is possible that VnfZ is a cytoplasmic regulator that binds vanadium.

10: Electron Transfer and Respiratory Protection

Large amounts of energy in the form of MgATP and low-potential electrons are required to sustain biological nitrogen fixation. Moreover, nitrogenase catalytic components, as well as certain proteins involved in metallocluster formation and trafficking, are readily inactivated by oxidative damage of their associated metalloclusters. Thus, as an obligately aerobic diazotrophic bacterium, *A. vinelandii* uses the respiratory electron transport chain to sustain both intermediary metabolism and protection of nitrogenase from O_2 inactivation, while also supplying the low-potential reducing equivalents necessary to support nitrogenase catalysis (Alleman, Mus, and Peters, 2021; Setubal et al., 2009). A complex electron transport chain consisting of several branches, including multiple dehydrogenases and terminal oxidases, is involved in these processes. In this way, demands imposed by nitrogen fixation are integrated with intermediary metabolism. Such integration involves the portioning of electrons supplied by NADH through

three pathway types. These include a fully coupled electron transport chain to maximize ATP production, a partially coupled electron transport chain to maximize O_2 consumption and pathways for the reduction of low-potential electron carriers that supply reducing equivalents for nitrogenase catalysis. The genes encoding various respiratory components involved in supporting intermediary metabolism and the supply of electrons to support nitrogenase catalysis, as well as a description of the function of their products, are summarized in **Tables S1** and **S2**.

Extensive branching at the level of the primary dehydrogenases allows oxidation of various substrates having widely differing redox potentials. Electrons enter the respiratory chain from NADH, NADPH, succinate, or malate and then subsequently enter the quinone pool (Oelze, 2000). NADH constitutes the major electron carrier that feeds the electron transport chain, via complex I and complex II, respectively (**Figure 27**). The *A. vinelandii* genome encodes four NADH-ubiquinone oxidoreductases. One of these is an ATP-coupled NADH oxidoreductase encoded by the *nuo* gene cluster (NDHI), and the others are ATP-uncoupled NADH-ubiquinone oxidoreductases. The latter includes a *ndhII* encoded NADH dehydrogenase II (NDHII) and membrane-associated cation-translocating NADH dehydrogenases, respectively encoded by the *nqr* and *sha* genes. The NDHI complex is comprised of at least thirteen subunits and promotes the oxidation of NADH through the reduction of Q to QH_2 in a reaction coupled with proton transfer across the membrane. Unlike NDHI that does not oxidize NADPH, NDHII can oxidize both NADH and NADPH, although the affinity for NADPH is very low (Bertsova, Bogachev, and Skulachev, 2001). Expression of NDHII only occurs when *A. vinelandii* is cultured diazotrophically under high O_2 concentrations (Bertsova, Bogachev, and Skulachev, 2001). The sodium translocating NADH dehydrogenases have six subunits each and oxidize NADH, transferring 2 electrons to ubiquinone and pumping out 2 sodium ions (Fadeeva et al.,

2007). Although there is no association between NDHI or the *nqr* and *sha* encoded membrane-associated cation-translocating NADH dehydrogenases with nitrogen fixation, NDHII is known to be important to sustain aerobic nitrogen fixation (Bertsova, Bogachev, and Skulachev, 2001; Hamilton et al., 2011). Subsequent ubiquinol-oxygen oxido-reduction occurs through either a two-step pathway, via cytochrome *c* reductase (Cyt bc_1 or complex III) followed by a cytochrome terminal oxidase (Cyt *o* or complex IV), or in a one-step process, via a ubiquinol-dependent cytochrome terminal oxidase. Five terminal oxidases are encoded within the *A. vinelandii* genome. These include two copies of cytochrome *bd* (designated CydAB I and CydAB II, respectively encoded by the *cydAB1* and *cydAB2* gene clusters), cytochrome c_4/c_5 oxidase (Cyt *c*, encoded by *cycA* and *cycB* annotated as Cyt c_4 and Cyt c_5), Cyt *o* (encoded by the *cox* gene cluster) and cytochrome cbb_3 oxidase (Cyt cbb_3, encoded by the *cco* gene cluster), (Setubal et al., 2009). The CydAB I respiratory complex displays high O_2 affinity ($K_{d(O_2)} = 0.5$ μM) and high O_2 consumption rates and low energetic yield (Belevich et al., 2007). The expression of this cytochrome increases and is apparently essential when *A. vinelandii* is cultured under conditions of diazotrophic growth and high O_2 (Kelly et al., 1990). In contrast to CydAB I, the Cyt *o* is dispensable for sustaining aerobic diazotrophic growth in *A. vinelandii* (Leung et al., 1994).

A. vinelandii tightly regulates O_2 consumption rates as a function of the culture conditions in response to the availability of fixed nitrogen and O_2 (Drozd, 1978; Post, Kleiner, and Oelze, 1983) by using different paths within the electron transport system. These include both a proton-coupled branch and a partially coupled branch. The proton-coupled branch is comprised of NDHI and the Cyt bc_1 complex, cytochrome c_4/c_5, and Cyt *o* or Cyt cbb_3 oxidases, whereas the partially coupled branch is comprised of NDHII and CydAB I (Bertsova, Bogachev,

and Skulachev, 1998). The activity of the partially coupled branch has been associated with a process known as “respiratory protection,” an important molecular mechanism for protecting nitrogenase from O_2 damage in *A. vinelandii* (Haaker and Veeger, 1976; Jones et al., 1973; Poole and Hill, 1997). Respiratory protection involves maintaining high respiration rates when diazotrophically growing cells are exposed to high O_2 concentrations, thereby maintaining low intracellular O_2 concentrations (Bertsova, Bogachev, and Skulachev, 1998; Kuhla and Oelze, 1988). The expression of the *cydAB1* and *ndhII* genes, encoding the corresponding respiratory chain components, is regulated at the transcriptional level by CydR (Bertsova, Bogachev, and Skulachev, 2001; Wu et al., 1997). An Fe-S cluster bound form of CydR is the active form of the repressor. Oxidative damage of the CydR associated Fe-S cluster, therefore, activates expression of *cydAB1* under conditions of high O_2.

Oxygen consumption by the terminal oxidases is not the only factor responsible for O_2 protection of nitrogenase in *A. vinelandii*. A recent study has indicated that the *nafU* gene product could be involved in cell membrane remodeling such that the capacity for diffusion of O_2 into nitrogen-fixing cells is lowered (Takimoto et al., 2022). Also, a [2Fe-2S] cluster-containing protein encoded by *nafO*, designated FeSII or the Shethna protein, forms a protective complex with nitrogenase when the enzyme is challenged by an O_2 shock (Moshiri et al., 1994; Schlesier et al., 2016). Cellular ATP levels also contribute to the protection of nitrogenase against O_2 damage (Linkerhagner and Oelze, 1997) by influencing the dissociation rate constant of the nitrogenase components. The most O_2 sensitive cluster in a nitrogenase catalytic unit is the surface located Fe protein [4Fe-4S] cluster which is sequestered from O_2 damage when the Fe protein and MoFe protein are complexed together. Two sets of ATP synthase machineries are located within the *A. vinelandii* genome (**Table S2**).

In addition to MgATP, nitrogenase catalysis requires a source of low-potential reducing equivalents. For *in vitro* nitrogenase assays, dithionite is commonly used as a source of reducing equivalents. *In vivo*, small redox-active proteins, a [4Fe-4S] cluster containing ferredoxin (Fd) or flavodoxin (Fld), serve as the direct physiological electron donors to nitrogenase. Reduction of Fd and Fld in *A. vinelandii* is catalyzed by two enzyme complexes designated Rnf1 and Fix (**Figures 27 & 28**). Both complexes couple the oxidation of NADH to the reduction of Fd or Fld by using distinct mechanisms. Rnf1 couples the endergonic electron transfer from NADH to reduce Fd or Fld using exergonic transport of ions/protons by proton motive force (Jeong and Jouanneau, 2000; Schmehl et al., 1993). *A. vinelandii* contains two differentially regulated *rnf* gene clusters. The *rnf1* genes are located within the minor nitrogen fixation gene cluster (see (B) in **Figure 5**), and their expression is increased under nitrogen-fixing conditions via NifA regulation, whereas the *rnf2* genes are constitutively expressed and unaffected by nitrogen status (Curatti et al., 2005; Hamilton et al., 2011). Inactivation of Rnf1 results in an extended growth lag when transitioning to diazotrophic growth but displays steady state diazotrophic growth rates comparable to wild type *A. vinelandii* (Curatti et al., 2005). Fd or Fld can also be reduced by an enzyme complex designated Fix. The Fix complex overcomes the energy barrier of Fd and Fld reduction by using flavin-based electron bifurcation, which couples the exergonic reduction of quinone with the endergonic reduction of Fd and Fld (Herrmann et al., 2008; Ledbetter et al., 2017). In *A. vinelandii*, inactivation of either Rnf1 or Fix has only a limited effect on diazotrophic growth. However, inactivation of Rnf1 and Fix in combination eliminates the capacity for diazotrophic growth (Ledbetter et al., 2017). Although the two systems have some functional redundancy, as already noted, Rnf1 harnesses free energy by using proton motive force for Fd or Fld reduction, whereas Fix effectively couples the endergonic reduction of Fd or

Fld with the highly exergonic reduction of quinone. Despite some functional redundancy, gene expression and physiological analyses have indicated distinct roles for Rnf1 and Fix under different growth conditions (Alleman, Mus, and Peters, 2021; Hamilton et al., 2011). Namely, Fix is the favored route for electron transport to support nitrogenase catalysis under O_2-limited conditions or when extra energy is required to sustain nitrogen fixation. In this system, bifurcation of electrons to quinol supplements ATP production while still enabling the reduction of Fd and Fld, thereby maximizing energy production necessary to sustain nitrogen fixation. In contrast, Rnf1 is favored to support nitrogenase catalysis under substrate and O_2 excess because its mechanism consumes proton motive force that helps balance ATP production and O_2 consumption. Thus, intrinsic physiological selection of either Fix or Rnf1 to support nitrogen fixation represents an elegant mechanism to enable rapid response to fluctuating environmental conditions.

11: Summary & Outlook.

Immense progress has been made towards understanding genetic, mechanistic, and regulatory factors that enable diazotrophy. Many fundamental principles associated with biological nitrogen fixation have been uncovered from studies performed using *A. vinelandii* as a model organism. In recent years common features associated with nitrogen fixation by *A. vinelandii* and several other diazotrophs have been used in genomic analyses to expand the inventory and taxonomic distribution of diazotrophic species. Likewise, computational analyses of sequenced genomes have led to a better understanding of components required for nitrogen fixation across a variety of physiological conditions and environmental niches. *A. vinelandii* continues to be a preferred model diazotrophic organism for exploration of outstanding questions concerning the

mechanistic details and structural features that promote common and distinct reactivities of the nitrogenase isozymes. Aspects of the biochemical assembly of both simple and complex Fe-S clusters, originally discovered in the analysis of nitrogen fixation by *A. vinelandii*, remains an important topic in contemporary metallobiochemistry. Furthermore, environmental, nutritional, and physiological factors controlling the expression and activity of critical components associated with nitrogen fixation constitute areas of interest that remain to be fully explored.

Insights gained from such studies are likely to have direct application in efforts to develop new strategies for ammonia production to improve crop productivity. For example, a complete understanding of the biochemical mechanism for N_2 reduction could guide synthetic chemical strategies for the development of novel catalysts for anthropogenic ammonia synthesis, having improved reactivities and lower energetic costs. The study of biological nitrogen fixation, specifically the research on *A. vinelandii,* has inspired efforts toward the development of artificial nitrogen fixation processes. Notably, structural, and mechanistic investigations of nitrogenase have guided the synthesis of metal complexes displaying reactivity towards dinitrogen and have recently been reviewed in the literature (Chalkley, Drover, and Peters, 2020). While meaningful progress has been made in this area, artificial systems display a low turnover number and require conditions far distinct from the biological process. Thus, the bottleneck in these processes remains their catalytic inefficiency which has, so far, denied their application as more environmentally friendly options to synthetic fertilizers.

Characterization of components involved in the synthesis and activation of the nitrogenase isozymes is also providing a road map for genetic engineering efforts aimed at extending the capacity for nitrogen fixation to cereal crops. The approach is incrementally proving successful as NifH and NifB proteins have been expressed in active form in the

mitochondria of transgenic rice plants (Baysal et al., 2022; He et al. 2022). The ability to circumvent complex regulatory networks also offers an opportunity to optimize ammonia secretion from diazotrophs for their potential application as biofertilizers.

Current soil management practices involving application of industrially produced fertilizers impose high agronomic, economic, and environmental costs that cannot be sustained. The application of fertilizers produced by the Haber-Bosch process for increased crop production accounts for 1-2% of the total global energy use worldwide (Smith, Hill, and Torrente-Murciano, 2020; Townsend and Howarth, 2010). Furthermore, indiscriminate application of ammonia fertilizer continues to grow and is expected to double by 2050. Only a fraction of nitrogen fertilizers applied to soils is assimilated to increase crop productivity, with the excess causing eutrophication of nearby watersheds. Furthermore, oxidation of ammonia through nitrification and denitrification pathways results in the formation of nitrous oxide (N_2O), a long-lived potent greenhouse gas that is able to react with the ozone layer, thereby contributing to global warming (Zhang, Ward, and Sigman, 2020). Such penalties associated with current agronomic practices underscore the importance of understanding and ultimately exploiting the principles of this biological process to achieve a more deliberate and efficient way to maximize crop productivity.

Supporting Information.

Table S1 – Description of *A. vinelandii* genes and products involved in nitrogen fixation

Table S2 – Description of *A. vinelandii* genes involved in respiration

Declaration of Interest

MBB and RD were supported by the UKRI Biotechnology and Biological Sciences Research Council, grants BB/W009986/1 to MBB, BB/N013476/1 and

BBS/E/J/000PR9797 to RD. MBB and RD were also supported by a grant from the Royal Society, ICA\R1\180088.LMR was supported by FEDER/Ministerio de Ciencia, Innovación y Universidades – Agencia Estatal de Investigación grant 2017-88475-R. J.W.P. was supported by the US DOE, Office of Science, Office of Basic Energy Sciences under award DE-SC0018143. Partial salary support for J. W. P. was provided by the United States Department of Agriculture National Institute of Food and Agriculture, Hatch umbrella project #15621. O.E. was supported by Deutsche Forschungsgemeinschaft (RTG 1976, project no. 235777276 and PP 1927, project no. 311061829). PDS and JR was supported by the National Science Foundation (MCB 1716535). DRD and JSMC were supported by the U.S. Department of Energy, Office of Science, Basic Energy DE-SC0010867.

Disclosure statement

No potential conflict of interest was reported by the author(s).

References

1. Addo MA, Dos Santos PC. 2020. Distribution of Nitrogen-Fixation Genes in Prokaryotes Containing Alternative Nitrogenases. Chembiochem, 21, 1749-59.
2. Alleman AB, Mus F, Peters JW. 2021. Metabolic Model of the Nitrogen-Fixing Obligate Aerobe *Azotobacter vinelandii* Predicts Its Adaptation to Oxygen Concentration and Metal Availability. mBio, 12, e0259321.
3. Appia-Ayme C, Little R, Chandra G, de Oliveira Martins C, Bueno Batista M and Dixon R. 2022. Interactions between paralogous bacterial enhancer-binding proteins enable metal-dependent regulation of alternative nitrogenases in *Azotobacter vinelandii*. Mol Microbiol 118, 105-124.
4. Arnold W, Rump A, Klipp W, Priefer UB, Puhler A. 1988. Nucleotide sequence of a 24,206-base-pair DNA fragment carrying the entire nitrogen fixation gene cluster of Klebsiella pneumoniae. J Mol Biol, 203, 715-38.
5. Arragain S, Jiménez-Vicente E, Scandurra AA, Burén S, Rubio LM, Echavarri-Erasun C. 2017. Diversity and Functional Analysis of the FeMo-Cofactor Maturase NifB. Fron Plant Sci, 8.
6. Bali A, Blanco G, Hill S, Kennedy C. 1992. Excretion of ammonium by a nifL mutant of *Azotobacter vinelandii* fixing nitrogen. Appl Environ Microbiol, 58, 1711-8.
7. Baradaran R, Berrisford JM, Minhas GS, Sazanov LA. 2013. Crystal structure of the entire respiratory complex I. Nature, 494, 443-48.
8. Barney BM, Plunkett MH, Natarajan V, Mus F, Knutson CM, Peters JW. 2017. Transcriptional Analysis of an Ammonium-Excreting Strain of *Azotobacter vinelandii* Deregulated for Nitrogen Fixation. Appl Environ Microbiol, 83, e01534-17

9. Baysal C, Buren S, He W, Capell T, Rubio LM, Christou P. 2022. Functional expression of the nitrogenase Fe protein in transgenic rice. Commun Biol, 5, 1006.
10. Belevich I, Borisov VB, Bloch DA, Konstantinov AA, Verkhovsky MI. 2007. Cytochrome bd from *Azotobacter vinelandii*: evidence for high-affinity oxygen binding. Biochemistry, 46, 11177-84.
11. Bellenger JP, Wichard T, Kustka AB, Kraepiel AML. 2008. Uptake of molybdenum and vanadium by a nitrogen-fixing soil bacterium using siderophores. Nat Geosci, 1, 243-46
12. Berry EA, Huang L-S, Saechao LK, Pon NG, Valkova-Valchanova M, Daldal F. 2004. X-Ray Structure of Rhodobacter Capsulatus Cytochrome bc1: Comparison with its Mitochondrial and Chloroplast Counterparts. Photosynthesis Research, 81, 251-75
13. Bertsova YV, Bogachev AV, Skulachev VP. 1998. Two NADH:ubiquinone oxidoreductases of *Azotobacter vinelandii* and their role in the respiratory protection. Biochimica et biophysica acta, 1363, 125-33.
14. Bertsova YV, Bogachev AV, Skulachev VP. 2001. Noncoupled NADH:ubiquinone oxidoreductase of *Azotobacter vinelandii* is required for diazotrophic growth at high oxygen concentrations. J Bacteriol, 183, 6869-74.
15. Bishop PE, Jarlenski DM, Hetherington DR. 1998. Evidence for an alternative nitrogen fixation system in *Azotobacter vinelandii*. Proc Natl Acad Sci U S A, 77, 7342-46.
16. Bishop PE, Premakumar R, Dean DR, Jacobson MR, Chisnell JR, Rizzo TM, Kopczynski J. 1986. Nitrogen fixation by *Azotobacter vinelandii* strains having deletions in structural genes for nitrogenase. Science, 232, 92-94.
17. Blanco G, Drummond M, Woodley P, Kennedy C. 1993. Sequence and molecular analysis of the nifL gene of *Azotobacter vinelandii*. Mol Microbiol, 9, 869-79.

18. Blum M, Chang H-Y, Chuguransky S, Grego T, Kandasaamy S, Mitchell A, Nuka G, Paysan-Lafosse T, Qureshi M, Raj S, Richardson L, Salazar GA, Williams L, Bork P, Bridge A, Gough J, Haft DH, Letunic I, Marchler-Bauer A, Mi H, Natale DA, Necci M, Orengo CA, Pandurangan AP, Rivoire C, Sigrist CJA, Sillitoe I, Thanki N, Thomas PD, Tosatto SCE, Wu CH, Bateman A, Finn RD. 2021. The InterPro protein families and domains database: 20 years on. Nucleic Acids Res, 49, D344-D54.

19. Bosch R, Rodriguez-Quinones F, Imperial J. 1997. Identification of gene products from the *Azotobacter vinelandii* nifBfdxNnifOQ operon. FEMS Microbiol Lett, 157, 19-25.

20. Boyd ES, Anbar AD, Miller S, Hamilton TL, Lavin M, Peters JW. 2011. A late methanogen origin for molybdenum-dependent nitrogenase. Geobiology, 9, 221-32.

21. Brigle KE, Setterquist RA, Dean DR, Cantwell JS, Weiss MC, Newton WE. 1987. Site-directed mutagenesis of the nitrogenase MoFe protein of *Azotobacter vinelandii*. Proc Natl Acad Sci USA, 84, 7066-69.

22. Brill WJ. 1975. Regulation and genetics of bacterial nitrogen fixation. Annu Rev Microbiol, 29, 109-29.

23. Broach RB, Rupnik K, Hu Y, Fay AW, Cotton M, Ribbe MW, Hales BJ. 2006. Variable-temperature, variable-field magnetic circular dichroism spectroscopic study of the metal clusters in the ΔnifB and ΔnifH MoFe proteins of nitrogenase from *Azotobacter vinelandii*. Biochemistry, 45, 15039-48.

24. Bueno Batista M, Brett P, Appia-Ayme C, Wang Y-P, Dixon R. 2021. Disrupting hierarchical control of nitrogen fixation enables carbon-dependent regulation of ammonia excretion in soil diazotrophs. PLOS Genet, 17, e1009617.

25. Bueno Batista M, Dixon R. 2019. Manipulating nitrogen regulation in diazotrophic bacteria for agronomic benefit. Biochem Soc Trans, 47, 603-14

26. Bulen WA, LeComte JR. 1966 . The nitrogenase system from Azotobacter: two-enzyme requirement for N2 reduction, ATP-dependent H2 evolution, and ATP hydrolysis. Proc Natl Acad Sci U S A, 56, 979-86.

27. Burén S, Jiménez-Vicente E, Echavarri-Erasun C, Rubio LM. 2020. Biosynthesis of Nitrogenase Cofactors. Chem Rev, 120, 4921-68.

28. Burén S, Rubio LM. 2018. State of the art in eukaryotic nitrogenase engineering. FEMS Microbiol Lett, 365, fnx274

29. Burgess BK, Lowe DJ. 1996. Mechanism of molybdenum nitrogenase. Chem Rev, 96, 2983-3012

30. Buscagan TM, Perez KA, Maggiolo AO, Rees DC, Spatzal T. 2021. Structural Characterization of Two CO Molecules Bound to the Nitrogenase Active Site. Angew Chem Int Ed, 60, 5704-07.

31. Bush JA, Wilson PW. 1959. A non-gummy chromogenic strain of *Azotobacter vinelandii*. Nature, 184, 381-84.

32. Bush M, Dixon R. 2012.The role of bacterial enhancer binding proteins as specialized activators of σ54-dependent transcription. Microbiol Mol Biol Rev: MMBR, 76, 497-529.

33. Catalytic N2-to-NH3 (or -N2H4) Conversion by Well-Defined Molecular Coordination Complexes

34. Chalkley J, Drover MW, Peters JC. 2020. Catalytic N2-to-NH3 (or -N2H4) Conversion by Well-Defined Molecular Coordination Complexes. Chem Rev, 12, 5582–5636.

35. Chisnell JR, Premakumar R, Bishop PE. 1988. Purification of a 2nd alternative nitrogenase from a *nifhdk* deletion strain of *Azotobacter vinelandii*. J Bacteriol, 170, 27-33.

36. Chiu H-J, Peters JW, Lanzilotta WN, Ryle MJ, Seefeldt LC, Howard JB, Rees DC. 2001. MgATP-Bound and Nucleotide-Free Structures of a Nitrogenase Protein Complex between the Leu 127Δ-Fe-Protein and the MoFe-Protein. Biochemistry, 40, 641-50.

37. Christiansen J, Goodwin PJ, Lanzilotta WN, Seefeldt LC, Dean DR. 1998. Catalytic and biophysical properties of a nitrogenase apo-MoFe protein produced by a nifB-deletion mutant of *Azotobacter vinelandii*. Biochemistry, 37, 12611-23.

38. Corbin D, Barran L, Ditta G. 1983. Organization and expression of *Rhizobium meliloti* nitrogen fixation genes. Proc.Natl Acad Sci USA, 80, 3005-09.

39. Cotton MS, Rupnik K, Broach RB, Hu Y, Fay AW, Ribbe MW, Hales BJ. 2009. VTVH-MCD study of the *ΔnifB ΔnifZ* MoFe protein from *Azotobacter vinelandii*. J Am Chem Soc, 131, 4558-59.

40. Cupp-Vickery JR, Silberg JJ, Ta DT, Vickery LE. 2004. Crystal structure of IscA, an iron-sulfur cluster assembly protein from *Escherichia coli*. J Mol Biol, 338, 127-37.

41. Curatti L, Brown CS, Ludden PW, Rubio LM. 2005. Genes required for rapid expression of nitrogenase activity in *Azotobacter vinelandii*. Proc Natl Acad Sci U S A, 102, 6291-6.

42. Curatti L, Hernandez JA, Igarashi RY, Soboh B, Zhao D, Rubio LM. 2007. In vitro synthesis of the iron–molybdenum cofactor of nitrogenase from iron, sulfur, molybdenum, and homocitrate using purified proteins. Proc.Natl Acad Sci USA, 104, 17626-31.

43. Danyal K, Dean DR, Hoffman BM, Seefeldt LC. 2011. Electron Transfer within Nitrogenase: Evidence for a Deficit-Spending Mechanism. Biochemistry, 50, 9255-63.

44. Danyal K, Shaw S, Page TR, Duval S, Horitani M, Marts AR, Lukoyanov D, Dean DR, Raugei S, Hoffman BM, Seefeldt LC, Antony E. 2016. Negative cooperativity in the nitrogenase Fe protein electron delivery cycle. Proc Natl Acad Sci USA, 113, E5783-E91.

45. Demtröder L, Narberhaus F, Masepohl B. 2019. Coordinated regulation of nitrogen fixation and molybdate transport by molybdenum. Mol Microbiol, 111, 17-30.

46. Denk D, Bock A. 1987. L-cysteine biosynthesis in *Escherichia coli*: nucleotide sequence and expression of the serine acetyltransferase (cysE) gene from the wild-type and a cysteine-excreting mutant. J Gen Microbiol, 133 (Pt 3), 515-25.

47. Desnoues N, Lin M, Guo X, Ma L, Carreño-Lopez R, Elmerich C. 2003. Nitrogen fixation genetics and regulation in a Pseudomonas stutzeri strain associated with rice. Microbiology, 149, 2251-62.

48. Dilworth MJ. 1966. Acetylene reduction by nitrogen-fixing preparations from *Clostridium pasteurianum*. Biochim Biophys Acta, 127, 285-94.

49. Dingler C, Kuhla J, Wassink H, Oelze J. 1988. Levels and activities of nitrogenase proteins in *Azotobacter vinelandii* grown at different dissolved oxygen concentrations. J Bacteriol, 170, 2148-52.

50. Dixon R, Eady RR, Espin G, Hill S, Iaccarino M, Kahn D, Merrick M. 1980. Analysis of regulation of *Klebsiella pneumoniae* nitrogen fixation (nif) gene cluster with gene fusions. Nature, 286, 128-32.

51. Dixon R, Kahn D. 2004. Genetic regulation of biological nitrogen fixation. Nat Rev Microbiol, 2, 621-31.

52. Dixon R, Kennedy C, Kondorosi A, Krishnapillai V, Merrick M. 1977. Complementation analysis of *Klebsiella pneumoniae* mutants defective in nitrogen fixation. Mol Gen Genetic: MGG, 157, 189-98.

53. Dixon R. 1998. The oxygen-responsive NIFL-NIFA complex: A novel two-component regulatory system controlling nitrogenase synthesis in γ-Proteobacteria. Arch Microbiol, 169, 371-80.

54. Dixon RA, Postgate JR. 1971. Transfer of Nitrogen-fixation Genes by Conjugation in *Klebsiella pneumoniae*. Nature, 234, 47-48.

55. Dixon RA. 1984. The Genetic Complexity of Nitrogen Fixation. Microbiol, 130, 2745-55.

56. Dos Santos PC, Dean DR. 2008. A newly discovered role for iron-sulfur clusters. Proc Natl Acad Sci U S A, 105, 11589-90.

57. Dos Santos PC, Fang Z, Mason SW, Setubal JC, Dixon R. 2012. Distribution of nitrogen fixation and nitrogenase-like sequences amongst microbial genomes. BMC Genomics, 13, 162

58. Dos Santos PC, Johnson DC, Ragle BE, Unciuleac M-C, Dean DR. 2007. Controlled Expression of nif and isc Iron-Sulfur Protein Maturation Components Reveals Target Specificity and Limited Functional Replacement between the Two Systems. J Bacteriol, 189, 2854-62.

59. Dos Santos PC, Mayer SM, Barney BM, Seefeldt LC, Dean DR. 2007. Alkyne substrate interaction within the nitrogenase MoFe protein. J Inorg Biochem. 101(11-12): 1642–1648.

60. Dos Santos PC, Smith AD, Frazzon J, Cash VL, Johnson MK, Dean DR. 2004. Iron-Sulfur Cluster Assembly: NifU-directed Activation of the Nitrogenase Fe protein. J Biol Chem, 279, 19705-11.

61. Dos Santos PC. 2012. Molecular biology and genetic engineering in nitrogen fixation. Methods Mol Biol, 766, 81-92.

62. Dos Santos PC, Dean DR. 2014. A retrospective on the discovery of [Fe-S] cluster biosynthetic machineries in *Azotobacter vinelandii*. In Rouault T, ed. Iron-Sulfur Clusters in Chemistry and Biology, Verlag Walter de Gruyter 267-96.

63. Drozd JW. 1978. Respiration and energy conservation in *Azotobacter vinelandii*. FEMS Microbiol Lett, 3, 47-49.

64. Duval S, Danyal K, Shaw S, Lytle AK, Dean DR, Hoffman BM, Antony E, Seefeldt LC. 2013. Electron transfer precedes ATP hydrolysis during nitrogenase catalysis. Proc Natl Acad Sci U S A, 110 (41) 16414-16419.

65. Dyer DH, Rubio LM, Thoden JB, Holden HM, Ludden PW, Rayment I. 2003. The three-dimensional structure of the core domain of NafY from *Azotobacter vinelandii* determined at 1.8-A resolution. J Biol Chem, 278, 32150-56.

66. Eady RR, Richardson TH, Miller RW, Hawkins M, Lowe DJ. 1988. The vanadium nitrogenase of *Azotobacter chroococcum*. Purification and properties of the Fe protein. Biochem J, 256, 189-96.

67. Eady RR, Robson RL, Richardson TH, Miller RW, Hawkins M. 1987. The vanadium nitrogenase of *Azotobacter chroococcum*: purification and properties of VFe protein. Biochem J, 244, 197-207.

68. Egener T, Sarkar A, Martin DE, Reinhold-Hurek B. 2002. Identification of a NifL-like protein in a diazotroph of the β-subgroup of the Proteobacteria, *Azoarcus* sp. strain BH72. Microbiology, 148, 3203-12.

69. Einsle O, Rees DC. 2020. Structural Enzymology of Nitrogenase Enzymes. Chem Rev, 120, 4969-5004.

70. Einsle O, Tezcan FA, Andrade Susana LA, Schmid B, Yoshida M, Howard James B, Rees Douglas C. 2002. Nitrogenase MoFe-Protein at 1.16 Å Resolution: A Central Ligand in the FeMo-Cofactor. Science, 297, 1696-700.

71. Emerich DW, Hageman RV, Burris RH. 1981. Interactions of dinitrogenase and dinitrogenase reductase. Adv Enzymol Relat Areas Mol Biol, 52, 1-22.

72. Emerich DW, Ljones T, Burris RH. 1978. Nitrogenase: properties of the catalytically inactive complex between the *Azotobacter vinelandii* MoFe protein and the *Clostridium pasteurianum* Fe protein. Biochimica et biophysica acta, 527, 359-69.

73. Erisman JW, Galloway JN, Seitzinger S, Bleeker A, Dise NB, Petrescu AMR, Leach AM, de Vries W. 2013. Consequences of human modification of the global nitrogen cycle. Philos Trans R Soc: Biol Sci, 368, 20130116.

74. Esquilin-Lebron K, Dubrac S, Barras F, Boyd JM, Yount J. 2021. Bacterial Approaches for Assembling Iron-Sulfur Proteins. mBio, 12, e02425-21.

75. Evans DJ, Jones R, Woodley PR, Wilborn JR, Robson RL. 1991. Nucleotide sequence and genetic analysis of the *Azotobacter chroococcum nifUSVWZM* gene cluster, including a new gene (nifP) which encodes a serine acetyltransferase. J Bacteriol, 173, 5457-69.

76. Eydmann T, Soderback E, Jones T, Hill S, Austin S, Dixon R. 1995.Transcriptional activation of the nitrogenase promoter in vitro: Adenosine nucleotides are required for inhibition of NIFA activity by NIFL. J Bacteriol, 177, 1186-95.

77. Fadeeva MS, Yakovtseva EA, Belevich GA, Bertsova YV, Bogachev AV. 2007. Regulation of expression of Na+ -translocating NADH:quinone oxidoreductase genes in *Vibrio harveyi* and *Klebsiella pneumoniae*. Arch Microbiol, 188, 341-8.

78. Fajardo AS, Legrand P, Payá-Tormo La, Martin L, Pellicer Martínez MT, Echavarri-Erasun C, Vernède X, Rubio LM, Nicolet Y. 2020. Structural Insights into the Mechanism of the Radical SAM Carbide Synthase NifB, a Key Nitrogenase Cofactor Maturating Enzyme. J Am Chem Soc, 142, 11006-12.

79. Fay AW, Blank MA, Lee CC, Hu Y, Hodgson KO, Hedman B, Ribbe MW. 2011. Spectroscopic characterization of the isolated iron-molybdenum cofactor (FeMoco) precursor from the protein NifEN. Angew Chem Int Ed Engl, 50, 7787-90.

80. Feng X, Schut Gerrit J, Lipscomb Gina L, Li H, Adams Michael WW. 2021. Cryoelectron microscopy structure and mechanism of the membrane-associated electron-bifurcating flavoprotein Fix/EtfABCX. Proc.Natl Acad Sci USA, 118, e2016978118.

81. Fenske D, Gnida M, Schneider K, Meyer-Klaucke W, Schemberg J, Henschel V, Meyer A-K, Knöchel A, Müller A. 2005. A New Type of Metalloprotein: The Mo Storage Protein from *Azotobacter vinelandii* Contains a Polynuclear Molybdenum–Oxide Cluster. ChemBioChem, 6, 405-13.

82. Forchhammer K, Lüddecke J. 2016. Sensory properties of the PII signalling protein family. The FEBS journal, 283, 425-37.

83. Fowler D, Coyle M, Skiba U, Sutton MA, Cape JN, Reis S, Sheppard LJ, Jenkins A, Grizzetti B, Galloway JN, Vitousek P, Leach A, Bouwman AF, Butterbach-Bahl K, Dentener F, Stevenson D, Amann M, Voss M. 2013. The global nitrogen cycle in the twenty-first century. Philos Trans R Soc Lond B Biol Sci, 368, 20130164-64.

84. Frise E, Green A, Drummond M. 1994. Chimeric transcriptional activators generated in vivo from VnfA and AnfA of *Azotobacter vinelandii*: N-terminal domain of AnfA is responsible for dependence on nitrogenase Fe protein. J Bacteriol, 176, 6545-9.

85. Galloway JN, Bleeker A, Erisman JW. 2021. The Human Creation and Use of Reactive Nitrogen: A Global and Regional Perspective. Annual Review of Environment and Resources, 46, 255-88.

86. Gavini N, Tungtur S, Pulakat L. 2006. Peptidyl-Prolyl cis/trans Isomerase-Independent Functional NifH Mutant of *Azotobacter vinelandii*. J Bacteriol, 188, 6020-25.

87. Georgiadis MM, Komiya H, Chakrabarti P, Woo D, Kornuc JJ, Rees DC. 1992. Crystallographic structure of the nitrogenase iron protein from *Azotobacter vinelandii*. Science, 257, 1653-59

88. Goodwin PJ, Agar JN, Roll JT, Roberts GP, Johnson MK, Dean DR. 1998. The *Azotobacter vinelandii* NifEN complex contains two identical [4Fe- 4S] clusters. Biochemistry, 37, 10420-28

89. Grunden AM, Shanmugam KT. 1997. Molybdate transport and regulation in bacteria. Arch Microbiol, 168, 345-54.

90. Guo Y, Echavarri-Erasun C, Demuez M, Jiménez-Vicente E, Bominaar EL, Rubio LM. 2016. The Nitrogenase FeMo-Cofactor Precursor Formed by NifB Protein: A Diamagnetic Cluster Containing Eight Iron Atoms. Angew Chem Int Ed, 55, 12764-67.

91. Haaker H, Veeger C. 1976. Regulation of respiration and nitrogen fixation in different types of *Azotobacter vinelandii*. Eur J Biochem, 63, 499-507.

92. Hageman RV, Burris RH. 1978. Kinetic studies on electron transfer and interaction between nitrogenase components from *Azotobacter vinelandii*. Biochemistry, 17, 4117-24.

93. Hageman RV, Burris RH. 1978. Nitrogenase and nitrogenase reductase associate and dissociate with each catalytic cycle. Proc Natl Acad Sci U S A, 75, 2699-26702.

94. Hageman RV, Burris RH. 1980. Electron allocation to alternative substrates of Azotobacter nitrogenase is controlled by the electron flux through dinitrogenase. Biochimica et biophysica acta, 591, 63-75.

95. Hales BJ, Case EE, Morningstar JE, Dzeda MF, Mauterer LA. 1986. Isolation of a new vanadium-containing nitrogenase from *Azotobacter vinelandii*. Biochemistry, 25, 7251-55.

96. Hamilton TL, Ludwig M, Dixon R, Boyd ES, Dos Santos PC, Setubal JC, Bryant DA, Dean DR, Peters JW. 2011. Transcriptional Profiling of Nitrogen Fixation in *Azotobacter vinelandii*. J Bacteriol, 193, 4477-86.

97. Hardy RWF, Holsten RD, Jackson EK, Burns RC. 1968. The acetylene-ethylene assay for N2 fixation: laboratory and field evaluation. Plant Physiol, 43, 1185-207.

98. Harris DF, Jimenez-Vicente E, Yang Z-Y, Hoffman BM, Dean DR, Seefeldt LC. 2020. CO as a substrate and inhibitor of H+ reduction for the Mo-, V-, and Fe-nitrogenase isozymes. J Inorg Biochem, 213, 111278.

99. Harris DF, Lukoyanov DA, Kallas H, Trncik C, Yang ZY, Compton P, Kelleher N, Einsle O, Dean DR, Hoffman BM, Seefeldt LC. 2019. Mo-, V-, and Fe-Nitrogenases Use a Universal Eight-Electron Reductive-Elimination Mechanism To Achieve N2 Reduction. Biochemistry, 58, 3293-301.

100. Harris GS, White TC, Flory JE, Orme-Johnson WH. 1990. Genes required for formation of the apoMoFe protein of *Klebsiella pneumoniae* nitrogenase in *Escherichia coli*. J Biol Chem, 265, 15909-19

101. He W, Burén S, Baysal C, Jiang X, Capell T, Christou P, Rubio LM. 2022. Nitrogenase Cofactor Maturase NifB Isolated from Transgenic Rice is Active in FeMo-co Synthesis. Acs Synth Biol,11, 3028–3036.
102. Hernandez JA, Curatti L, Aznar CP, Perova Z, Britt RD, Rubio LM. 2008. Metal trafficking for nitrogen fixation: NifQ donates molybdenum to NifEN/NifH for the biosynthesis of the nitrogenase FeMo-cofactor. Proc Natl Acad Sci USA, 105, 11679-84.
103. Hernandez JA, George SJ, Rubio LM. 2009. Molybdenum Trafficking for Nitrogen Fixation. Biochemistry, 48, 9711-21.
104. Hernandez JA, Igarashi RY, Soboh B, Curatti L, Dean DR, Ludden PW, Rubio LM. 2007. NifX and NifEN exchange NifB cofactor and the VK-cluster, a newly isolated intermediate of the iron-molybdenum cofactor biosynthetic pathway. Mol Microbiol, 63, 177-92.
105. Hernandez JA, Phillips AH, Erbil WK, Zhao D, Demuez M, Zeymer C, Pelton JG, Wemmer DE, Rubio LM. 2011. A Sterile α-Motif Domain in NafY Targets Apo-NifDK for Iron-Molybdenum Cofactor Delivery via a Tethered Domain. J Biol Chem, 286, 6321-28.
106. Herrmann G, Jayamani E, Mai G, Buckel W. 2008. Energy conservation via electron-transferring flavoprotein in anaerobic bacteria. J Bacteriol, 190, 784-91.
107. Hill S, Austin S, Eydmann T, Jones T, Dixon R. 1996. *Azotobacter vinelandii* NIFL is a flavoprotein that modulates transcriptional activation of nitrogen-fixation genes via a redox-sensitive switch. Proc.Natl Acad Sci USA, 93, 2143-48.
108. Homer MJ, Dean DR, Roberts GP. 1995. Characterization of the gamma protein and its involvement in the metallocluster assembly and maturation of dinitrogenase from *Azotobacter vinelandii*. J Biol Chem, 270, 24745-52.

109. Hoover TR, Imperial J, Ludden PW, Shah VK. 1989. Homocitrate is a component of the iron-molybdenum cofactor of nitrogenase. Biochemistry, 28, 2768-71.

110. Hoover TR, Robertson AD, Cerny RL, Hayes RN, Imperial J, Shah VK, Ludden PW. 1987. Identification of the V factor needed for synthesis of the iron-molybdenum cofactor of nitrogenase as homocitrate. Nature, 329, 855-57.

111. Howard JB, Rees DC. 1994. Nitrogenase: a nucleotide-dependent molecular switch. Annu Rev Biochem, 63, 235-64.

112. Hreha TN, Mezic KG, Herce HD, Duffy EB, Bourges A, Pryshchep S, Juarez O, Barquera B. 2015. Complete Topology of the RNF Complex from *Vibrio cholerae*. Biochemistry, 54, 2443-55.

113. Hu Y, Corbett MC, Fay AW, Webber JA, Hedman B, Hodgson KO, Ribbe MW. 2005. Nitrogenase reactivity with P-cluster variants. Proc Natl Acad Sci U S A, 102, 13825-30.

114. Hu Y, Fay AW, Dos Santos PC, Naderi F, Ribbe MW. 2004.Characterization of *Azotobacter vinelandii* nifZ deletion strains: Indication of stepwise MoFe protein Assembly. J Biol Chem, 279, 54963-71.

115. Hu Y, Fay AW, Lee CC, Ribbe MW. 2007. P-cluster maturation on nitrogenase MoFe protein. Proc Natl Acad Sci USA, 104, 10424-29.

116. Hu Y, Lee CC, Ribbe MW. 2011. Extending the carbon chain: hydrocarbon formation catalyzed by vanadium/molybdenum nitrogenases. Science, 333, 753.

117. Huergo LF, Chandra G, Merrick M. 2013. P(II) signal transduction proteins: nitrogen regulation and beyond. FEMS microbiology reviews, 37, 251-83.

118. Imperial J, Shah VK, Ugalde RA, Ludden PW, Brill WJ. 1987. Iron-molybdenum cofactor synthesis in *Azotobacter vinelandii* Nif- mutants. J Bacteriol, 169, 1784-86.

119. Imperial J, Ugalde RA, Shah VK, Brill WJ. 1984. Role of the *nifQ* gene product in the incorporation of molybdenum into nitrogenase in *Klebsiella pneumoniae*. J Bacteriol, 158, 187-94.

120. Jacobs D, Mitchell D, Watt GD. 1995. The Concentration of Cellular Nitrogenase Proteins in *Azotobacter vinelandii* Whole Cells as Determined by Activity Measurements and Electron Paramagnetic Resonance Spectroscopy. Archives of Biochemistry and Biophysics, 324, 317-24.

121. Jacobson MR, Brigle KE, Bennett LT, Setterquist RA, Wilson MS, Cash VL, Beynon J, Newton WE, Dean DR. 1989. Physical and genetic map of the major *nif* gene cluster from *Azotobacter vinelandii*. J Bacteriol, 171, 1017-27.

122. Jacobson MR, Cash VL, Weiss MC, Laird NF, Newton WE, Dean DR. 1989. Biochemical and genetic analysis of the *nifUSVWZM* cluster from *Azotobacter vinelandii*. Mol Gen Genet, 219, 49-57.

123. Jang SB, Seefeldt LC, Peters JW. 2000.Insights into Nucleotide Signal Transduction in Nitrogenase: Structure of an Iron Protein with MgADP Bound. Biochemistry, 39, 14745-52.

124. Jasniewski AJ, Lee CC, Ribbe MW, Hu Y. 2020. Reactivity, Mechanism, and Assembly of the Alternative Nitrogenases. Chem Rev, 120, 5107-57.

125. Jenner LP, Cherrier MV, Amara P, Rubio LM, Nicolet Y. 2021. An unexpected P-cluster like intermediate en route to the nitrogenase FeMo-co. Chem Sci, 12, 5269-74.

126. Jeong HS, Jouanneau Y. 2000.Enhanced nitrogenase activity in strains of *Rhodobacter capsulatus* that overexpress the rnf genes. J Bacteriol, 182, 1208-14.

127. Jiang X, Payá-Tormo L, Coroian D, García-Rubio I, Castellanos-Rueda R, Eseverri Á, López-Torrejón G, Burén S, Rubio LM. 2021. Exploiting genetic diversity and gene synthesis to identify superior nitrogenase NifH protein variants to engineer N2-fixation in plants. Comm Biol, 4, 4.

128. Jimenez-Vicente E, Dean DR. 2017. Keeping the nitrogen-fixation dream alive. Proc.Natl Acad Sci USA, 114, 3009-11.

129. Jimenez-Vicente E, Navarro-Rodriguez M, Poza-Carrion C, Rubio LM. 2014. Role of *Azotobacter vinelandii* FdxN in FeMo-co biosynthesis. FEBS Lett, 588, 512-6.

130. Jimenez-Vicente E, Yang ZY, Martin Del Campo JS, Cash VL, Seefeldt LC, Dean DR. 2019. The NifZ accessory protein has an equivalent function in maturation of both nitrogenase MoFe protein P-clusters. J Biol Chem, 294, 6204-13.

131. Jimenez-Vicente E, Yang ZY, Ray WK, Echavarri-Erasun C, Cash VL, Rubio LM, Seefeldt LC, Dean DR. 2018. Sequential and differential interaction of assembly factors during nitrogenase MoFe protein maturation. J Biol Chem, 293, 9812-23.

132. Joerger RD, Bishop PE. 1990. Genetics and Molecular Biology of Alternative Nitrogen Fixation Systems. Annu Rev Plant Phys Plant Mol Biol, 41, 109-125.

133. Joerger RD, Bishop PE. 1988. Nucleotide sequence and genetic analysis of the *nifB-nifQ* region from *Azotobacter vinelandii*. J Bacteriol, 170, 1475-87.

134. Joerger RD, Jacobson MR, Bishop PE. 1989. Two nifA-like genes required for expression of alternative nitrogenases by *Azotobacter vinelandii*. J Bacteriol, 171, 3258-67.

135. Joerger RD, Jacobson MR, Premakumar R, Wolfinger ED, Bishop PE. 1989. Nucleotide-sequence and mutational analysis of the structural genes (*anfhdgk*) for the 2nd alternative nitrogenase from *Azotobacter vinelandii*. J Bacteriol, 171, 1075-86.

136. Joerger RD, Loveless TM, Pau RN, Mitchenall LA, Simon BH, Bishop PE. 1990. Nucleotide-sequences and mutational analysis of the structural genes for nitrogenase-2 of *Azotobacter vinelandii*. J Bacteriol, 172, 3400-08.

137. Joerger RD, Wolfinger ED, Bishop PE. 1991. The gene encoding dinitrogenase reductase 2 is required for expression of the second alternative nitrogenase from *Azotobacter vinelandii*. JBacteriol, 173, 4440-46.

138. Johnson DC, Dos Santos PC, Dean DR. 2005. NifU and NifS are required for the maturation of nitrogenase and cannot replace the function of isc-gene products in *Azotobacter vinelandii*. Biochem Soc Trans, 33, 90-3.

139. Jones CW, Brice JM, Wright V, Ackrell BA. 1973. Respiratory protection of nitrogenase in *Azotobacter vinelandii*. FEBS Lett, 29, 77-81.

140. Jumper J, Evans R, Pritzel A, Green T, Figurnov M, Ronneberger O, Tunyasuvunakool K, Bates R, Žídek A, Potapenko A, Bridgland A, Meyer C, Kohl SAA, Ballard AJ, Cowie A, Romera-Paredes B, Nikolov S, Jain R, Adler J, Back T, Petersen S, Reiman D, Clancy E, Zielinski M, Steinegger M, Pacholska M, Berghammer T, Bodenstein S, Silver D, Vinyals O, Senior AW, Kavukcuoglu K, Kohli P, Hassabis D. 2021. Highly accurate protein structure prediction with AlphaFold. Nature, 596, 583-89.

141. Kaiser JT, Hu Y, Wiig JA, Rees DC, Ribbe MW. 2011. Structure of Precursor-Bound NifEN: A Nitrogenase FeMo Cofactor Maturase/Insertase. Science, 331, 91-94.

142. Kakuta Y, Horio T, Takahashi Y, Fukuyama K. 2001.Crystal Structure of *Escherichia coli* Fdx, an Adrenodoxin-Type Ferredoxin Involved in the Assembly of Iron−Sulfur Clusters. Biochemistry, 40, 11007-12.

143. Kang W, Rettberg L, Stiebritz M, Jasniewski A, Tanifuji K, Lee CC, Ribbe MW, Hu Y. 2021. X-Ray Crystallographic analysis of NifB with a full complement of clusters: Structural insights into the radical SAM-dependent carbide insertion during nitrogenase cofactor assembly. Angew Chem Int Ed, 60, 2364-70.

144. Kelly MJ, Poole RK, Yates MG, Kennedy C. 1990. Cloning and mutagenesis of genes encoding the cytochrome bd terminal oxidase complex in *Azotobacter vinelandii*: mutants deficient in the cytochrome d complex are unable to fix nitrogen in air. J Bacteriol, 172, 6010-19.

145. Kennedy C, Dean D. 1992. The nifU, nifS and nifV gene products are required for activity of all three nitrogenases of *Azotobacter vinelandii*. Mol Gen Genetic: MGG, 231, 494-98.

146. Kennedy C, Gamal R, Humphrey R, Ramos J, Brigle K, Dean D. 1986. The nifH, nifM and nifN genes of *Azotobcater vinelandii*: characterisation by Tn5 mutagenesis and isolation from pLAFR1 gene banks. Mol Gen Genet, 205, 318-25.

147. Kim CH, Newton WE, Dean DR. 1995. Role of the MoFe protein alpha-subunit histidine-195 residue in FeMo-cofactor binding and nitrogenase catalysis. Biochemistry, 34, 2798-808.

148. Kim J, Rees DC. 1992. Crystallographic structure and functional implications of the nitrogenase molybdenum-iron protein from *Azotobacter vinelandii*. Nature, 360, 553-60.

149. Kim JH, Tonelli M, Kim T, Markley JL. 2012. Three-Dimensional Structure and Determinants of Stability of the Iron–Sulfur Cluster Scaffold Protein IscU from *Escherichia coli*. Biochemistry, 51, 5557-63.

150. Kleiner D, Kleinschmidt JA. 1976. Selective inactivation of nitrogenase in *Azotobacter vinelandii* batch cultures. J Bacteriol, 128, 117-22.

151. Kleinschmidt JA, Kleiner D. 1978. The Glutamine Synthetase from *Azotobacter vinelandii*: Purification, Characterization, Regulation and Localization. European Journal of Biochemistry, 89, 51-60.

152. Knutson CM, Pieper MN, Barney BM, Becker A. 2021. Gene Fitness of *Azotobacter vinelandii* under Diazotrophic Growth. *J Bacteriol,* 203, e00404-00421.

153. Krebs C, Agar JN, Smith AD, Frazzon J, Dean DR, Huynh BH, Johnson MK. 2001.IscA, an Alternate Scaffold for Fe-S Cluster Biosynthesis. Biochemistry, 40, 14069-80.

154. Kuhla J, Oelze J. 1988. Dependence of nitrogenase switch-off upon oxygen stress on the nitrogenase activity in *Azotobacter vinelandii*. J Bacteriol, 170, 5325-29.

155. Ledbetter RN, Garcia Costas AM, Lubner CE, Mulder DW, Tokmina-Lukaszewska M, Artz JH, Patterson A, Magnuson TS, Jay ZJ, Duan HD, Miller J, Plunkett MH, Hoben JP, Barney BM, Carlson RP, Miller AF, Bothner B, King PW, Peters JW, Seefeldt LC. 2017. The Electron Bifurcating FixABCX Protein Complex from *Azotobacter vinelandii*: Generation of Low-Potential Reducing Equivalents for Nitrogenase Catalysis. Biochemistry, 56, 4177-90.

156. Lei S, Pulakat L, Gavini N. 1999. Regulated Expression of the nifM of *Azotobacter vinelandii* in Response to Molybdenum and Vanadium Supplements in Burk's Nitrogen-Free Growth Medium. Biochemical and Biophysical Research Communications, 264, 186-90.

157. Leung D, van der Oost J, Kelly M, Saraste M, Hill S, Poole RK. 1994. Mutagenesis of a gene encoding a cytochrome o-like terminal oxidase of *Azotobacter vinelandii*: a cytochrome o mutant is aero-tolerant during nitrogen fixation. FEMS Microbiol Lett, 119, 351-7

158. Liedtke J, Lee CC, Tanifuji K, Jasniewski AJ, Ribbe MW, Hu Y. 2021. Characterization of a Mo-Nitrogenase Variant Containing a Citrate-Substituted Cofactor. ChemBioChem, 22, 151-55.

159. Linkerhagner K, Oelze J. 1997. Nitrogenase activity and regeneration of the cellular ATP pool in *Azotobacter vinelandii* adapted to different oxygen concentrations. J Bacteriol, 179, 1362-67.

160. Lipman JG. 1903. Experiments on the transformation and fixation of nitrogen by bacteria.ed. New Jersey state agricultural experiment station, 17th annual report. New Jersey, 215–85.

161. Little R, Colombo V, Leech A, Dixon R. 2002. Direct Interaction of the NifL Regulatory Protein with the GlnK Signal Transducer Enables the *Azotobacter vinelandii* NifL-NifA Regulatory System to Respond to Conditions Replete for Nitrogen. J Biol Chem, 277, 15472-81.

162. Little R, Martinez-Argudo I, Dixon R. 2006. Role of the central region of NifL in conformational switches that regulate nitrogen fixation. Biochem Soc Trans, 34, 162-64.

163. Little R, Martinez-Argudo I, Perry S, Dixon R. 2007. Role of the H Domain of the Histidine Kinase-like Protein NifL in Signal Transmission. J Biol Chem, 282, 13429-37.

164. Little R, Reyes-Ramirez F, Zhang Y, van Heeswijk WC, Dixon R. 2000.Signal transduction to the *Azotobacter vinelandii* NIFL-NIFA regulatory system is influenced directly by interaction with 2-oxoglutarate and the PII regulatory protein. The EMBO Journal, 19, 6041-50.

165. Ljones T, Burris RH. 1978. Evidence for one-electron transfer by the Fe protein of nitrogenase. Biochem Biophys Res Commun, 80, 22-25.

166. López-Torrejón G, Burén S, Veldhuizen M, Rubio LM. 2021. Biosynthesis of cofactor-activatable iron-only nitrogenase in Saccharomyces cerevisiae. Microbial Biotechnology, 14, 1073-83.

167. Lopez-Torrejon G, Jimenez-Vicente E, Buesa JM, Hernandez JA, Verma HK, Rubio LM. 2016. Expression of a functional oxygen-labile nitrogenase component in the mitochondrial matrix of aerobically grown yeast. Nat Commun, 7, 11426.

168. Lowe DJ, Thorneley RN. 1984. The mechanism of *Klebsiella pneumoniae* nitrogenase action. The determination of rate constants required for the simulation of the kinetics of N2 reduction and H2 evolution. Biochem J, 224, 895-901.

169. Lukoyanov D, Khadka N, Yang Z-Y, Dean DR, Seefeldt LC, Hoffman BM. 2016. Reductive Elimination of H2 Activates Nitrogenase to Reduce the N≡N Triple Bond: Characterization of the E4(4H) Janus Intermediate in Wild-Type Enzyme. J Am Chem Soc, 138, 10674-83.

170. Lukoyanov D, Khadka N, Yang Z-Y, Dean DR, Seefeldt LC, Hoffman BM. 2016. Reversible Photoinduced Reductive Elimination of H2 from the Nitrogenase Dihydride State, the E4(4H) Janus Intermediate. J Am Chem Soc, 138, 1320-27.

171. Macheroux P, Hill S, Austin S, Eydmann T, Jones T, Kim S-O, Poole R, Dixon R. 1998. Electron donation to the flavoprotein NifL, a redox-sensing transcriptional regulator. Biochemical Journal, 332, 413-19.

172. MacKellar D, Lieber L, Norman JS, Bolger A, Tobin C, Murray JW, Oksaksin M, Chang RL, Ford TJ, Nguyen PQ, Woodward J, Permingeat HR, Joshi NS, Silver PA, Usadel B, Rutherford AW, Friesen ML, Prell J. 2016. *Streptomyces thermoautotrophicus* does not fix nitrogen. Sci Rep, 6, 20086.

173. MacNeil D, Howe MM, Brill WJ. 1980. Isolation and characterization of lambda specialized transducing bacteriophages carrying *Klebsiella pneumoniae* nif genes. J Bacteriol, 141, 1264-71.

174. MacNeil T, MacNeil D, Roberts GP, Supiano MA, Brill WJ. 1978. Fine-structure mapping and complementation analysis of nif (nitrogen fixation) genes in Klebsiella pneumoniae. J Bacteriol, 136, 253-66.

175. Martinez-Argudo I, Little R, Shearer N, Johnson P, Dixon R. 2004.The NifL-NifA System: a Multidomain Transcriptional Regulatory Complex That Integrates Environmental Signals. J Bacteriol, 186, 601-10.

176. Martinez-Argudo I, Little R, Shearer N, Johnson P, Dixon R. 2005. Nitrogen fixation: key genetic regulatory mechanisms. Biochem Soc Trans, 33, 152-6.

177. McLean PA, Dixon RA. 1981. Requirement of nifV gene for production of wild-type nitrogenase enzyme in Klebsiella pneumoniae. Nature, 292, 655-56.

178. McRose DL, Baars O, Morel FMM, Kraepiel AML. (2017).Siderophore production in *Azotobacter vinelandii* in response to Fe-, Mo- and V-limitation. Environ Microbiol, 19, 3595-605.

179. Mitra R, Das HK, Dixit A. 2005. Identification of a Positive Transcription Regulatory Element within the Coding Region of the nifLA Operon in *Azotobacter vinelandii*. Appl Environ Microbiol, 71, 3716-24.

180. Moreno-Vivian C, Schmehl M, Masepohl B, Arnold W, Klipp W. 1989. DNA sequence and genetic analysis of the *Rhodobacter capsulatus nifENX* gene region: homology between NifX and NifB suggests involvement of NifX in processing of the iron-molybdenum cofactor. Mol Gen Genetic: MGG, 216, 353-63.

181. Moshiri F, Kim JW, Fu C, Maier RJ. 1994. The FeSII protein of *Azotobacter vinelandii* is not essential for aerobic nitrogen fixation, but confers significant protection to oxygen-mediated inactivation of nitrogenase in vitro and in vivo. Mol Microbiol, 14, 101-14.

182. Mouncey NJ, Mitchenall LA, Pau RN. 1995. Mutational analysis of genes of the mod locus involved in molybdenum transport, homeostasis and processing in *Azotobacter vinelandii*. J Bacteriol, 177, 5294-302.

183. Mouncey NJ, Mitchenall LA, Pau RN. 1996. The modE gene product mediates molybdenum-dependent expression of genes for the high-affinity molybdate transporter and modG in *Azotobacter vinelandii*. Microbiology, 142, 1997-2004.

184. Mus F, Alleman AB, Pence N, Seefeldt LC, Peters JW 2018. Exploring the alternatives of biological nitrogen fixation. Metallomics, 10, 4, 523–538.

185. Mus F, Crook Matthew B, Garcia K, Garcia Costas A, Geddes Barney A, Kouri Evangelia D, Paramasivan P, Ryu M-H, Oldroyd Giles ED, Poole Philip S, Udvardi Michael K, Voigt Christopher A, Ané J-M, Peters John W, Kelly RM. 2016. Symbiotic Nitrogen Fixation and the Challenges to Its Extension to Nonlegumes. Appl Environ Microbiol, 82, 3698-710.

186. Nakajima H, Takatani N, Yoshimitsu K, Itoh M, Aono S, Takahashi Y, Watanabe Y. 2010. The role of the Fe-S cluster in the sensory domain of nitrogenase transcriptional activator VnfA from *Azotobacter vinelandii*. FEBS Journal, 277, 817-32.

187. Navarro-Rodríguez M, Buesa JM, Rubio LM. 2019. Genetic and Biochemical Analysis of the *Azotobacter vinelandii* Molybdenum Storage Protein. Frontiers in Microbiology, 10.

188. Ninfa AJ, Jiang P. 2005. PII signal transduction proteins: sensors of alpha-ketoglutarate that regulate nitrogen metabolism. Current opinion in microbiology, 8, 168-73.

189. Oelze J. 2000.Respiratory protection of nitrogenase in Azotobacter species: is a widely held hypothesis unequivocally supported by experimental evidence? FEMS Microbiology Reviews, 24, 321-33.

190. Oldroyd GED, Dixon R. 2014. Biotechnological solutions to the nitrogen problem. Current Opinion in Biotechnology, 26, 19-24.

191. Pau RN, Lawson DM. 2002. Transport, homeostasis, regulation, and binding of molybdate and Tungstate to proteins. Met Ions Biol Syst, 39, 31-74.

192. Paustian TD, Shah VK, Roberts GP. 1989. Purification and characterisation of the nifN and nifE gene products from *Azotobacter vinelandii* mutant UW45. Proc Natl Acad Sci USA, 86, 6082-86.

193. Paustian TD, Shah VK, Roberts GP. 1990. Apodinitrogenase: purification, association with a 20-kilodalton protein, and activation by the iron-molybdenum cofactor in the absence of dinitrogenase reductase. Biochemistry, 29, 3515-22.

194. Pence N, Lewis N, Alleman AB, Seefeldt LC, Peters JW. 2021. Revealing a role for the G subunit in mediating interactions between the nitrogenase component proteins. 214.

195. Pérez-González A, Jimenez-Vicente E, Gies-Elterlein J, Salinero-Lanzarote A, Yang Z-Y, Einsle O, Seefeldt LC, Dean DR, David Leslie Johnson M. 2021. Specificity of NifEN and VnfEN for the Assembly of Nitrogenase Active Site Cofactors in *Azotobacter vinelandii*. mBio, 12, e01568-21.

196. Pérez-González A, Jimenez-Vicente E, Salinero-Lanzarote A, Harris DF, Seefeldt LC, Dean DR. 2022. AnfO controls fidelity of nitrogenase FeFe protein maturation by preventing misincorporation of FeV-cofactor. Mol Microbiol, n/a doi.org/10.1111/mmi.14890

197. Phillips AH, Hernandez JA, Erbil KM, Pelton JG, Wemmer DE, Rubio LM.(2010. Biological activity and solution structure of the apo-dinitrogenase binding domain of NafY. DOI:10.2210/pdb2kic/pdb.

198. Phillips AH, Hernandez JA, Payá-Tormo L, Burén S, Cuevas-Zuviría B, Pacios LF, Pelton JG, Wemmer DE, Rubio LM. 2021. Environment and coordination of FeMo–co in the nitrogenase metallochaperone NafY. RSC Chemical Biology, 2, 1462-65.

199. Pollock RC, Lee HI, Cameron LM, Derose VJ, Hales BJ, Ormejohnson WH, Hoffman BM. 1995. Investigation of co bound to inhibited forms of nitrogenase MoFe protein by c-13 endor. J Am Chem Soc, 117, 8686-87.

200. Poole RK, Hill S. 1997. Respiratory protection of nitrogenase activity in *Azotobacter vinelandii* - Roles of the terminal oxidases. Biosci Rep, 17, 303-17.

201. Post E, Kleiner D, Oelze J. (1983).Whole cell respiration and nitrogenase activities in *Azotobacter vinelandii* growing in oxygen controlled continuous culture. Arch Microbiol, 134, 68-72.

202. Poza-Carrión C, Jiménez-Vicente E, Navarro-Rodríguez M, Echavarri-Erasun C, Rubio LM. 2014. Kinetics of nif Gene Expression in a Nitrogen-Fixing Bacterium. J Bacteriol, 196, 595-603.

203. Premakumar R, Loveless TM, Bishop PE. 1994. Effect of amino acid substitutions in a potential metal-binding site of AnfA on expression from the anfH promoter in *Azotobacter vinelandii*. J Bacteriol, 176, 6139-42.

204. Premakumar R, Pau RN, Mitchenall LA, Easo M, Bishop PE. 1998. Regulation of the transcriptional activators AnfA and VnfA by metals and ammonium in *Azotobacter vinelandii*. FEMS Microbiol Lett, 164, 63-8.

205. Puerta-Fernández E, Vioque A. 2011. Hfq Is Required for Optimal Nitrate Assimilation in the Cyanobacterium Anabaena sp. Strain PCC 7120. J Bacteriol, 193, 3546-55.

206. Pye VE, Tingey AP, Robson RL, Moody PCE. 2004.The Structure and Mechanism of Serine Acetyltransferase from *Escherichia coli*. J Biol Chem, 279, 40729-36.

207. Raina R, Bageshwar UK, Das HK. 1993. The *Azotobacter vinelandii* nifL-like gene: nucleotide sequence analysis and regulation of expression. Mol Gen Genetic: MGG, 237, 400-6.

208. Raymond J, Siefert JL, Staples CR, Blankenship RE. 2004.The Natural History of Nitrogen Fixation. Mol Biol Evol, 21, 541-54.

209. Rebelein JG, Lee CC, Newcomb M, Hu Y, Ribbe MW, Lovley DR, Buckel W, Tezcan A. 2018. Characterization of an M-Cluster-Substituted Nitrogenase VFe Protein. mBio, 9, e00310-18.

210. Rettberg LA, Wilcoxen J, Lee CC, Stiebritz MT, Tanifuji K, Britt RD, Hu Y. 2018. Probing the coordination and function of Fe4S4 modules in nitrogenase assembly protein NifB. Nat Comm, 9, 2824.

211. Reyes-Ramirez F, Little R, Dixon R. 2001.Role of *Escherichia coli* Nitrogen Regulatory Genes in the Nitrogen Response of the *Azotobacter vinelandii* NifL-NifA Complex. J Bacteriol, 183, 3076-82.

212. Ribbe MW, Hu Y, Guo M, Schmid B, Burgess BK. 2002. The FeMoco-deficient MoFe protein produced by a nifH deletion strain of *Azotobacter vinelandii* shows unusual P-cluster features. J Biol Chem, 277, 23469-76.

213. Rivera-Ortiz JM, Burris RH. 1975. Interactions among substrates and inhibitors of nitrogenase. J Bacteriol, 123, 537-45.

214. Robinson AC, Burgess BK, Dean DR. 1986. Activity, reconstitution, and accumulation of nitrogenase components in *Azotobacter vinelandii* mutant strains containing defined deletions within the nitrogenase structural gene cluster. J Bacteriol, 166, 180-86.

215. Rohde M, Grunau K, Einsle O. 2020. CO Binding to the FeV Cofactor of CO-Reducing Vanadium Nitrogenase at Atomic Resolution. Angew Chem Int Ed, 59, 23626-30.

216. Rohde M, Laun K, Zebger I, Stripp ST, Einsle O. 2021. Two ligand-binding sites in CO-reducing V nitrogenase reveal a general mechanistic principle. Sci Adv, 7, eabg4474.

217. Rohde M, Sippel D, Trncik C, Andrade SLA, Einsle O. 2018. The Critical E4 State of Nitrogenase Catalysis. Biochemistry, 57, 5497-504.

218. Rohde M, Trncik C, Sippel D, Gerhardt S, Einsle O. 2018. Crystal structure of VnfH, the iron protein component of vanadium nitrogenase. J Biol Inorg Chem, 23, 1049-56

219. Roll JT, Shah VK, Dean DR, Roberts GP. 1995. Characteristics of NIFNE in *Azotobacter vinelandii* strains. Implications for the synthesis of the iron-molybdenum cofactor of dinitrogenase. J Biol Chem, 270, 4432-7.

220. Rubio LM, Ludden PW. 2008. Biosynthesis of the Iron-Molybdenum Cofactor of Nitrogenase. Annual Review of Microbiology, 62, 93-111.

221. Rubio LM, Rangaraj P, Homer MJ, Roberts GP, Ludden PW. 2002. Cloning and mutational analysis of the gamma gene from *Azotobacter vinelandii* defines a new family of proteins capable of metallocluster binding and protein stabilization. J Biol Chem, 277, 14299-305.

222. Rubio LM, Singer SW, Ludden PW. 2004.Purification and Characterization of NafY (Apodinitrogenase γ Subunit) from *Azotobacter vinelandii*. J Biol Chem, 279, 19739-46.

223. Rudnick P, Kunz C, Gunatilaka MK, Hines ER, Kennedy C. 2002. Role of GlnK in NifL-Mediated Regulation of NifA Activity in *Azotobacter vinelandii*. J Bacteriol, 184, 812-20.

224. Rutledge HL, Tezcan FA. 2020. Electron Transfer in Nitrogenase. Chem Rev, 120, 5158-93.

225. Ruttimann-Johnson C, Rangaraj P, Shah VK, Ludden PW. 2001.Requirement of Homocitrate for the Transfer of a 49V-Labeled Precursor of the Iron-Vanadium Cofactor from VnfX to nif-apodinitrogenase. J Biol Chem, 276, 4522-6.

226. Ruttimann-Johnson C, Rubio LM, Dean DR, Ludden PW. 2003. VnfY is required for full activity of the vanadium-containing dinitrogenase in *Azotobacter vinelandii*. J Bacteriol, 185, 2383-86.

227. Rüttimann-Johnson C, Staples CR, Rangaraj P, Shah VK, Ludden PW. 1999. A vanadium and iron cluster accumulates on VnfX during iron-vanadium-cofactor synthesis for the vanadium nitrogenase in *Azotobacter vinelandii*. J Biol Chem, 274, 18087-92.

228. Saio T, Kumeta H, Ogura K, Yokochi M, Asayama M, Katoh S, Katoh E, Teshima K, Inagaki F. 2007. The Cooperative Role of OsCnfU-1A Domain I and Domain II in the Iron–Sulphur Cluster Transfer Process as Revealed by NMR. J Biochem, 142, 113-21.

229. Schlesier J, Rohde M, Gerhardt S, Einsle O. 2016. A Conformational Switch Triggers Nitrogenase Protection from Oxygen Damage by Shethna Protein II (FeSII). J Am Chem Soc, 138, 239-47.

230. Schmehl M, Jahn A, Meyer zu Vilsendorf A, Hennecke S, Masepohl B, Schuppler M, Marxer M, Oelze J, Klipp W. 1993. Identification of a new class of nitrogen fixation genes in Rhodobacter capsulatus: a putative membrane complex involved in electron transport to nitrogenase. Mol Gen Genetic: MGG, 241, 602-15.

231. Schmid B, Einsle O, Chiu H-J, Willing A, Yoshida M, Howard JB, Rees DC. 2002. Biochemical and Structural Characterization of the Cross-Linked Complex of Nitrogenase: Comparison to the ADP-AlF4--Stabilized Structure. Biochemistry, 41, 15557-65.

232. Schmid B, Ribbe MW, Einsle O, Yoshida M, Thomas LM, Dean DR, Rees DC, Burgess BK. 2002. Structure of a cofactor-deficient nitrogenase MoFe protein. Science, 296, 352-56.

233. Schoch CL, Ciufo S, Domrachev M, Hotton CL, Kannan S, Khovanskaya R, Leipe D, McVeigh R, O'Neill K, Robbertse B, Sharma S, Soussov V, Sullivan JP, Sun L, Turner S, Karsch-Mizrachi I. 2020. NCBI Taxonomy: a comprehensive update on curation, resources and tools. Database (Oxford), 2020, baaa062.

234. Scott DJ, May HD, Newton WE, Brigle KE, Dean DR. 1990. Role for the nitrogenase MoFe protein alpha-subunit in FeMo-cofactor binding and catalysis. Nature, 343, 188-90.

235. Seefeldt LC, Hoffman BM, Peters JW, Raugei S, Beratan DN, Antony E, Dean DR. 2018. Energy Transduction in Nitrogenase. Acc Chem Res, 51, 2179-86.

236. Seefeldt LC, Yang Z-Y, Lukoyanov DA, Harris DF, Dean DR, Raugei S, Hoffman BM. 2020. Reduction of Substrates by Nitrogenases. Chem Rev, 120, 5082-106.

237. Seefeldt LC, Yang ZY, Duval S, Dean DR. 2013. Nitrogenase reduction of carbon-containing compounds. Biochim Biophys Acta, 1827, 1102-11.

238. Segal HM, Spatzal T, Hill MG, Udit AK, Rees DC. 2017. Electrochemical and structural characterization of *Azotobacter vinelandii* flavodoxin II. Prot Sci, 26, 1984-93.

239. Setubal JC, dos Santos P, Goldman BS, Ertesvag H, Espin G, Rubio LM, Valla S, Almeida NF, Balasubramanian D, Cromes L, Curatti L, Du Z, Godsy E, Goodner B, Hellner-Burris K, Hernandez JA, Houmiel K, Imperial J, Kennedy C, Larson TJ, Latreille P, Ligon LS, Lu

J, Maerk M, Miller NM, Norton S, O'Carroll IP, Paulsen I, Raulfs EC, Roemer R, Rosser J, Segura D, Slater S, Stricklin SL, Studholme DJ, Sun J, Viana CJ, Wallin E, Wang B, Wheeler C, Zhu H, Dean DR, Dixon R, Wood D. 2009. Genome sequence of *Azotobacter vinelandii*, an obligate aerobe specialized to support diverse anaerobic metabolic processes. J Bacteriol, 191, 4534-45.

240. Shah VK, Allen JR, Spangler NJ, Ludden PW. 1994. In vitro synthesis of the iron-molybdenum cofactor of nitrogenase. Purification and characterization of NifB cofactor, the product of NIFB protein. J Biol Chem, 269, 1154-58.
241. Shah VK, Brill WJ. 1981. Isolation of a molybdenum-iron cluster from nitrogenase. Proc.Natl Acad Sci USA, 78, 3438-40.
242. Shah VK, Imperial J, Ugalde RA, Ludden PW, Brill WJ. 1986. In vitro synthesis of the iron-molybdenum cofactor of nitrogenase. Proc Natl Acad Sci USA, 83, 1636-40.
243. Shi R, Proteau A, Villarroya M, Moukadiri I, Zhang L, Trempe J-F, Matte A, Armengod ME, Cygler M. 2010. Structural Basis for Fe–S Cluster Assembly and tRNA Thiolation Mediated by IscS Protein–Protein Interactions. PLOS Biol, 8, e1000354.
244. Shin Sang H, Kim S, Kim Jae Y, Lee S, Um Y, Oh M-K, Kim Y-R, Lee J, Yang K-S. 2012. Complete Genome Sequence of Klebsiella oxytoca KCTC 1686, Used in Production of 2,3-Butanediol. J Bacteriol, 194, 2371-72.
245. Simpson FB, Burris RH. 1984. A nitrogen pressure of 50 atmospheres does not prevent evolution of hydrogen by nitrogenase. Science, 224, 1095-97.
246. Sippel D, Einsle O. 2017. The structure of vanadium nitrogenase reveals an unusual bridging ligand. Nat Chem Biol, 13, 956-60.

247. Sippel D, Schlesier J, Rohde M, Trncik C, Decamps L, Djurdjevic I, Spatzal T, Andrade SLA, Einsle O. 2017) Production and isolation of vanadium nitrogenase from *Azotobacter vinelandii* by molybdenum depletion. J Biol Inorg Chem, 22, 161-68

248. Slavny P, Little R, Salinas P, Clarke TA, Dixon R. 2010. Quaternary structure changes in a second Per-Arnt-Sim domain mediate intramolecular redox signal relay in the NifL regulatory protein. Mol Microbiol, 75, 61-75.

249. Smil V. 2000.Enriching the earth: Fritz Haber, Carl Bosch, and the transformation of world food production. Cambridge, Massachusetts, MIT Press.

250. Smith AD, Jameson GNL, Dos Santos PC, Agar JN, Naik S, Krebs C, Frazzon J, Dean DR, Huynh BH, Johnson MK. 2005. NifS-mediated assembly of [4Fe-4S] clusters in the N- and C-terminal domains of the NifU scaffold protein. Biochemistry, 44, 12955-69.

251. Smith C, Hill AK, Torrente-Murciano L. 2020. Current and future role of Haber–Bosch ammonia in a carbon-free energy landscape. Energy Environ Sci, 13, 331-44.

252. Soboh B, Boyd ES, Zhao D, Peters JW, Rubio LM. 2010. Substrate specificity and evolutionary implications of a NifDK enzyme carrying NifB-co at its active site. FEBS Lett, 584, 1487-92.

253. Sobti M, Walshe JL, Wu D, Ishmukhametov R, Zeng YC, Robinson CV, Berry RM, Stewart AG. 2020. Cryo-EM structures provide insight into how E. coli F1Fo ATP synthase accommodates symmetry mismatch. Nat Comm, 11, 2615.

254. Söderbäck E, Reyes-Ramirez F, Eydmann T, Austin S, Hill S, Dixon R. 1998. The redox- and fixed nitrogen-responsive regulatory protein NIFL from *Azotobacter vinelandii* comprises discrete flavin and nucleotide-binding domains. Mol Microbiol, 28, 179-92.

255. Soulimane T, Buse G, Bourenkov GP, Bartunik HD, Huber R, Than ME. 2000.Structure and mechanism of the aberrant ba3-cytochrome c oxidase from Thermus thermophilus. The EMBO J, 19, 1766-76.

256. Sousa FM, Sena FV, Batista AP, Athayde D, Brito JA, Archer M, Oliveira ASF, Soares CM, Catarino T, Pereira MM. 2017. The key role of glutamate 172 in the mechanism of type II NADH:quinone oxidoreductase of Staphylococcus aureus. Biochim et Biophys Acta : Bioenerg, 1858, 823-32.

257. Spatzal T, Aksoyoglu M, Zhang L, Andrade SL, Schleicher E, Weber S, Rees DC, Einsle O. 2011. Evidence for interstitial carbon in nitrogenase FeMo cofactor. Science, 334, 940.

258. Spatzal T, Perez KA, Einsle O, Howard JB, Rees DC. 2014. Ligand binding to the FeMo-cofactor: structures of CO-bound and reactivated nitrogenase. Science (New York, NY), 345, 1620-23.

259. Srisantitham S, Badding ED, Suess DLM. 2021. Postbiosynthetic modification of a precursor to the nitrogenase iron–molybdenum cofactor. Proc.Natl Acad Sci USA, 118, e2015361118.

260. Steuber J, Vohl G, Casutt MS, Vorburger T, Diederichs K, Fritz G. 2014. Structure of the *V. cholerae* Na+-pumping NADH:quinone oxidoreductase. Nature, 516, 62-67.

261. Streicher S, Gurney E, Valentine RC. 1971. Transduction of the Nitrogen-Fixation Genes in Klebsiella pneumoniae. Proc.Natl Acad Sci USA, 68, 1174-77.

262. Takimoto R, Tatemichi Y, Aoki W, Kosaka Y, Minakuchi H, Ueda M, Kuroda K. 2022. A critical role of an oxygen-responsive gene for aerobic nitrogenase activity in *Azotobacter vinelandii* and its application to *Escherichia coli*. Sci Rep, 12, 4182.

263. Tanabe Y, Nishibayashi Y. 2021. Comprehensive insights into synthetic nitrogen fixation assisted by molecular catalysts under ambient or mild conditions. Chem Soc Rev, 50, 5201-42.

264. Tanifuji K, Lee CC, Sickerman NS, Tatsumi K, Ohki Y, Hu Y, Ribbe MW. 2018. Tracing the 'ninth sulfur' of the nitrogenase cofactor via a semi-synthetic approach. Nat Chem, 10, 568-72.

265. Tezcan FA, Kaiser JT, Mustafi D, Walton MY, Howard JB, Rees DC. 2005. Nitrogenase Complexes: Multiple Docking Sites for a Nucleotide Switch Protein. Science, 309, 1377-80.

266. Than ME, Hof P, Huber R, Bourenkov GP, Bartunik HD, Buse G, Soulimane T. 1997. *Thermus thermophilus* cytochrome-c552: a new highly thermostable cytochrome-c structure obtained by MAD phasing11Edited by K. Nagai. J Mol Biol, 271, 629-44.

267. Townsend AR, Howarth RW. 2010. FIXING THE GLOBAL Nitrogen Problem. Sci Am, 302, 64-71.

268. Trncik C, Müller T, Franke P, Einsle O. 2022. Structural analysis of the reductase component AnfH of iron-only nitrogenase from *Azotobacter vinelandii*. J Inorg Biochem, 227, 111690.

269. Ugalde RA, Imperial J, Shah VK, Brill WJ. 1984. Biosynthesis of iron-molybdenum cofactor in the absence of nitrogenase. J Bacteriol, 159, 888-93.

270. Ugalde RA, Imperial J, Shah VK, Brill WJ. 1985. Biosynthesis of the iron-molybdenum cofactor and the molybdenum cofactor in *Klebsiella pneumoniae*: effect of sulfur source. J Bacteriol, 164, 1081-87.

271. van Heeswijk WC, Westerhoff HV, Boogerd FC. 2013. Nitrogen assimilation in *Escherichia coli*: putting molecular data into a systems perspective. Microbiol Mol Biol Rev: MMBR, 77, 628-95.

272. Van Stappen C, Decamps L, Cutsail GE, Bjornsson R, Henthorn JT, Birrell JA, DeBeer S. 2020. The Spectroscopy of Nitrogenases. Chem Rev, 120, 5005-81.

273. Van Stappen C, Jiménez-Vicente E, Pérez-González A, Yang Z-Y, Seefeldt LC, DeBeer S, Dean DR, Decamps L. 2022. A conformational role for NifW in the maturation of molybdenum nitrogenase P-cluster. Chem Sci, 13, 3489-3500.

274. Varadi M, Anyango S, Deshpande M, Nair S, Natassia C, Yordanova G, Yuan D, Stroe O, Wood G, Laydon A, Žídek A, Green T, Tunyasuvunakool K, Petersen S, Jumper J, Clancy E, Green R, Vora A, Lutfi M, Figurnov M, Cowie A, Hobbs N, Kohli P, Kleywegt G, Birney E, Hassabis D, Velankar S. 2022. AlphaFold Protein Structure Database: massively expanding the structural coverage of protein-sequence space with high-accuracy models. Nucleic Acids Res, 50, D439-D44.

275. Walmsley J, Toukdarian A, Kennedy C. 1994. The role of regulatory genes *nifA, vnfA, anfA, nfrX, ntrC,* and *rpoN* in expression of genes encoding the three nitrogenases of *Azotobacter vinelandii*. Arch Microbiol, 162, 422-29.

276. Wiethaus J, Wirsing A, Narberhaus F, Masepohl B. 2006. Overlapping and Specialized Functions of the Molybdenum-Dependent Regulators MopA and MopB in *Rhodobacter capsulatus*. J Bacteriol, 188, 8441-51.

277. Wiig J, Hu Y, Lee Chi C, Ribbe Markus W. 2012. Radical SAM-Dependent Carbon Insertion into the Nitrogenase M-Cluster. Science, 337, 1672-75.

278. Wilcoxen J, Arragain S, Scandurra AA, Jimenez-Vicente E, Echavarri-Erasun C, Pollmann S, Britt RD, Rubio LM. 2016. Electron Paramagnetic Resonance Characterization of Three Iron–Sulfur Clusters Present in the Nitrogenase Cofactor Maturase NifB from *Methanocaldococcus infernus*. J Am Chem Soc, 138, 7468-71.

279. Wolfinger ED, Bishop PE. 1991. Nucleotide sequence and mutational analysis of the *vnfENX* region of *Azotobacter vinelandii*. J Bacteriol, 173, 7565-72.

280. Wu G, Hill S, Kelly MJ, Sawers G, Poole RK. 1997. The cydR gene product, required for regulation of cytochrome bd expression in the obligate aerobe *Azotobacter vinelandii*, is an Fnr- like protein. Microbiol, 143, 2197-207.

281. Yan Y, Yang J, Dou Y, Chen M, Ping S, Peng J, Lu W, Zhang W, Yao Z, Li H, Liu W, He S, Geng L, Zhang X, Yang F, Yu H, Zhan Y, Li D, Lin Z, Wang Y, Elmerich C, Lin M, Jin Q. 2008. Nitrogen fixation island and rhizosphere competence traits in the genome of root-associated *Pseudomonas stutzeri* A1501. Proc.Natl Acad Sci USA, 105, 7564-69.

282. Yang J, Xie X, Wang X, Dixon R, Wang Y-P. 2014. Reconstruction and minimal gene requirements for the alternative iron-only nitrogenase in *Escherichia coli*. Proc.Natl Acad Sci USA, 111, E3718-E25.

283. Yang Z-Y, Dean DR, Seefeldt LC. 2011. Molybdenum Nitrogenase Catalyzes the Reduction and Coupling of CO to Form Hydrocarbons. J Biol Chem, 286, 19417-21.

284. Yang Z-Y, Jimenez-Vicente E, Kallas H, Lukoyanov DA, Yang H, Martin del Campo JS, Dean DR, Hoffman BM, Seefeldt LC. 2021. The electronic structure of FeV-cofactor in vanadium-dependent nitrogenase. Chem Sci, 12, 6913-22.

285. Yang ZY, Khadka N, Lukoyanov D, Hoffman BM, Dean DR, Seefeldt LC. 2013. On reversible H2 loss upon N2 binding to FeMo-cofactor of nitrogenase. Proc Natl Acad Sci U S A, 16327-32.

286. Yankovskaya V, Horsefield R, Törnroth S, Luna-Chavez C, Miyoshi H, Léger C, Byrne B, Cecchini G, Iwata S. 2003. Architecture of Succinate Dehydrogenase and Reactive Oxygen Species Generation. Science, 299, 700-04.

287. Yoshimitsu K, Takatani N, Miura Y, Watanabe Y, Nakajima H. 2011. The role of the GAF and central domains of the transcriptional activator VnfA in *Azotobacter vinelandii*. FEBS J, 278, 3287-97.

288. Yuvaniyama P, Agar JN, Cash VL, Johnson MK, Dean DR. 2000.NifS-directed assembly of a transient [2Fe-2S] cluster within the NifU protein. Proc.Natl Acad Sci USA, 97, 599-604.

289. Zhang X, Ward BB, Sigman DM. 2020. Global Nitrogen Cycle: Critical Enzymes, Organisms, and Processes for Nitrogen Budgets and Dynamics. Chem Rev, 120, 5308-51.

290. Zheng C, Dos Santos PC. 2018. Metallocluster transactions: dynamic protein interactions guide the biosynthesis of Fe-S clusters in bacteria. Biochem Soc Trans, 46, 1593-603.

291. Zheng L, Cash VL, Flint DH, Dean DR. 1998. Assembly of iron-sulfur clusters. Identification of an *iscSUA-hscBA-fdx* gene cluster from *Azotobacter vinelandii*. J Biol Chem, 273, 13264-72.

292. Zheng L, White RH, Cash VL, Dean DR. 1994. Mechanism for the desulfurization of L-cysteine catalyzed by the nifS gene product. Biochemistry, 33, 4714-20.

293. Zheng L, White RH, Cash VL, Jack RF, Dean DR. 1993. Cysteine desulfurase activity indicates a role for NifS in metallocluster biosynthesis. Proc Natl Acad Sci U S A, 90, 2754-8.

294. Zheng L, White RH, Dean DR. 1997. Purification of the *Azotobacter vinelandii* nifV-encoded homocitrate synthase. J Bacteriol, 179, 5963-6.

295. Zimmermann R, Munck E, Brill WJ, Shah VK, Henzl MT, Rawlings J, Orme-Johnson WH. 1978. Nitrogenase X: Mossbauer and EPR studies on reversibly oxidized MoFe protein from *Azotobacter vinelandii* OP. Nature of the iron centers. Biochim et Biophys Acta, 537, 185-207

Figure Legends

Figure 1 Schematic representation of three major pathways for the input of fixed nitrogen into the biosphere. It has been estimated that the Haber-Bosch process contributes approximately 65% of fixed nitrogen input to the biosphere, biological nitrogen fixation 32%, and lightning about 3% (Galloway, Bleeker, and Erisman, 2021; Smil, 2000). Note that these figures only account for the terrestrial contribution provided by biological nitrogen fixation. The Haber-Bosch industrial process requires extraordinarily high temperature and pressure, whereas biological nitrogen fixation occurs at ambient temperature and pressure. The Haber-Bosch process has made an enormous impact on humanity and has been the major driver for sustained population growth for the past 100 years (Smith, Hill, and Torrente-Murciano, 2020; Townsend and Howarth, 2010). Without the application of nitrogenous fertilizers produced by the Haber-Bosch process to increase crop productivity, it is estimated that 3.5 billion people representing nearly 40% of the world's existing human population, could not be sustained. Nevertheless, there are numerous unfavorable ecological, agronomic, and economic consequences associated with the Haber-Bosch process. The process consumes approximately 2% of the world's non-renewable energy supply and contributes about 1.6% of worldwide emissions of the greenhouse gas CO_2. An additional contribution to global warming associated with the industrial process is the production of the powerful greenhouse gas N_2O resulting from microbial denitrification of applied nitrogenous fertilizers (Zhang, Ward, and Sigman, 2020). It is notable that N_2O has 300 times the global warming power relative to CO_2 emissions, and it is estimated that ¾ of N_2O emission levels are attributed to the use of fertilizers in agriculture. Eutrophication of watersheds because of run-off of applied fertilizers, as well as costs associated with fertilizer transport and application, are also penalties associated with industrial nitrogen fixation (Erisman et al., 2013).

There have also been unfavorable social and geopolitical consequences linked to the rapid growth in the human population because of industrial nitrogen fixation.

Figure 2. Standard Gibbs free energy change (ΔG^o) for intermediates in the N_2 reduction pathway. The overall reduction of nitrogen to ammonia is an exothermic process (thermodynamically favored). The energetically limiting step in the overall reaction is the endergonic activation of N_2 to form diazene (HN=NH). The catalytic function of nitrogenase in the reduction of N_2 is to lower the activation energy of the reactants by stabilizing the transition state (Seefeldt et al., 2013).

Figure 3. Micrographs of *A. vinelandii* cells. (A) Scanning- and (B)-transmission-electron micrographs are from the laboratory strain designated DJ. *A. vinelandii* DJ (Setubal et al., 2009), which is a high frequency genetically transformable strain derived from *A. vinelandii* OP (Bush and Wilson, 1959), a non-gummy strain deficient in the formation of exopolysaccharides and unable to form cysts. The original *A. vinelandii* type strain, from which strain OP was derived, was isolated from Vineland, New Jersey soil samples in 1903 (Lipman, 1903). It is an obligately aerobic *gammaproteobacteria* closely related to the *Pseudomonas* (Setubal et al., 2009). Other commonly used *A. vinelandii* strains, for example, strains UW and CA, were also derived from the OP strain. Membrane invaginations that include respiratory complexes can be recognized at the cell periphery and polyhydroxybutyrate granules appear as bright spots within the transmission electron micrograph. Electron micrographs courtesy of Sandy Hancock, Virginia Tech. Color version of this figure is available online.

Figure 4 Two-dimensional gel electrophoretic profile of total proteins from diazotrophically grown *A. vinelandii*. The horizontal dimension represents separation by isoelectric focusing and the vertical dimension represents separation based on size. Notice the relative abundance of proteins representing the two Mo-dependent nitrogenase catalytic components. Fe protein is designated by an H (product of *nifH*), and the α- and β-subunits of the MoFe protein are respectively indicated as D (product of *nifD*) and K (product of *nifK*). When cultured under nitrogen fixing conditions, accumulation of nitrogenase components is abundant, comprising as much as 10% of the total protein cellular pool (Jacobs, Mitchell, and Watt, 1995; Zheng and Dos Santos, 2018).

Figure 5. Identity and genomic arrangement of *A. vinelandii* genes associated with nitrogen fixation. Individual gene cluster regions are alphabetized with their corresponding genomic locations indicated within parentheses and by the circular chromosome map. The exact chromosomal locations of all genes included in the figure, as well as the known, proposed, or predicted characteristics of their corresponding products are provided in Table S1. The PDB IDs of known or related structures of certain gene products are also included in Table S1. The basis for gene designations used in the figure is described in the text. Arrows indicate identified transcriptional units and, where indicated, color-coded dots denote transcription start sites controlled by associated trans-acting regulatory proteins shown on the right side of the bottom panel. Color version of this figure is available online.

Figure 6. Surface structure of the docked catalytic units of the Mo-dependent nitrogenase and commonly used nomenclatures. The designations Fe protein and MoFe protein reflect the

metal composition of the cofactors associated with the two catalytic partners (see **Figure 7**). The nomenclature NifH (or $NifH_2$) and NifDK (or $NifD_2K_2$) is based on the corresponding genes that respectively encode the Fe protein (*nifH*) and the MoFe protein (*nifDK*). Subscripts are sometimes used to indicate subunit organizations. Component I and Component II refer to their order of elution during ion-exchange chromatography (Bulen and LeComte, 1966). Dinitrogenase reductase and dinitrogenase is a nomenclature used to indicate that during catalysis Fe protein is a reductase that delivers electrons to the MoFe protein, which harbors the site for N_2 reduction (Emerich, Hageman, and Burris, 1981). Av1 and Av2 respectively correspond to MoFe protein (Component I) and Fe protein (Component II) and is a convenient nomenclature used to distinguish nitrogenase components from different organisms. For example, Av2 and Cp2 respectively correspond to Fe protein from *A. vinelandii* and *Clostridium pasteurianum* (Emerich, Ljones, and Burris, 1978). PDB file used to generate the figure include 1G21 (Chiu et al., 2001). Color version of this figure is available online.

Figure 7. Ribbon representations of an Fe protein and MoFe protein catalytic unit highlighting the nucleotide binding sites and associated metalloclusters. The Fe protein homodimer is shown on the left in light pink. It contains one nucleotide binding site in each subunit and a single [4Fe-4S] cluster bridged between the subunits. The α- and β-subunits of a MoFe protein heterodimeric unit is shown on the right in light brown and light green. The P-cluster designation refers to the fact that it cannot be extracted intact from the MoFe protein and is therefore obligately Protein- or "P"-bound (Zimmermann et al., 1978). FeMo-cofactor (or FeMo-co) can be extracted intact from the MoFe protein using chaotropic solvents and is named on the basis that it contains both Fe and Mo (Shah and Brill, 1981). "M-cluster" or "M-center"

are also common designations for FeMo-cofactor found in the literature (Zimmermann et al., 1978). These nomenclatures are derived from the fact that FeMo-cofactor contained in the as-isolated resting state of MoFe protein exhibits a characteristic electron paramagnetic spectroscopic signature. Metal-containing cofactor atoms are indicated as; rust (Fe), yellow (S), purple (Mo), red (O), and grey (C). PDB file used to generate the figure include 1G21 (Chiu et al., 2001). Color version of this figure is available online.

Figure 8. Examples of Mo-dependent nitrogenase catalyzed reactions. The ideal stoichiometry for N_2 reduction catalyzed by Mo-dependent nitrogenase involves the consumption of eight electrons and eight protons. Each electron transfer event requires the hydrolysis of two MgATP. Six electrons/protons are necessary for protonation of N_2 to yield two NH_3. An additional two electrons/protons are required for the N_2 activation step resulting in the obligate evolution of one H_2 for each N_2 reduced. N_2 is the only known nitrogenase substrate that requires H_2 evolution as an obligate aspect of substrate activation. In the absence of N_2 or any other substrate, electrons are used for proton reduction resulting in hydrolysis of four MgATP for each H_2 evolved. Acetylene (C_2H_2) is a non-physiological substrate that nitrogenase can reduce by two electrons to yield ethylene (C_2H_4), also requiring the hydrolysis of four MgATP.

Figure 9. Fe protein cycle. (Step 1) Reduced and MgATP-bound Fe protein docks with the MoFe protein. (Step 2) Intra- and intermolecular electron transfer events result in oxidation of the Fe protein's $[4Fe\text{-}4S]^{1+}$ cluster by one electron and reduction of the FeMo-cofactor resting state by an increment of one electron. These events are described by a proposed "deficit spending" model shown in **Figure 10**. (Step 3) MgATP is hydrolyzed. (Step 4) P_i release is

proposed to be the rate-limiting step in the cycle. (Step 5) Oxidized Fe protein dissociates from the MoFe protein. (Step 6) Fe protein is re-reduced by a flavodoxin in its fully reduced hydroquinone state or a ferredoxin by a reduced Fe-S cluster (not shown). Other redox-active species can also be utilized for reduction of the Fe protein. For example, dithionite is often used as an Fe protein reducing agent for *in vitro* assays. (Step 7) MgATP is exchanged for MgADP. MgATP-bound forms of Fe protein are indicated in pink and the MgADP bound forms are indicated in blue. Reduced species are indicated by a yellow halo. PDB files used to generate the figure include: 1G20 (Chiu et al., 2001), 2AFI (Tezcan et al., 2005), 5K9B (Segal et al., 2017), and 1FP6 (Jang, Seefeldt, and Peters, 2000). Color version of this figure is available online.

Figure 10. Deficit spending model for intra- and inter-molecular electron transfer. In this model (Step 2 in **Figure 9**), docking of the Fe protein (shown in light pink) and MoFe protein (shown in light green and light orange) triggers a single intramolecular electron transfer from P-cluster to FeMo-cofactor. The electron deficit within the P-cluster is then rapidly filled by intermolecular electron transfer from the reduced Fe protein $[4Fe\text{-}4S]^{1+}$ cluster to the one-electron oxidized P-cluster. For clarity, the size of metalloclusters is scaled up relative to their cognate proteins. In this model, MgATP hydrolysis is proposed to occur after the electron transfer events and release of Pi is the rate-limiting step. PDB file used to generate the figure include 1G20 (Chiu et al., 2001).

Figure 11. MoFe protein cycle. (A) The resting state of the enzyme is indicated as E_0. Each turn of the Fe protein cycle results in the progressive accumulation of one electron/proton within FeMo-cofactor, or a FeMo-cofactor-bound semi-reduced N_2 intermediate, indicated as $E_1(H)$,

$E_2(2H)$, $E_3(3H)$ *etc*. The four electrons accumulated at the $E_4(4H)$ state are stored as two hydrides bridged between Fe sites located within FeMo-cofactor. (B) Once the enzyme reaches the $E_4(4H)$ state, N_2 can be activated by reductive elimination resulting in an Fe-bound diazene or hydrazido species and evolution of one H_2. The reductive elimination reaction can be reversed by oxidative addition of H_2 and displacement of N_2. None of the steps beyond the $E_4(N_2H_2)$ stage are known to be reversible. The nature of the proposed cofactor-bound semi-reduced intermediate species (end on, side on, bridging *etc.*) is not known. Although it is not clearly established whether steps following initial N_2 binding at $E_4(H4)$ proceed through distal or alternating protonation of N atoms the sequence of NH_3 release shown in (A) represents an alternating mechanism. In the absence of N_2, or other substrates, H_2 is evolved by protonolysis after two or more electrons have accumulated, thereby reversing the cycle by two steps. Similarly, once the enzyme has accumulated two or more electrons the artificial substrate acetylene (C_2H_2) can be reduced via hydride insertion to yield ethylene (C_2H_4), also reversing the cycle by two steps. Substrate activation by reductive elimination could be unique to N_2 among all the known nitrogenase substrates. Color version of this figure is available online.

Figure 12. Mo-dependent nitrogenase active site cofactor. (A) FeMo-cofactor contains the 7Fe-Mo-9S-C framework with homocitrate attached to the apical Mo-atom. (B) FeMo-cofactor is coordinated by two apical protein ligands α-Cys^{275} and α-His^{442}. (C) View of FeMo-cofactor is shown down the long axis. Homocitrate and the amino acid ligands are removed for clarity and several amino acids (α-Gln^{191}, α-His^{195}, and α-Arg^{359}) located within immediate proximity to the the FeMo-cofactor are shown. This view also highlights the three symmetrical Fe/S faces of FeMo-cofactor, one of which includes irons 2-3-6-7, which is approached by α-Val^{70}.

Substitution of α-Val^{70} by an Ala or Ile, respectively increases or decreases the size of short-chain alkynes (for example, acetylene, propyne, butyne) that can be reduced by the altered proteins (Dos Santos et al., 2007). (D & E) Crystallographically determined models of FeMo-cofactor contained within MoFe protein inhibited by either low or high concentrations of the inhibitor CO. For (D) a single CO is bridged between Fe2 and Fe6 and for (E) one CO is bridged between Fe2 and Fe6 and an addition CO is bound end-on to Fe6. For both structures, the S bridging Fe2 and E6 has been displaced. In aggregate structural features of FeMo-cofactor contained in CO-inhibited enzyme, catalytic features associated with amino acid substitution studies, as well as biophysical analyses suggest a key role for Fe2 and Fe6 in substrate activation. PDB file used to generate the figure include 1M1N (Einsle et al., 2002). Color-coding of atoms is the same as in **Figure 7**. Color version of this figure is available online.

Figure 13. Schematic representation of pathways for the assembly of simple [Fe-S] clusters. (A) Pathway for assembly of [Fe-S] clusters for the activation of general *A. vinelandii* cellular proteins that contain [Fe-S] clusters. CysE is a serine acetyltransferase that constitutes the rate-limiting step in L-cysteine. IscS is a cysteine desulfurase, that delivers S for simple [Fe-S] cluster formation to IscU which provides a scaffold for [Fe-S] cluster formation. The physiological source of Fe for [Fe-S] cluster formation on the IscU scaffold is not known. Electrons required for the release of a NifS-bound persulfide for S delivery to the IscU scaffold are provided by a [2Fe-2S] cluster containing ferredoxin. After their formation on the IscU scaffold, [Fe-S] species are transferred to a variety of intermediate carrier proteins such, as NfuA, and IscA, involved in the delivery of [Fe-S] clusters to target proteins. Molecular chaperones, not shown in the figure, are involved in the delivery of [Fe-S] clusters from the IscU scaffold to intermediate carriers. (B)

The parallel *A. vinelandii* nitrogen fixation specific pathway for the formation of [Fe-S] cluster building blocks used for the maturation of nitrogenase components. Parallel functions are color-coded. Note that based on primary structure comparisons and an AlphaFold (Jumper et al., 2021; Varadi et al., 2022) structural model NifU is a modular protein for which the scaffold, electron transfer, and intermediate carrier functions are fused within a single polypeptide. There are no chaperones known to participate in nitrogen fixation specific assembly of [Fe-S] cluster building blocks. (C) Summary of parallel features shown in (A) and (B). PDB files used to generate the figure: 1T3D (Pye et al., 2004), 3LVM (Shi et al., 2010), 2L4X (Kim et al., 2012), 1H7H (Kakuta et al., 2001), 2JNV (Saio et al., 2007), and 1S98 (Cupp-Vickery et al., 2004). Color version of this figure is available online.

Figure 14. Activation of sulfur by NifS for [Fe-S] cluster assembly. Sulfur is mobilized by NifS for [Fe-S] cluster assembly using pyridoxal phosphate (PLP) chemistry. (1) Substrate L-cysteine forms an adduct with PLP involving the displacement of the resting state NifS Lys^{202} residue; (2) PLP-bound L-cysteine undergoes nucleophilic attack by the active site NifS Cys^{325} residue to form a NifS bound persulfide species; (3) the NifS bound persulfide is transferred to the NifU scaffold in a process involving interaction between NifU and NifS, and NifS is returned to the resting state. Color version of this figure is available online.

Figure 15. Schematic representation of a model for MoFe protein P-cluster formation. The P-cluster precursor is proposed to be comprised of two proximal [4Fe-4S] clusters, one contained in the α-subunit, and one contained within the β-subunit, with each respectively coordinated by three cysteines provided by each subunit. [4Fe-4S] clusters within proteins typically have four

coordinating ligands. Whether or not there is a fourth coordinating ligand for either of the P-cluster precursor [4Fe-4S] subclusters is not known. The subclusters are fused by a proposed reductive coupling process that requires a source of reducing equivalents, MgATP, and the Fe protein (NifH), resulting in the elimination of a single S atom. P-cluster maturation is assisted by three accessory proteins, NafH, NifW, and NifZ that sequentially and differentially interact with the immature MoFe protein in the sequence shown in the figure. NafH, NifW, and NifZ optimize P-cluster formation but are not required. There is no evidence that these accessory proteins are involved in P-cluster formation for either the V-dependent or Fe-only nitrogenase. Color-coding of atoms is the same as indicated in **Figure 7**. Color version of this figure is available online.

Figure 16. Assembly nodes involved in formation of FeMo-cofactor. The first node is provided by NifU, which provides a scaffold necessary for the formation of [4Fe-4S] cluster building blocks. The second node is provided by NifB, which provides a scaffold for the fusion of two [4Fe-4S] subclusters and incorporation of an interstitial carbide provide by S-adenosyl methionine to form an 8Fe-9S-C precursor to FeMo-cofactor designated NifB-co (also called L-cluster by some investigators). A working model for NifB-co formation is described in **Figure 17**. The third node is provided by the NifEN complex, which provides a scaffold that enables the replacement of an apical Fe atom by Mo and attachment of the organic constituent R-homocitrate to the Mo atom. Fe protein (NifH), MgATP, and electrons are required for the terminal assembly of FeMo-cofactor within the NifEN scaffold. NifV catalyzes R-homocitrate formation and a [3Fe-Mo-4S] cluster bound to NifQ is proposed to be the physiological source of Mo. Details of Mo insertion, and R-homocitrate attachment, at the atomic level are not known. Color-coding of atoms is the same as indicated in **Figure 7**. Color version of this figure is available online.

Figure 17. Plausible NifB-cofactor biosynthetic scheme that occurs on the NifB scaffold. A) Substrate K1 and K2 sub-clusters are reductively coupled to generate an [8Fe-8S] K-cluster. K-cluster is a nomenclature used to indicate that it is a precursor to the L-cluster, which is an alternative nomenclature used to designate NifB-co. The next step involves a separate catalytic [4Fe-4S] cluster, designated as the RS-cluster, which promotes the transfer of a methyl group from the RS-cluster-bound S-Adenosyl Methionine (SAM) to the K-cluster μ2-sulfide ion. S-Adenosyl Homocysteine (SAH) formed in this reaction is then exchanged by a second SAM molecule, which is reductively cleaved to produce the 5′-deoxyadenosyl radical. Formation of this radical leads to abstraction of one H atom from the methyl group, facilitating subsequent deprotonation events to generate carbide. These steps are followed by exchange of carbide with the μ6-sulfide ion, and incorporation of an additional μ2-sulfide ion to complete NifB-co synthesis. B) SAM and SAH structures highlighting the methyl group position in SAM (green shade). C) Relative positions of the catalytic RS-cluster and the K-cluster reaction intermediate on the reconstituted, dithionite-reduced structure of *Methanotermobacter thermautotrophicus* NifB (PDB 7B17, (Jenner et al., 2021). Analysis of crystallographic data shows the arrangement of the unique Fe site of the RS-cluster, indicated by a red arrow, and the μ2-sulfide ion of the K-cluster, indicated by a yellow arrow, before methyl transfer. This structure lacks the SAM molecule that would bind to the unique Fe site. Color-coding of atoms is the same as indicated in **Figure 7**. Color version of this figure is available online.

Figure 18. Common structural features between the MoFe protein and the NifEN scaffold. (A) Ribbons structure of an αβ- half of the MoFe protein tetramer poised for interaction with the

Fe protein. The location of the P-cluster and FeMo-cofactor have been determined crystallographically. The scheme shown is the same as presented in **Figure 7**. (B) Ribbons structure of an αβ-half of the NifEN tetramer also poised for interaction with the Fe protein. The location of the [4Fe-4S] cluster bridged between the NifE- and NifN-subunits subunits was determined crystallographically but the location of NifB-co, highlighted in yellow, was modeled into a plausible processing site. The presence of NifB-co at a possible NifB-co binding site located at the NifE surface near the docking surface is not shown. (C) Expanded view of the relative positions of the P-cluster and FeMo-cofactor within an αβ-unit of the MoFe protein shown in (A). (D) Expanded view of the relative positions of the [4Fe-4S] cluster and NifB-co located at a possible processing site within a NifEN unit. PDB files used to generate the figure include 1G21 (Chiu et al., 2001) and 3PDI (Kaiser et al., 2011). Color-coding of atoms is the same as indicated in **Figure 7**. Color version of this figure is available online.

Figure 19. Common and differentiating features among the Mo-dependent, V-dependent, and Fe-only nitrogenases. (A) Catalytic components of the Mo-dependent nitrogenase poised for interaction and its associated FeMo-cofactor with iron positions Fe2 and Fe6 indicated. (B) Catalytic components of the V-dependent nitrogenase poised for interaction and its associated FeV-cofactor. (C) Catalytic components of the Fe-only nitrogenase poised for interaction and its associated FeFe-cofactor (Trncik et al., 2022). Differentiating features to note are the presence of δ-subunits (VnfG and AnfG, shown in blue) within the VnfDGK (VFe protein) and AnfDGK (FeFe protein) structures but not the NifDK (MoFe protein) structure. Also, the corresponding cofactors have Mo, V, or Fe as the apical metal that is attached to homocitrate. The FeV-cofactor has one of the bridging sulfides present in FeMo-cofactor and FeFe-cofactor replaced by a

carbonate. PDB files used to generate the figure include 1G21 (Chiu et al., 2001), 5N6Y (Sippel and Einsle, 2017) and 6Q93 (Rohde et al., 2018). Color-coding of atoms is the same as indicated in **Figure 7**. Vanadium is indicated as light purple. Color version of this figure is available online.

Figure 20. Comparison of P-clusters and active site cofactors associated with the MoFe protein, VFe protein and FeFe protein highlighting similarities in the polypeptide environments. References to PDB ID files used to generate the figure can be found in Table S1. Color-coding of atoms is the same as indicated in **Figure 7**. Vanadium is indicated in light purple. The P-clusters of all three isoenzymes share the same architecture and are shown in the all-ferrous P^N state. Upon one-electron reduction, a nearby, conserved serine becomes a new ligand. The three active-site cofactors are topologically equivalent, but in the FeV cofactor of vanadium nitrogenase one bridging sulfide is replaced by carbonate. Color version of this figure is available online.

Figure 21. Comparison of pathways for the assembly of FeMo-cofactor, FeFe-cofactor, and FeV-cofactor. NifB-co is a common precursor and homocitrate, electrons, and MgATP are necessary for the formation of all three cofactors. Completion of FeMo-cofactor assembly occurs on the NifEN scaffold, which involves the replacement of an apical Fe by Mo and attachment of homocitrate in a process requiring *nifH* encoded Fe protein (NifH). FeV-cofactor formation follows a parallel path utilizing a VnfEN scaffold, analogous to the NifEN scaffold, with the proposed involvement of the *vnfH* encoded Fe protein (VnfH) for the insertion of V and attachment of homocitrate. Insertion of the proposed bridging carbonate constituent within FeV-

cofactor is not known. Completion of FeFe-cofactor formation does not involve an intermediate assembly scaffold analogous to NifEN and VnfEN but is likely to require the *anfH* encoded Fe protein (AnfH) for homocitrate attachment. Color-coding of atoms is the same as indicated in **Figure 7**. Vanadium is indicated by light purple. Color version of this figure is available online.

Figure 22. A common structural motif is predicted for members of the NifX family of proposed metallocluster carrier proteins. (A) Comparison of possible NifX-like metallocluster binding domains present within the NifX family of proteins. Arrows indicate the location of the N-terminal and C-terminal residue of the corresponding NifX-like domains. A structure for the NifX-like domain within NafY was determined by crystallography (Dyer et al., 2003), and structural predictions for the other NifX-like domains were obtained using AlphaFold software (Jumper et al., 2021; Varadi et al., 2022). B) Structure of the tethered N-terminal and C-terminal domains of NafY determined by NMR (Hernandez et al., 2011; Phillips et al., 2021). The relative orientation of the structural domains was obtained by superimposing the AlphaFold model of the entire NafY sequence with the reported structural domains. Color version of this figure is available online.

Figure 23. Overview of *A. vinelandii* NifL and NifA domain organization and regulatory models dependent on different environmental signals. In (A) and (B) schematic representations of NifL and NifA domain organizations, respectively. Domains were drawn to scale based on boundaries delimited by InterPro (Blum et al., 2021), except for the H domain in NifL (A), which was manually annotated based on (Little et al., 2007). C) Regulatory model for the NifL-NifA system dependent on redox changes triggered by fluctuation in the oxygen levels.

Under excess oxygen conditions (C, left), the FAD cofactor in the NifL PAS1 domain is oxidized, allowing NifL to adopt an inhibitory conformation capable of forming a binary complex to inactivate NifA. Under limiting oxygen conditions (C, right), the FAD is fully protonated to its reduced form ($FADH_2$). Reduction of the FAD cofactor triggers conformational changes in NifL prompting changes in its quaternary structure that prevents interaction with NifA, releasing its activity. In the reduced state, NifL can still inhibit NifA in response to the levels of nitrogen and carbon. (D) Regulatory model for the NifL-NifA system dependent on nitrogen and carbon signaling. Under nitrogen excess conditions (D, upper left N^{High}), non-uridylylated GlnK forms a ternary GlnK-NifL-NifA complex that inhibits NifA activity. Upon a shift to low nitrogen (D, upper right N^{Low}) signaled by a decrease in the level of glutamine (Gln), GlnK is uridylylated (GlnK-UMP). Under optimal carbon supply, a reduction in Gln is accompanied by an increase in 2-oxoglutarate levels (2-OG). 2-OG binds the GAF domain of NifA, allowing complete dissociation of the ternary complex to release NifA activity. Under nitrogen excess conditions, the GlnK-NifL-NifA ternary complex is stable even if the GAF domain in NifA is saturated with 2-OG (D, bottom left). Under nitrogen limitation, if 2-OG is limiting (D, bottom right), an inhibitory binary complex between NifL and NifA can still be formed. Color version of this figure is available online.

Figure 24. Model for integration of nitrogen metabolism in *A. vinelandii*. The main enzymatic reactions coupling nitrogen fixation (catalyzed by the nitrogenase complex) to its assimilation (catalyzed by the GS-GOGAT pathway) are represented at the top of the figure. Glutamine (Gln), an intermediate metabolite of the GS-GOGAT coupled reaction and a metabolic signal of nitrogen sufficiency, stimulates the uridylyl-removing (UR) activity of GlnD,

yielding non-modified (or non-uridylylated) GlnK. Non-uridylylated GlnK can form a ternary complex, GlnK-NifL-NifA, to inhibit NifA activity (top right). Non-uridylylated GlnK also stimulates the adenylyltransferase activity (ATase) of GlnE to inactivate the glutamine synthetase (GS) via adenylylation, to form GS-AMP (left). Upon reduction in the fixed nitrogen levels, the uridylyltransferase activity (UTase) of GlnD is stimulated, yielding modified/uridylylated GlnK (GlnK-UMP), which is no longer competent to stimulate NifL inhibition of NifA, provided that sufficient 2-oxoglutarate (2-OG) is available. GlnK-UMP also stimulates the adenylyl removal (AR) activity of GlnE, activating the GS enzyme (top left). In its active form, NifA triggers transcriptional activation at σ^{54} -dependent *nif* promoters, resulting in expression of genes required for Mo nitrogenase synthesis and activity (bottom). For simplicity only the structural genes are shown here. For further details, see main text and references therein. Color version of this figure is available online.

Figure 25. Domain structures of σ^{54}-dependent bacterial enhancer binding proteins that regulate expression of alternative nitrogenases, showing homologies between VnfA paralogs. Boundaries of the N-terminal region, regulatory GAF domain, the catalytic AAA+ σ^{54} -RNA polymerase interaction domain and the C-terminal helix-turn-helix motif (H-T-H) in the DNA binding domain are indicated at the top of the figure. Domain boundaries were assigned by InterPro (Blum et al., 2021). The percentage identity between individual domains is shown and conserved cysteine residues located at the N-terminal region of each protein are highlighted in yellow. N-terminal and C-terminal regions of each protein are expanded below the domain diagrams to show the cysteine residue conservation and homology between the DNA recognition helices (C-terminal helix of the H-T-H motif), respectively. Residue numbers are indicated at the

right of each sequence. Protein sequences were derived from the original genome annotation reported in Setubal et al 2009. More recent annotations in the NCBI database result in truncation of the N-terminus of VnfA2 and consequent removal of one of the conserved cysteine residues. Color version of this figure is available online.

Figure 26. Model for regulation of the alternative nitrogenases in response to metal availability. Under Mo replete conditions, ModE1 and ModE2 repress transcription of the *vnfUA1* and *anfA* operons, preventing expression of VnfA1 and AnfA, and, consequently, expression of the V-dependent and Fe-only nitrogenases. In the absence of Mo and presence of V, VnfA1 activates expression of the *vnf* structural and biosynthesis genes, enabling expression of the V-dependent nitrogenase. In the presence of V, (but not in Fe-only conditions), VnfA1 represses transcription of *nifHDK,* the structural genes for the Mo-dependent nitrogenase and also *anfA,* thus preventing expression of Fe-only nitrogenase. In the absence of Mo and V, AnfA is expressed and activated by NifH, enabling the expression of Fe-only nitrogenase. VnfA1 also activates expression of the *vnfZ-vnfA3* operon. In Fe-only conditions, VnfZ forms a complex with VnfA3 permitting co-activation of the *anfH* promoter by VnfA1 and VnfA3. Other genes co-activated by VnfA1 and VnfA3 are not shown in this diagram. Positive gene activation (green arrows) is indicated by +V +Fe, when this occurs either in V excess or V-limiting conditions, and is indicated as +Fe, when activation only occurs in the absence of V. Negative gene regulation by VnfA1 (red arrows) only occurs in the presence of V and is indicated by +V. Colored dots in promoter regions indicate binding sites for regulatory proteins as indicated in **Figure 5**. Color version of this figure is available online.

Figure 27. Schematic representation of the electron transport chains in *A. vinelandii*. The electron transport system in *A. vinelandii* can use two pathways to achieve O_2 reduction. The pathway coupled to ATP formation (fully coupled branch) begins with NDHI (complex I) or SDH (succinate dehydrogenase, complex II) leading to formation of ubiquinol (QH_2) from oxidation of NADH and succinate, respectively. QH_2 is subsequently oxidized by Cyt bc_1 (complex III). Reduced cytochrome *c* (Cyt *c*) then drives the reduction of oxygen to water by the terminal oxidase, Cyt *o* (complex IV). The partially coupled branch, also known as the respiratory protection pathway, consists of an uncoupled type II NADH dehydrogenase (NDHII) and terminal oxidase cytochrome *bd* (Cyd *bd1* also known as CydAB I). Each branch translocates a different number of protons per electron. The uncoupled NDHII/CydAB I branch (highlighted in orange) promotes translocation of $4H^+/O_2$ reduced, whereas the coupled NDHI/Cyt bc_1/Cyt *o* branch (components illustrated in blue) generates $20H^+/O_2$ reduced. Low-potential reducing equivalents required for nitrogen reductions are provided through Fix and Rnf1 via the reduction of ferredoxin (Fd) and flavodoxin (Fld) from NADH (highlighted in green). A proton gradient generated through these complexes drives the synthesis of ATP by ATP-synthase (indicated in purple). PDB files used to generate the figure include 5NA1 (Sousa et al., 2017), 4HEA (Baradaran et al., 2013), 1NEK (Yankovskaya et al., 2003), 1ZRT (Berry et al., 2004), 1EHK (Soulimane et al., 2000), 1C52 (Than et al., 1997), 6OQW (Sobti et al., 2020), 4P6V (Steuber et al., 2014), and 7KOE (Feng et al., 2021). For a more detailed description of Rnf1 and Fix, see the legend to **Figure 28**. Color version of this figure is available online.

Figure 28. Schematic representations of Rnf1 and Fix complexes. Reduction of ferredoxin or flavodoxin (Fd/Fld) in *A. vinelandii* is catalyzed by two different electron complexes called Rnf1

and Fix. Both complexes oxidize NADH and reduce Fd/Fld through distinct mechanisms. Rnf couples the endergonic electron transfer from NADH to Fd/Fld to the exergonic transport of ions/protons with the proton motive force. Rnf1 complex reduces 2 Fd/Fld per NADH. Fix complex overcomes the energy barrier of Fd/Fld reduction by using flavin-based electron bifurcation, which couples the exergonic reduction of quinone with the endergonic reduction of Fd/Fld. Fix protein complex oxidizes two NADH to NAD^+ while reducing one quinone to quinol and two Fd/Fld. RnfB was modeled using Alphafold, and the assembled Rnf1 was sketched following the reported organization of the Rnf system (Hreha et al., 2015). PDB files used to generate the figure include 4P6V (Steuber et al., 2014), and 7KOE (Feng et al., 2021). Color version of this figure is available online.

Nitrogen Fixation

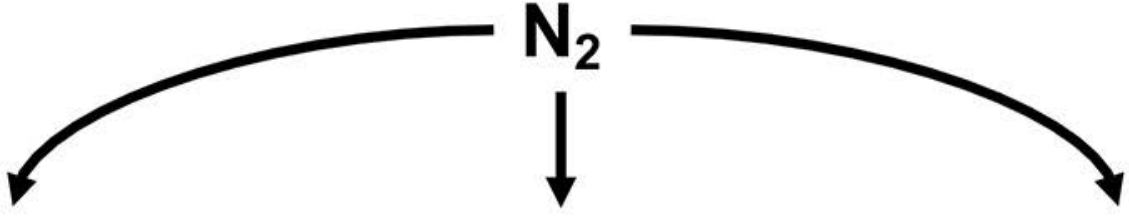

NH_3

Industrial

~65%

Haber-Bosch process

- 300–550 °C
- 150–250 atm
- Fe catalyst

NH_3

Lightning

~3%

Geochemical

NH_3

Diazotrophy

~32%

Terrestrial biological N_2 fixation

- Ambient Temperature
- Ambient Pressure
- Nitrogenase

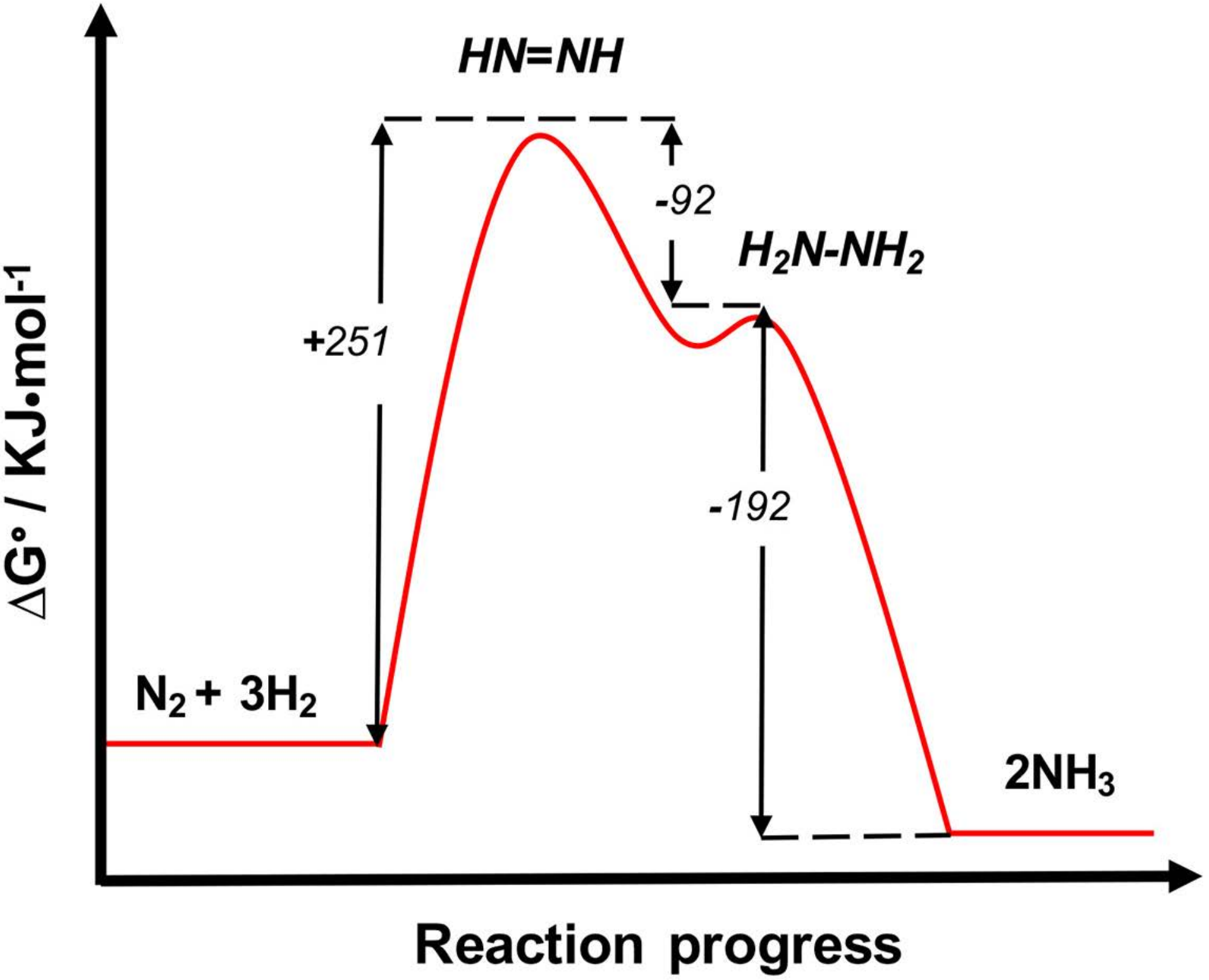
HN=NH
-92
H2N-NH2
+251
-192
N2 + 3H2
2NH3
ΔG° / KJ•mol-1
Reaction progress

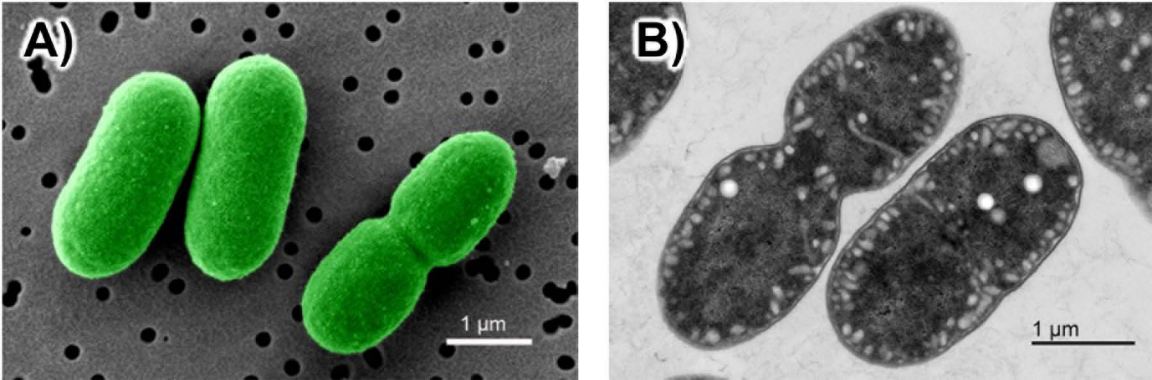
A)
1 µm
B)
1 µm

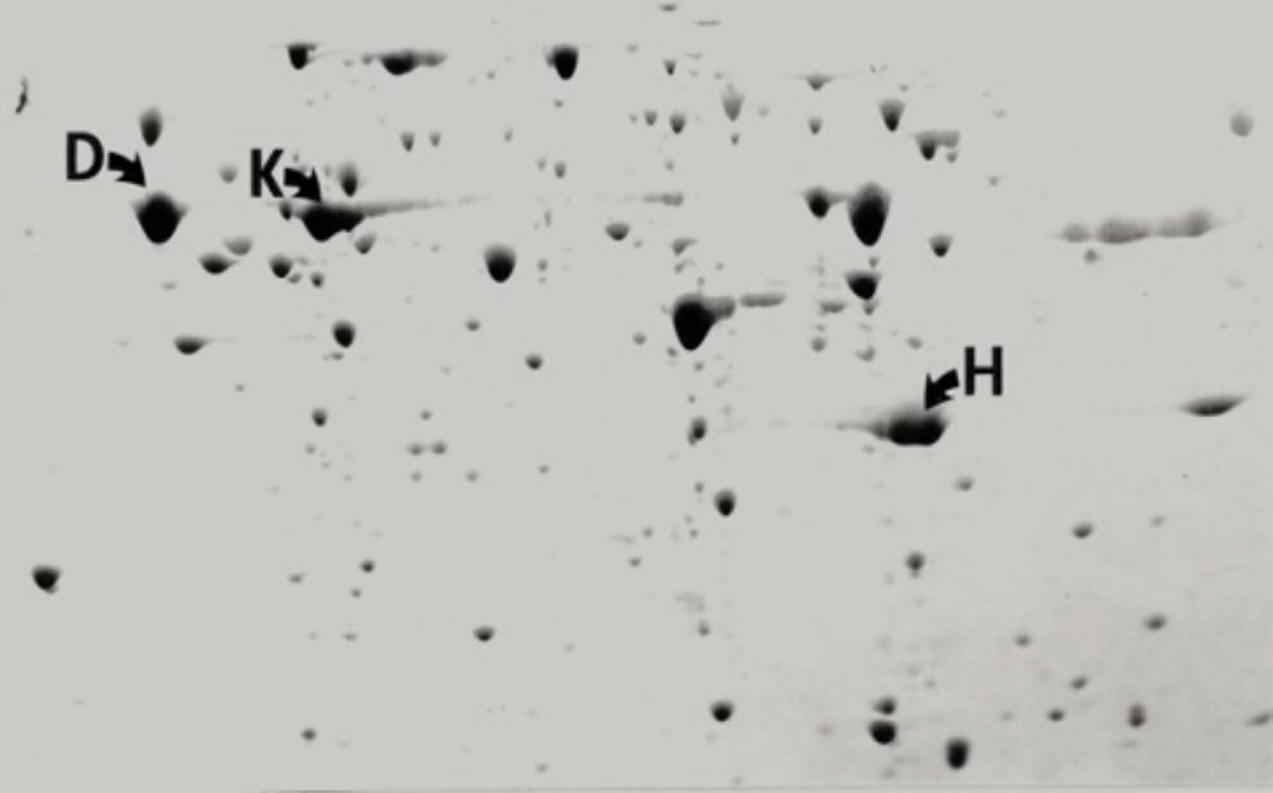
D
K
H

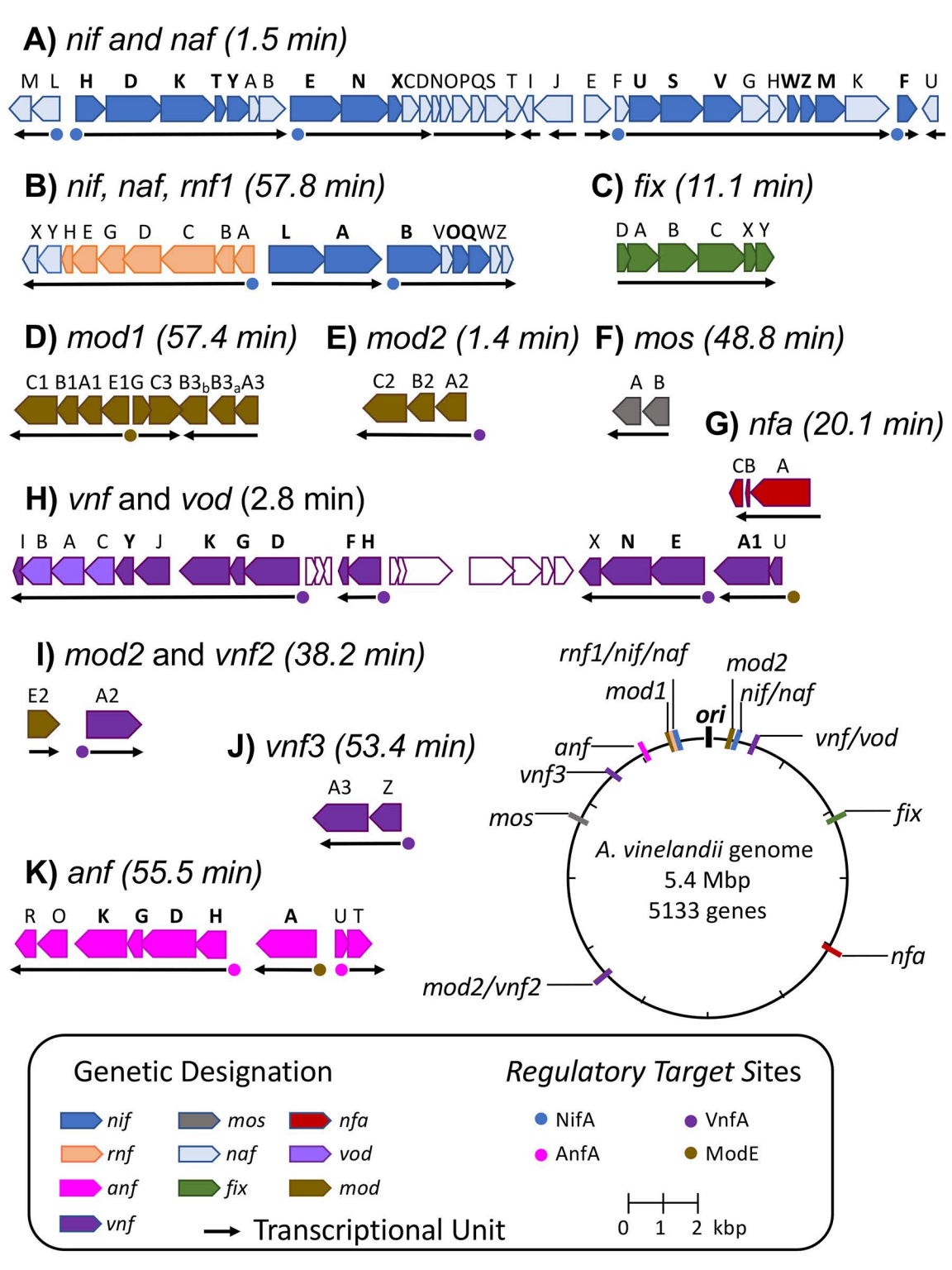
A) nif and naf (1.5 min)
M L H D K TY A B E N XCDNOPQS T I J E F U S V G HWZ M K F U
B) nif, naf, rnf1 (57.8 min)
X Y H E G D C B A L A B VOQWZ
C) fix (11.1 min)
D A B C X Y
D) mod1 (57.4 min)
C1 B1A1 E1G C3 B3b B3a A3
E) mod2 (1.4 min)
C2 B2 A2
F) mos (48.8 min)
A B
G) nfa (20.1 min)
CB A
H) vnf and vod (2.8 min)
I B A C Y J K G D F H X N E A1 U
I) mod2 and vnf2 (38.2 min)
E2 A2
J) vnf3 (53.4 min)
A3 Z
K) anf (55.5 min)
R O K G D H A U T
rnf1/nif/naf
mod2
mod1
nif/naf
ori
anf
vnf/vod
vnf3
mos
fix
A. vinelandii genome
5.4 Mbp
5133 genes
nfa
mod2/vnf2
Genetic Designation
nif
mos
nfa
rnf
naf
vod
anf
fix
mod
vnf
Transcriptional Unit
Regulatory Target Sites
NifA
VnfA
AnfA
ModE
0 1 2 kbp

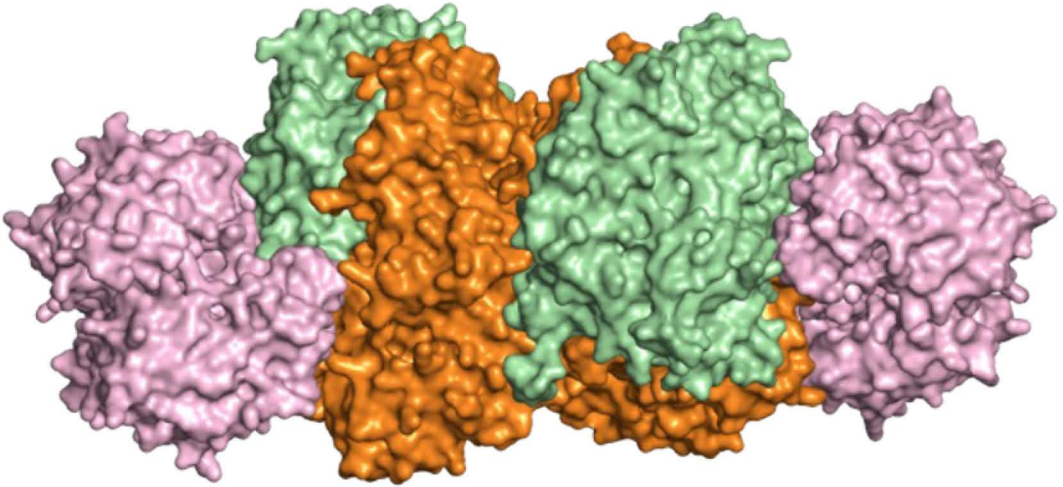

Fe protein (γ_2)
NifH ($NifH_2$)
Component II
Dinitrogenase Reductase
Av_2

MoFe protein ($\alpha_2\beta_2$)
NifDK ($NifD_2K_2$)
Component I
Dinitrogenase
Av_1

Fe protein (γ_2)
NifH ($NifH_2$)
Component II
Dinitrogenase Reductase
Av_2

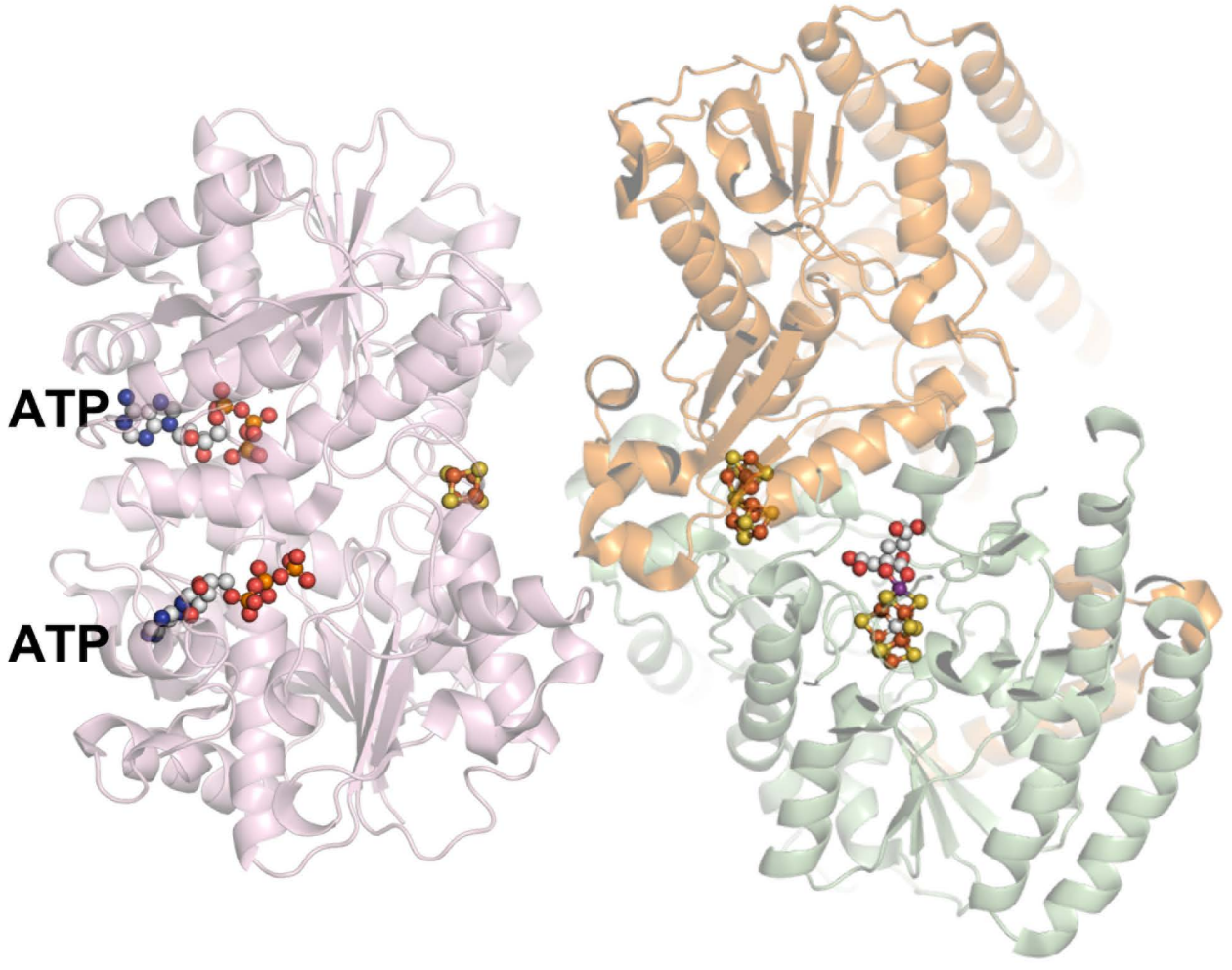

[4Fe-4S]

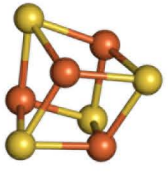

4 Iron-4 Sulfur cluster

[8Fe-7S]

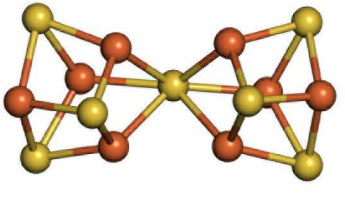

P-cluster

[7Fe-Mo-9S-C]-Homocitrate

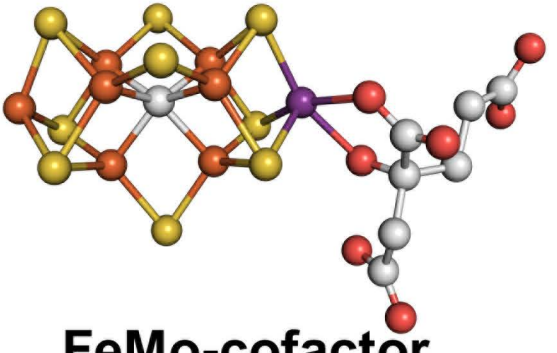

FeMo-cofactor

$$N_2 + 8H^+ + 8e^- + 16MgATP \rightarrow 2NH_3 + H_2 + 16MgADP + 16P_i$$

$$2H^+ + 2e^- + 4MgATP \rightarrow H_2 + 4MgADP + 4P_i$$

$$C_2H_2 + 2H^+ + 2e^- + 4MgATP \rightarrow C_2H_4 + 4MgADP + 4P_i$$

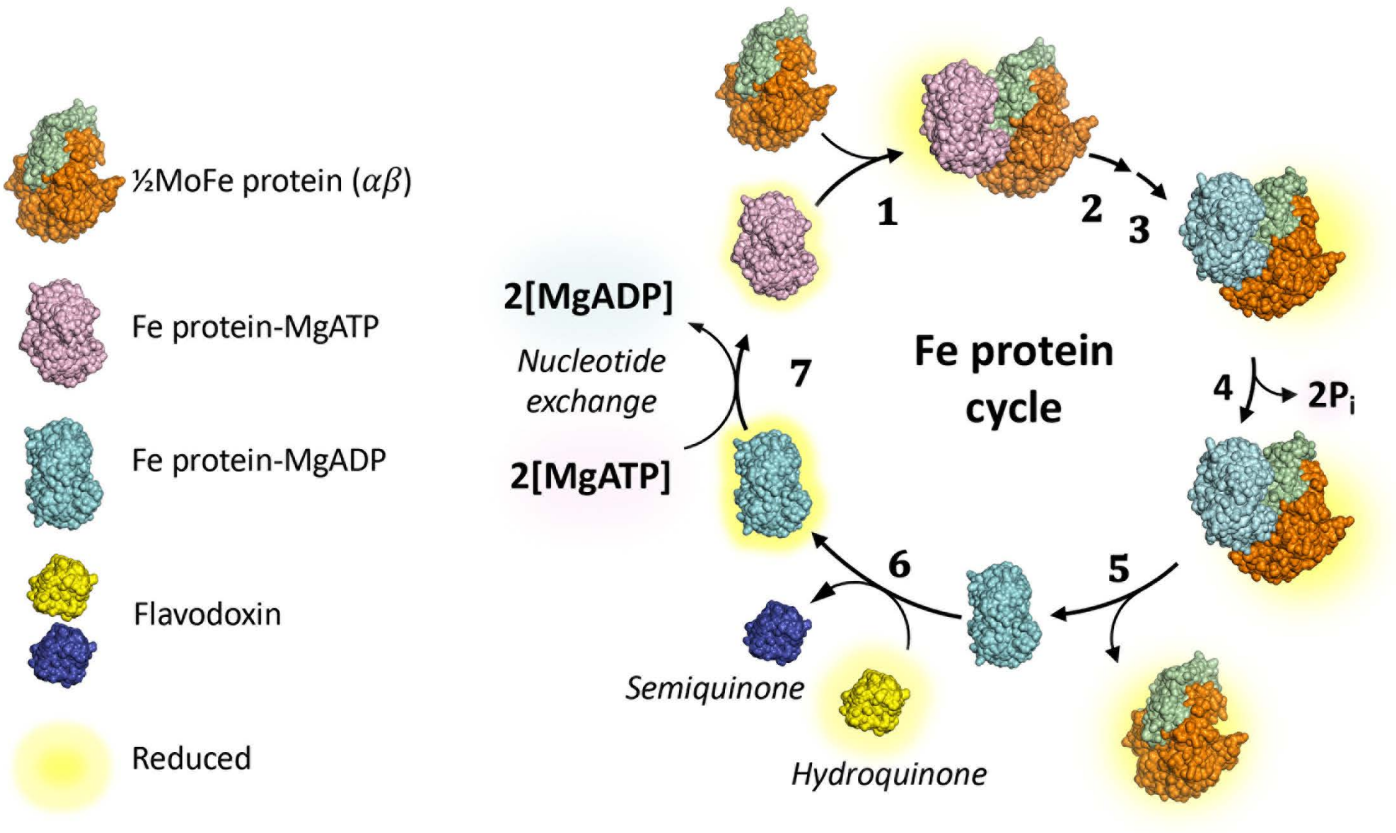
½MoFe protein (αβ)
Fe protein-MgATP
Fe protein-MgADP
Flavodoxin
Reduced
1
2
3
4
2Pi
5
6
7
2[MgADP]
Nucleotide exchange
2[MgATP]
Fe protein cycle
Semiquinone
Hydroquinone

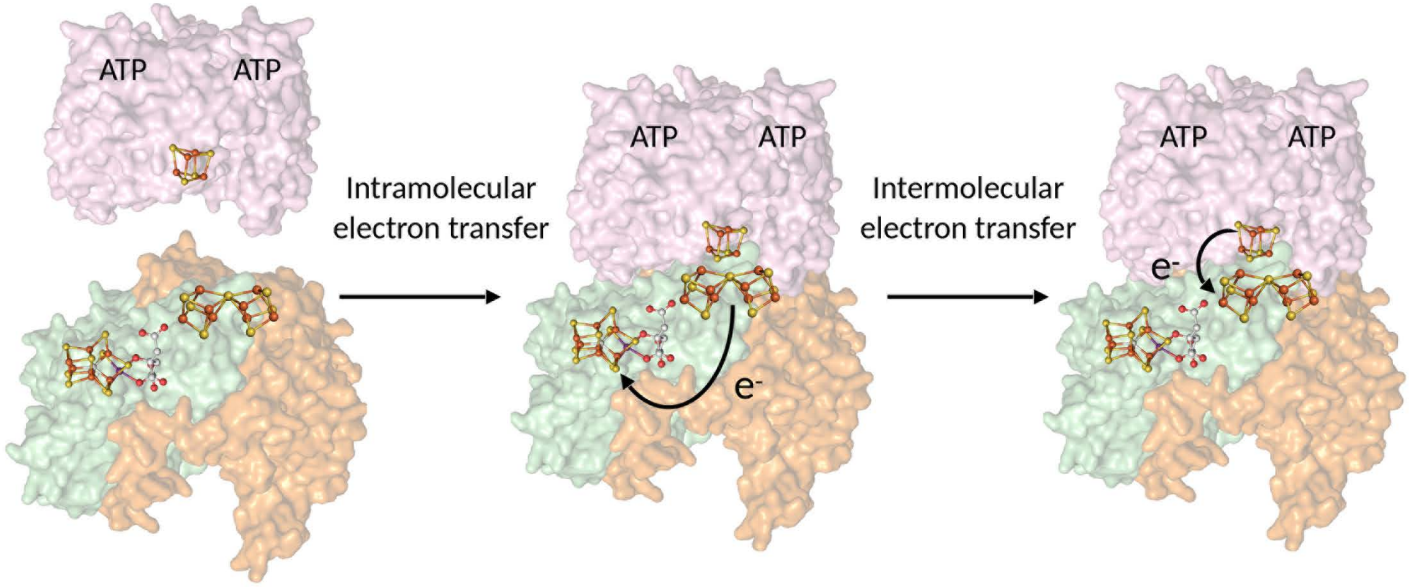
ATP
ATP
Intramolecular
electron transfer
ATP
ATP
e-
Intermolecular
electron transfer
ATP
ATP
e-

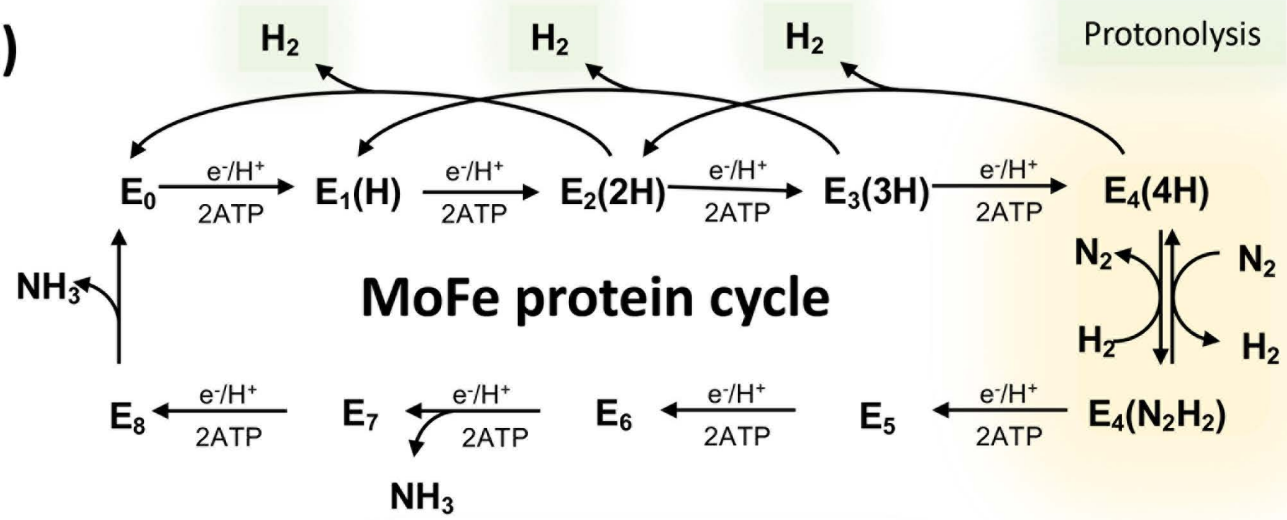
A)
H2
H2
H2
Protonolysis
E0
e-/H+
2ATP
E1(H)
e-/H+
2ATP
E2(2H)
e-/H+
2ATP
E3(3H)
e-/H+
2ATP
E4(4H)
NH3
MoFe protein cycle
N2
N2
H2
H2
E8
e-/H+
2ATP
E7
e-/H+
2ATP
E6
e-/H+
2ATP
E5
e-/H+
2ATP
E4(N2H2)
NH3

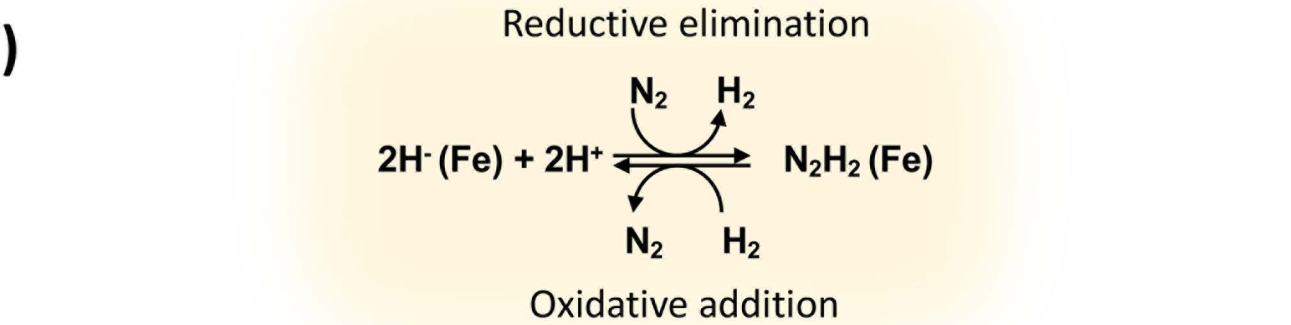
B)
Reductive elimination
N2
H2
2H- (Fe) + 2H+
N2H2 (Fe)
N2
H2
Oxidative addition

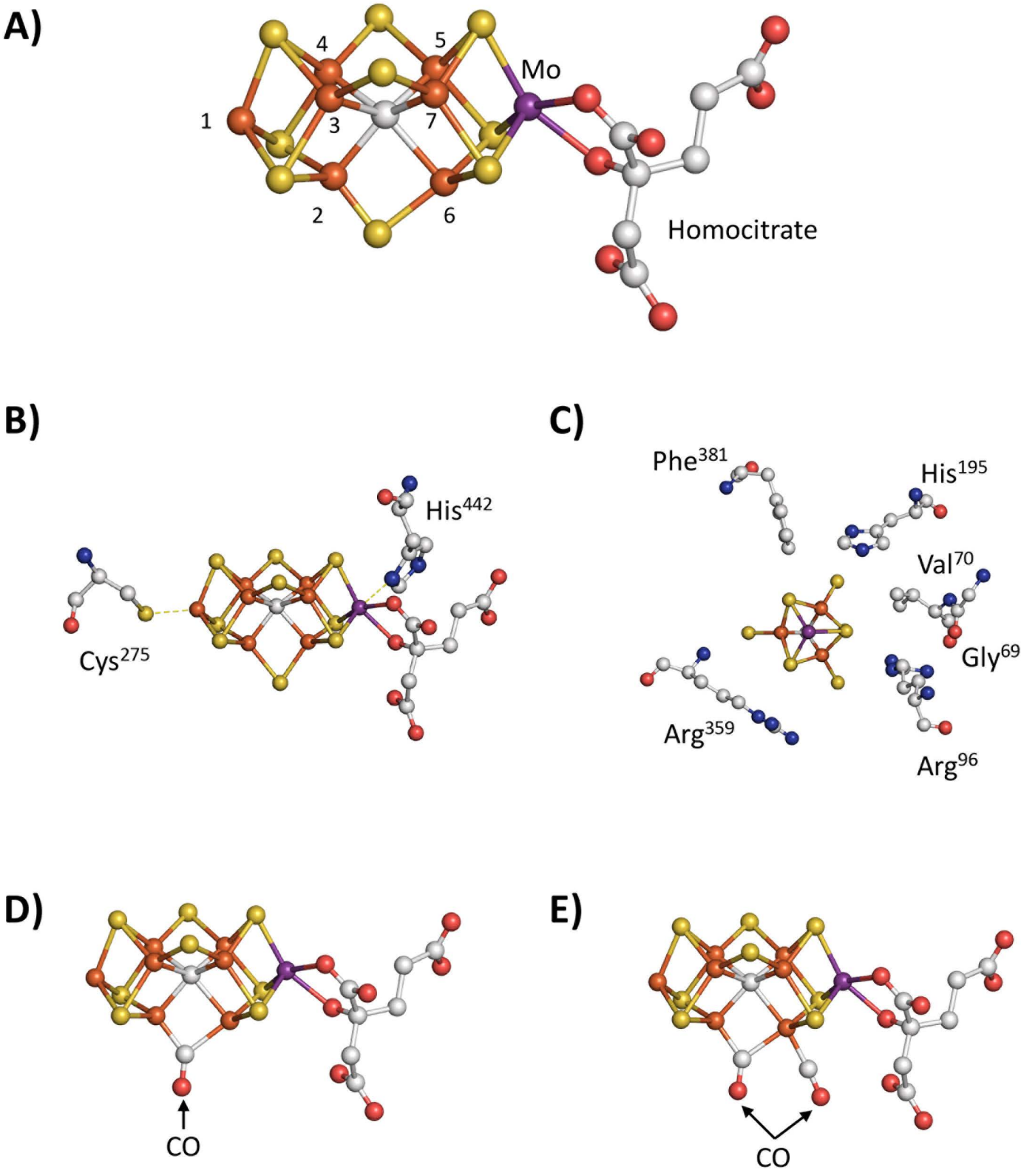
A)
4
5
Mo
1
3
7
2
6
Homocitrate
B)
His442
Cys275
C)
Phe381
His195
Val70
Gly69
Arg359
Arg96
D)
CO
E)
CO

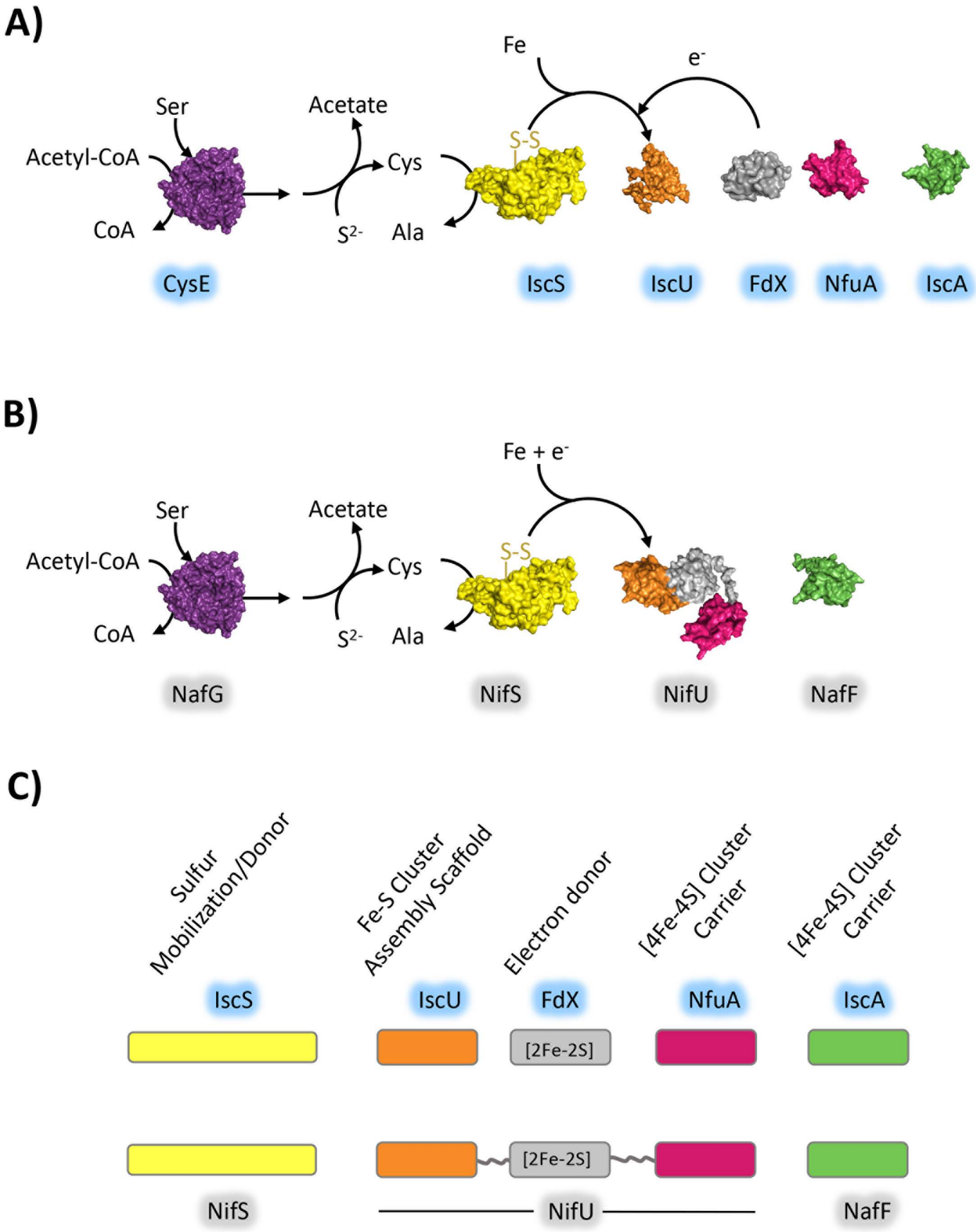
A)
Ser
Acetyl-CoA
CoA
CysE
Acetate
Cys
S2-
Ala
Fe
e-
S-S
IscS
IscU
FdX
NfuA
IscA
B)
Ser
Acetyl-CoA
CoA
NafG
Acetate
Cys
S2-
Ala
Fe + e-
S-S
NifS
NifU
NafF
C)
Sulfur Mobilization/Donor
Fe-S Cluster Assembly Scaffold
Electron donor
[4Fe-4S] Cluster Carrier
[4Fe-4S] Cluster Carrier
IscS
IscU
FdX
NfuA
IscA
[2Fe-2S]
[2Fe-2S]
NifS
NifU
NafF

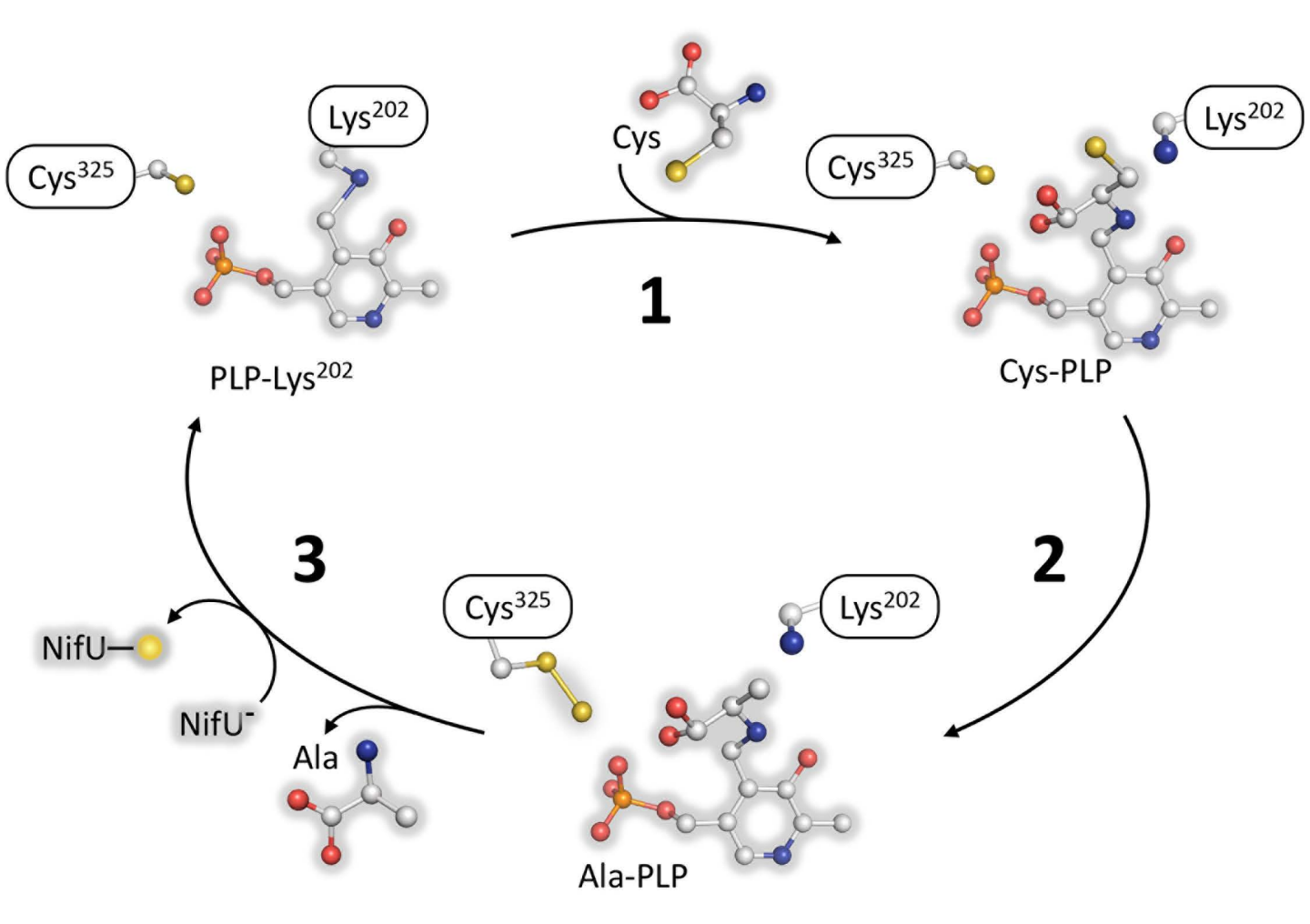
Cys325
Lys202
PLP-Lys202
Cys
1
Cys325
Lys202
Cys-PLP
2
Cys325
Lys202
Ala-PLP
3
NifU—
NifU-
Ala

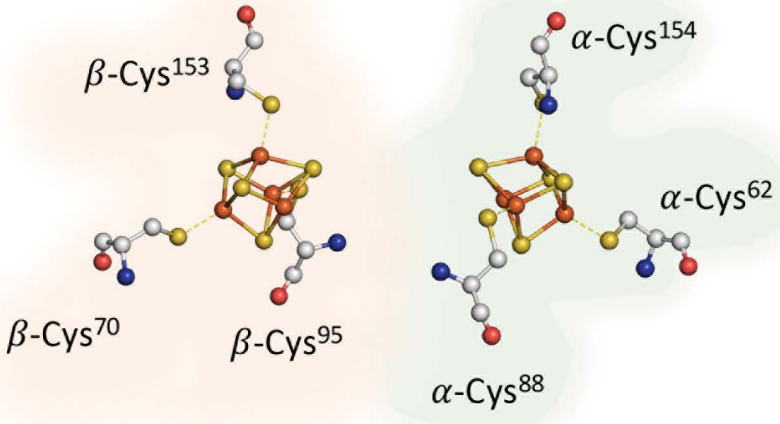

P-cluster precursor

NafH

NifW

NifZ

ATP

e-

NifH

S

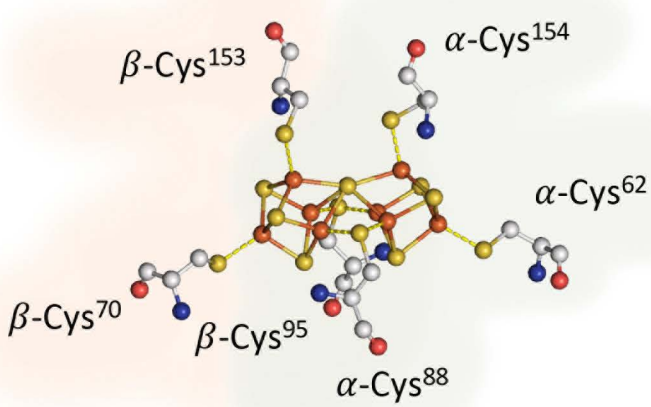

P-cluster

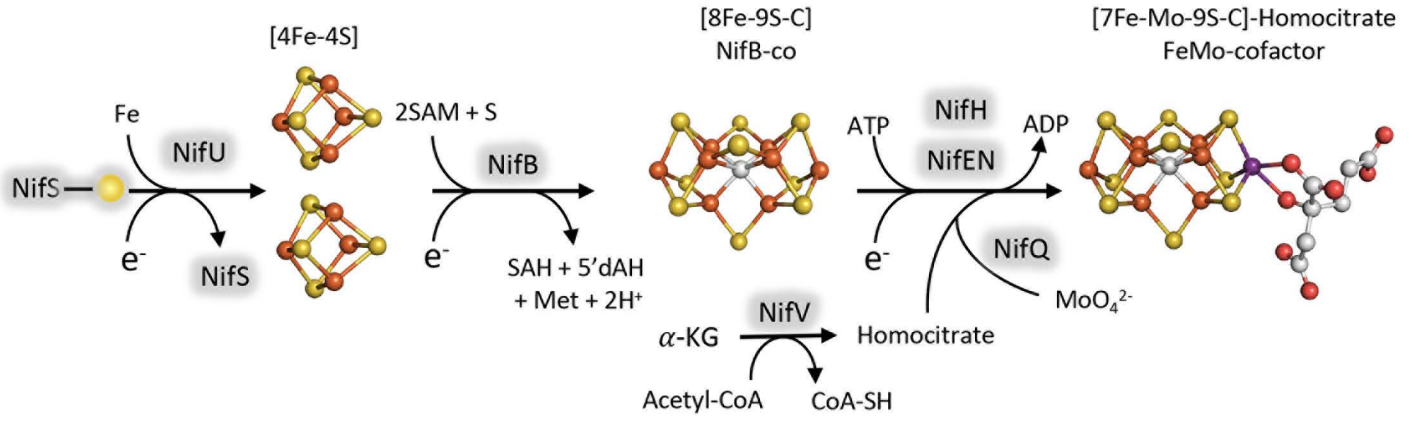
[4Fe-4S]
Fe
NifU
NifS
e-
NifS
2SAM + S
NifB
e-
SAH + 5'dAH
+ Met + 2H+
[8Fe-9S-C]
NifB-co
ATP
NifH
NifEN
ADP
e-
NifQ
MoO4 2-
[7Fe-Mo-9S-C]-Homocitrate
FeMo-cofactor
α-KG
NifV
Homocitrate
Acetyl-CoA
CoA-SH

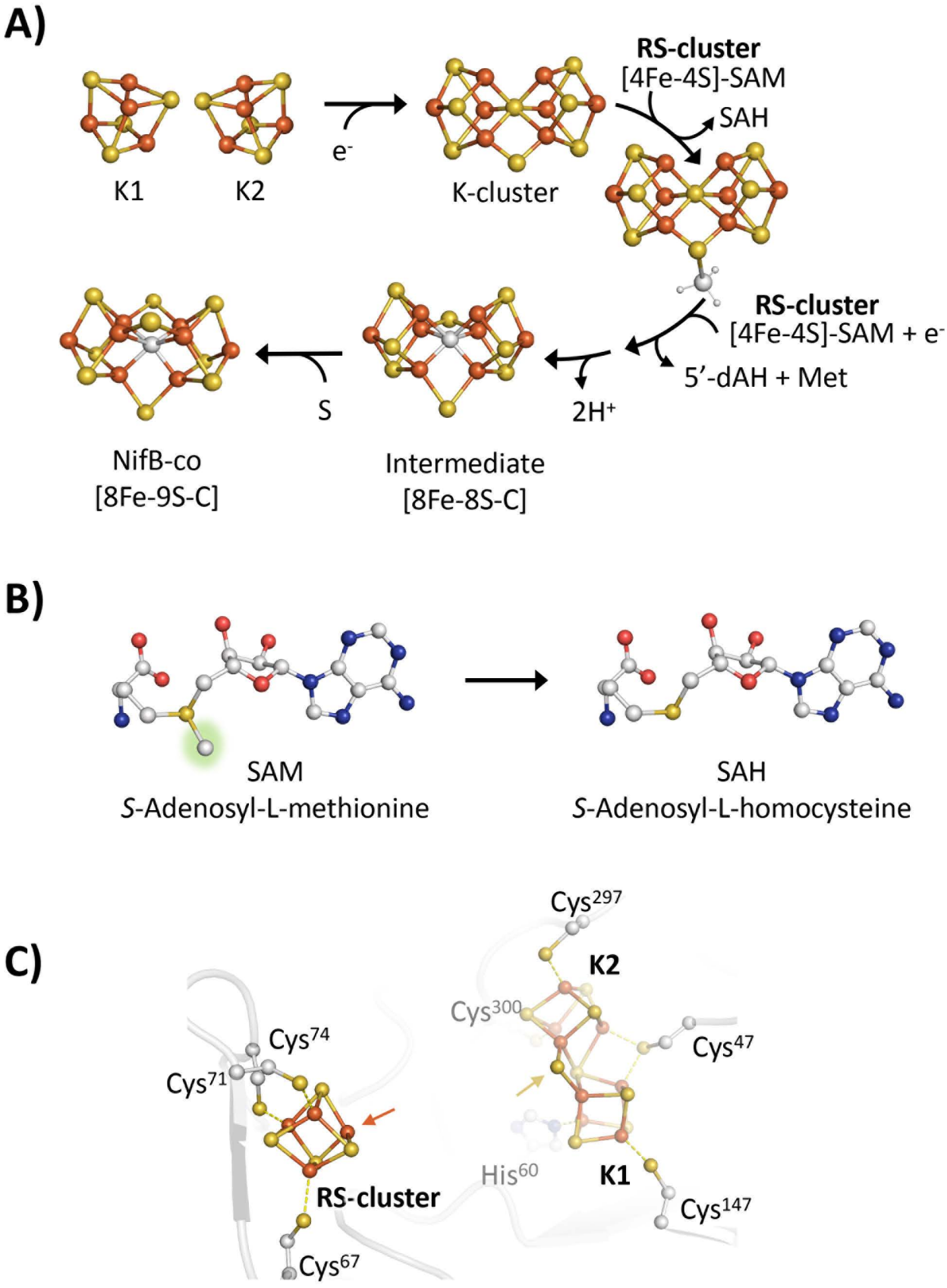
A)
K1
K2
e-
K-cluster
RS-cluster
[4Fe-4S]-SAM
SAH
RS-cluster
[4Fe-4S]-SAM + e-
5'-dAH + Met
2H+
S
NifB-co
[8Fe-9S-C]
Intermediate
[8Fe-8S-C]
B)
SAM
S-Adenosyl-L-methionine
SAH
S-Adenosyl-L-homocysteine
C)
Cys297
K2
Cys300
Cys47
Cys74
Cys71
RS-cluster
His60
K1
Cys147
Cys67

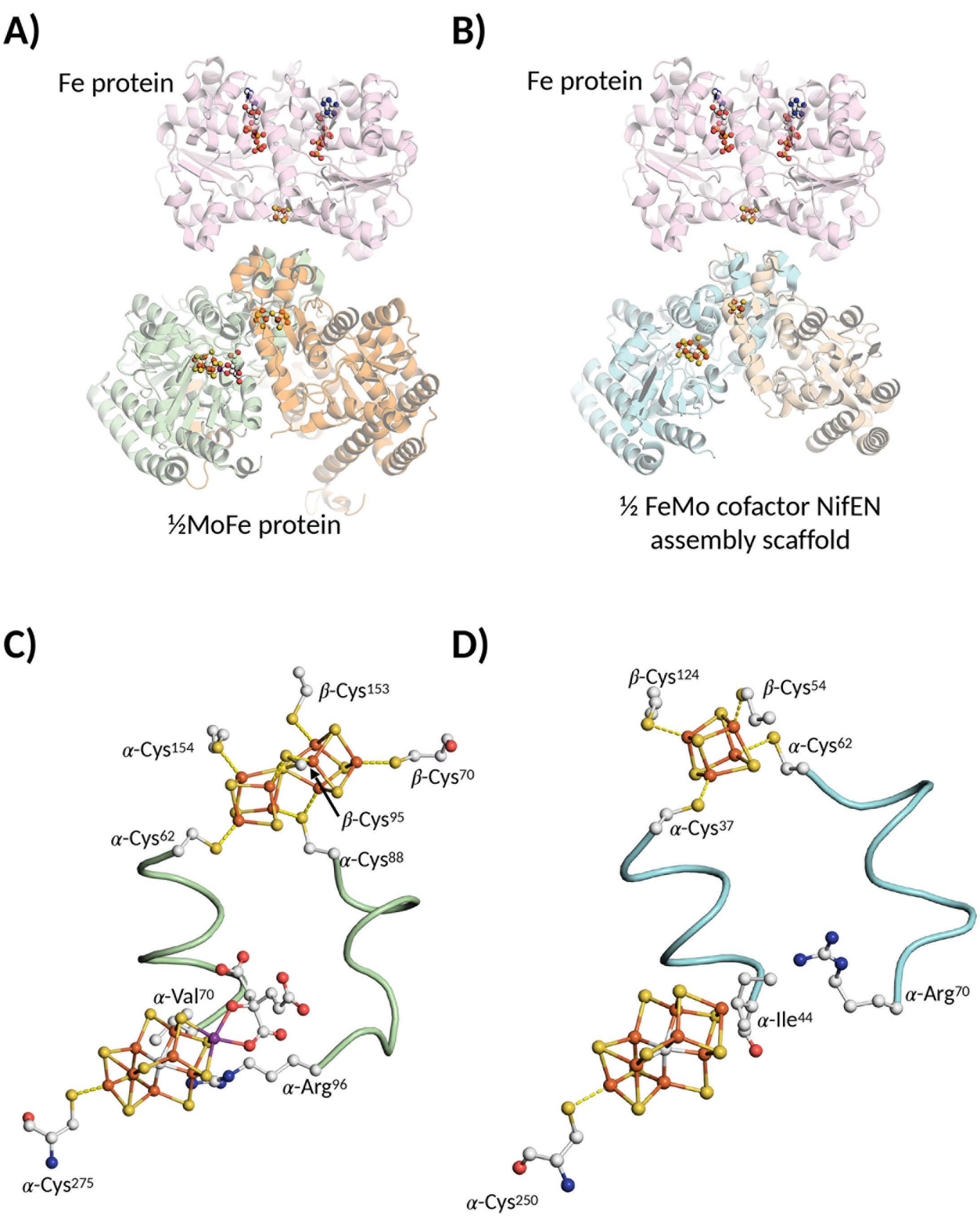
A)
Fe protein
½MoFe protein
B)
Fe protein
½ FeMo cofactor NifEN
assembly scaffold
C)
β-Cys153
α-Cys154
β-Cys70
β-Cys95
α-Cys62
α-Cys88
α-Val70
α-Arg96
α-Cys275
D)
β-Cys124
β-Cys54
α-Cys62
α-Cys37
α-Arg70
α-Ile44
α-Cys250

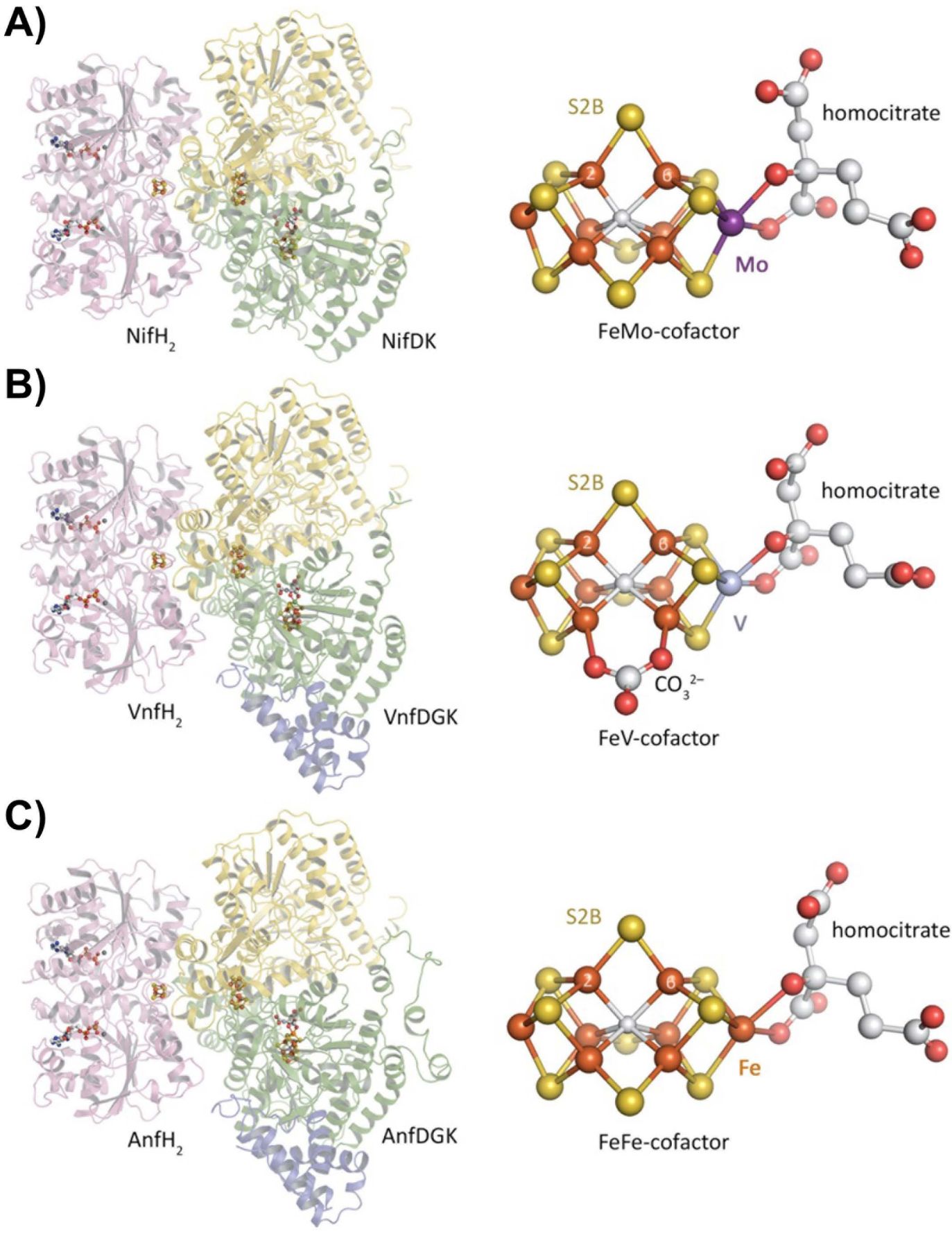
A)
NifH2
NifDK
S2B
homocitrate
Mo
FeMo-cofactor
B)
VnfH2
VnfDGK
S2B
homocitrate
V
CO3 2–
FeV-cofactor
C)
AnfH2
AnfDGK
S2B
homocitrate
Fe
FeFe-cofactor

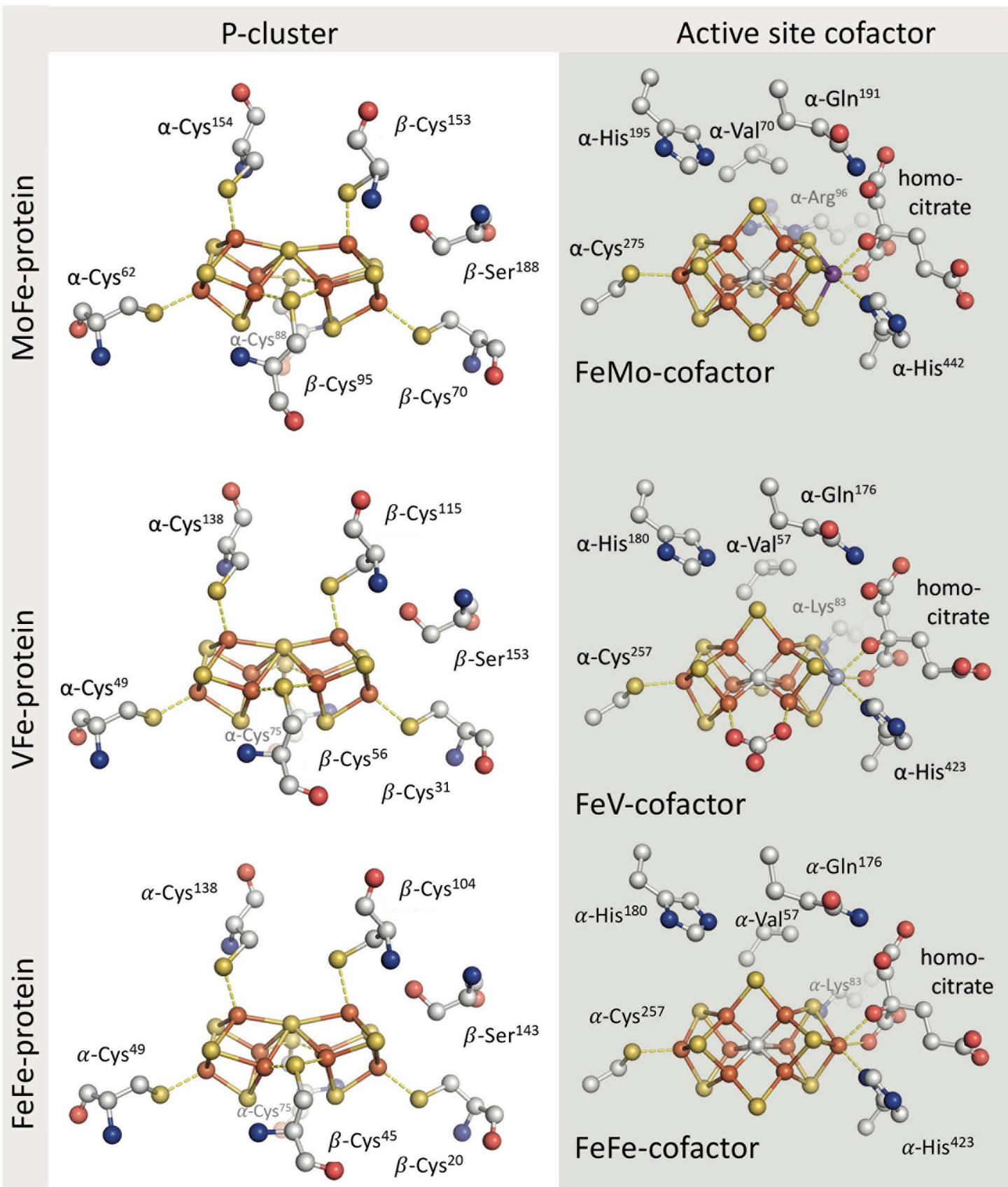
P-cluster
Active site cofactor
MoFe-protein
VFe-protein
FeFe-protein
α-Cys154
β-Cys153
α-Cys62
β-Ser188
α-Cys88
β-Cys95
β-Cys70
α-Gln191
α-His195
α-Val70
homo-citrate
α-Arg96
α-Cys275
FeMo-cofactor
α-His442
α-Cys138
β-Cys115
β-Ser153
α-Cys49
α-Cys75
β-Cys56
β-Cys31
α-Gln176
α-His180
α-Val57
homo-citrate
α-Lys83
α-Cys257
α-His423
FeV-cofactor
α-Cys138
β-Cys104
β-Ser143
α-Cys49
α-Cys75
β-Cys45
β-Cys20
α-Gln176
α-His180
α-Val57
homo-citrate
α-Lys83
α-Cys257
FeFe-cofactor
α-His423

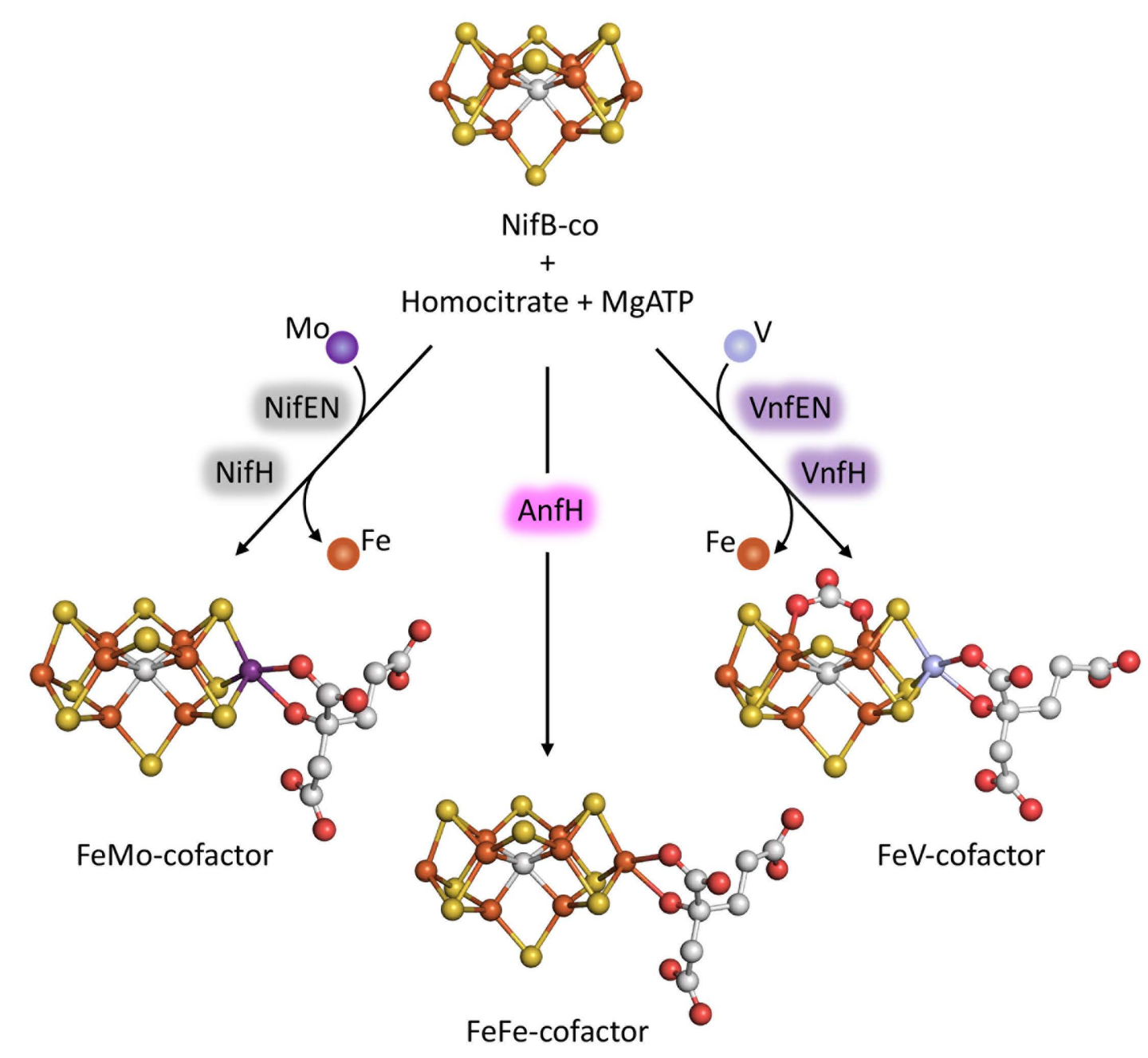
NifB-co
+
Homocitrate + MgATP
Mo
NifEN
NifH
Fe
AnfH
V
VnfEN
VnfH
Fe
FeMo-cofactor
FeV-cofactor
FeFe-cofactor

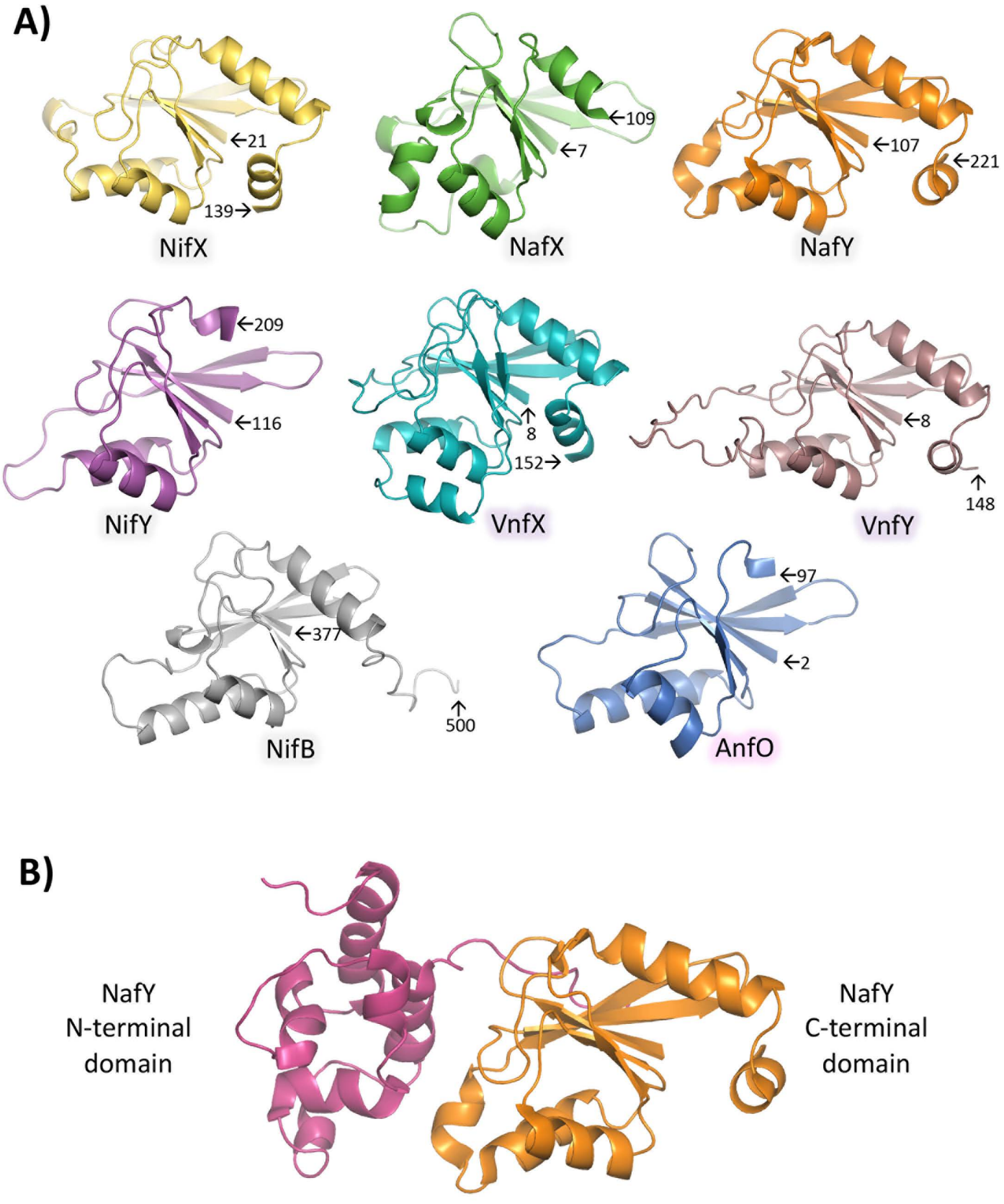
A)
←21
139→
NifX
←109
←7
NafX
←107
←221
NafY
←209
←116
NifY
8
152→
VnfX
←8
148
VnfY
←377
500
NifB
←97
←2
AnfO
B)
NafY
N-terminal
domain
NafY
C-terminal
domain

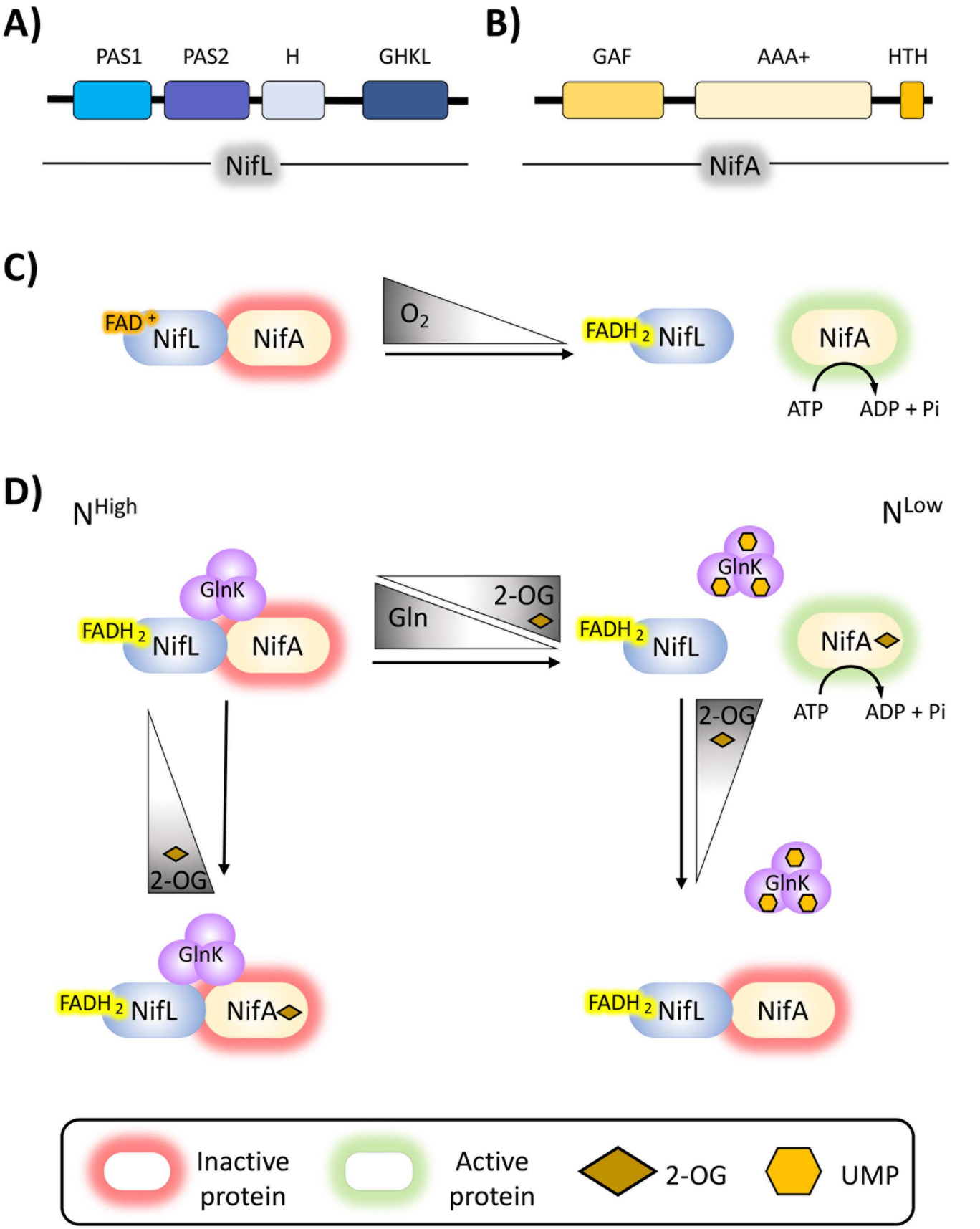
A)
PAS1
PAS2
H
GHKL
NifL
B)
GAF
AAA+
HTH
NifA
C)
FAD +
NifL
NifA
O2
FADH 2
NifL
NifA
ATP
ADP + Pi
D)
N High
N Low
GlnK
FADH 2
NifL
NifA
Gln
2-OG
2-OG
GlnK
FADH 2
NifL
NifA
ATP
ADP + Pi
2-OG
GlnK
FADH 2
NifL
NifA
FADH 2
NifL
NifA
Inactive protein
Active protein
2-OG
UMP

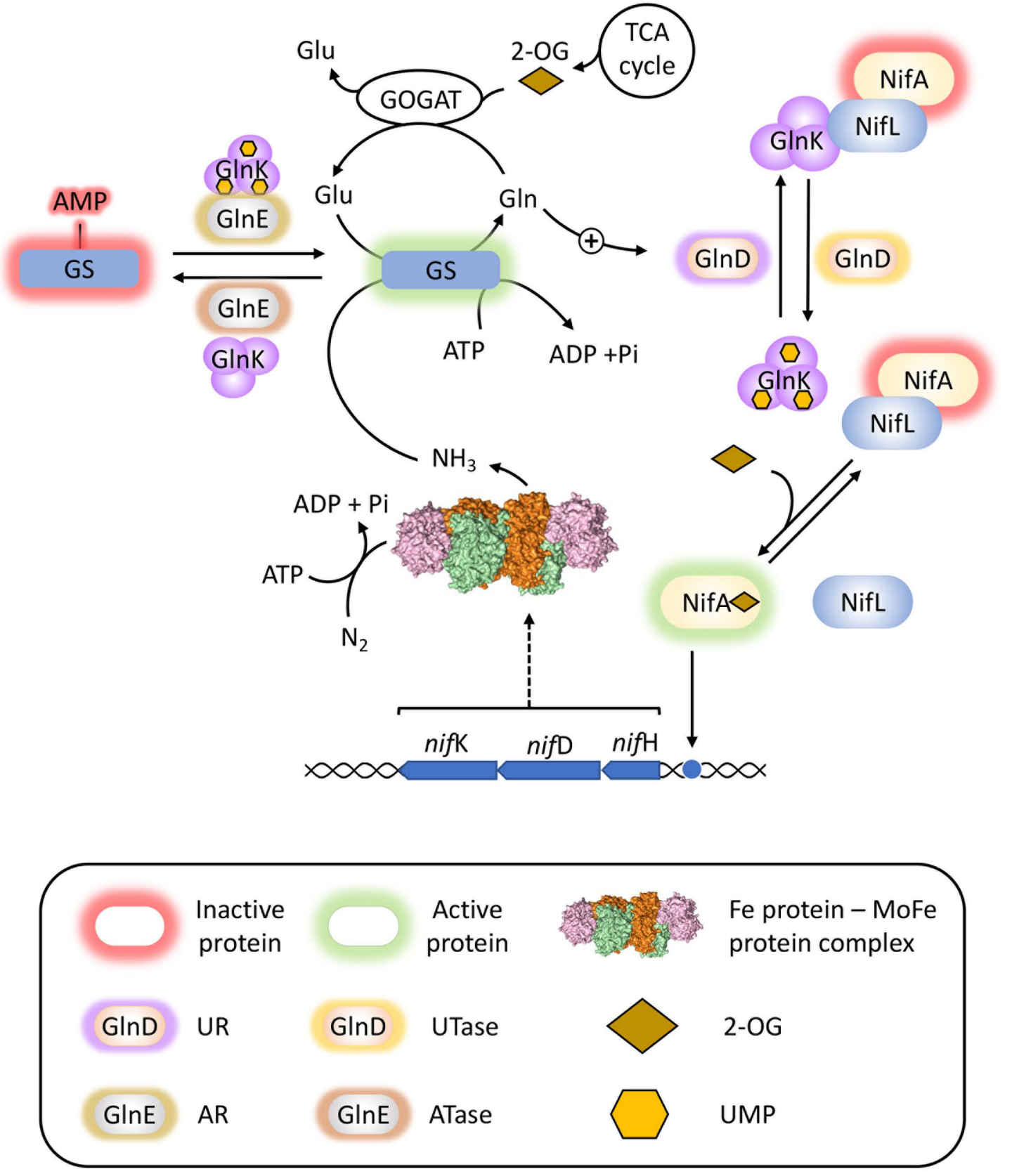
Glu
2-OG
TCA cycle
GOGAT
NifA
NifL
GlnK
GlnE
AMP
GS
Glu
Gln
GlnD
GlnD
GlnE
GlnK
ATP
ADP +Pi
NH3
ADP + Pi
ATP
N2
NifA
NifL
nifK
nifD
nifH
Inactive protein
Active protein
Fe protein – MoFe protein complex
GlnD
UR
GlnD
UTase
2-OG
GlnE
AR
GlnE
ATase
UMP

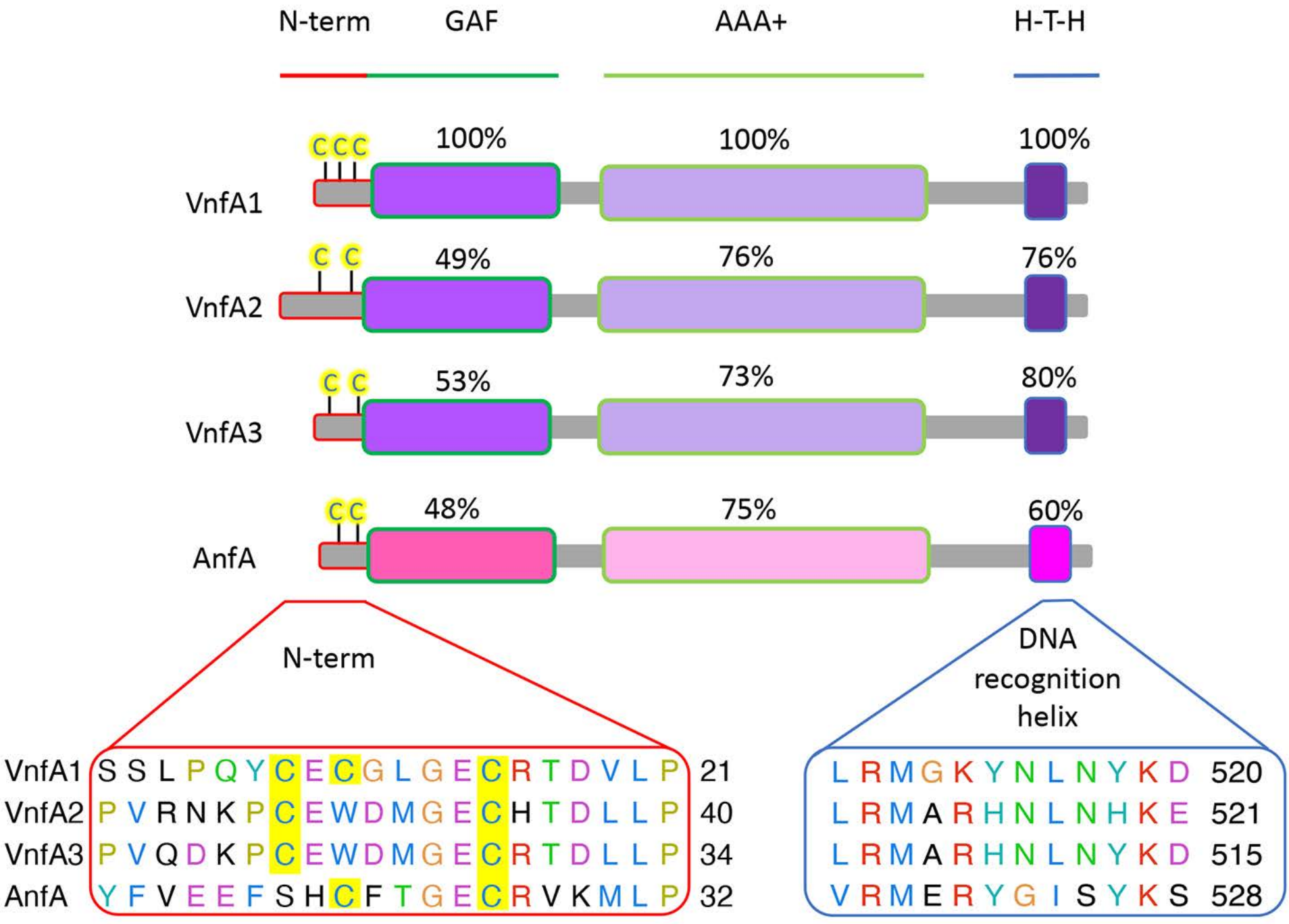
N-term
GAF
AAA+
H-T-H
VnfA1
100%
100%
100%
VnfA2
49%
76%
76%
VnfA3
53%
73%
80%
AnfA
48%
75%
60%
N-term
DNA recognition helix
VnfA1 S S L P Q Y C E C G L G E C R T D V L P 21
VnfA2 P V R N K P C E W D M G E C H T D L L P 40
VnfA3 P V Q D K P C E W D M G E C R T D L L P 34
AnfA Y F V E E F S H C F T G E C R V K M L P 32
L R M G K Y N L N Y K D 520
L R M A R H N L N H K E 521
L R M A R H N L N Y K D 515
V R M E R Y G I S Y K S 528

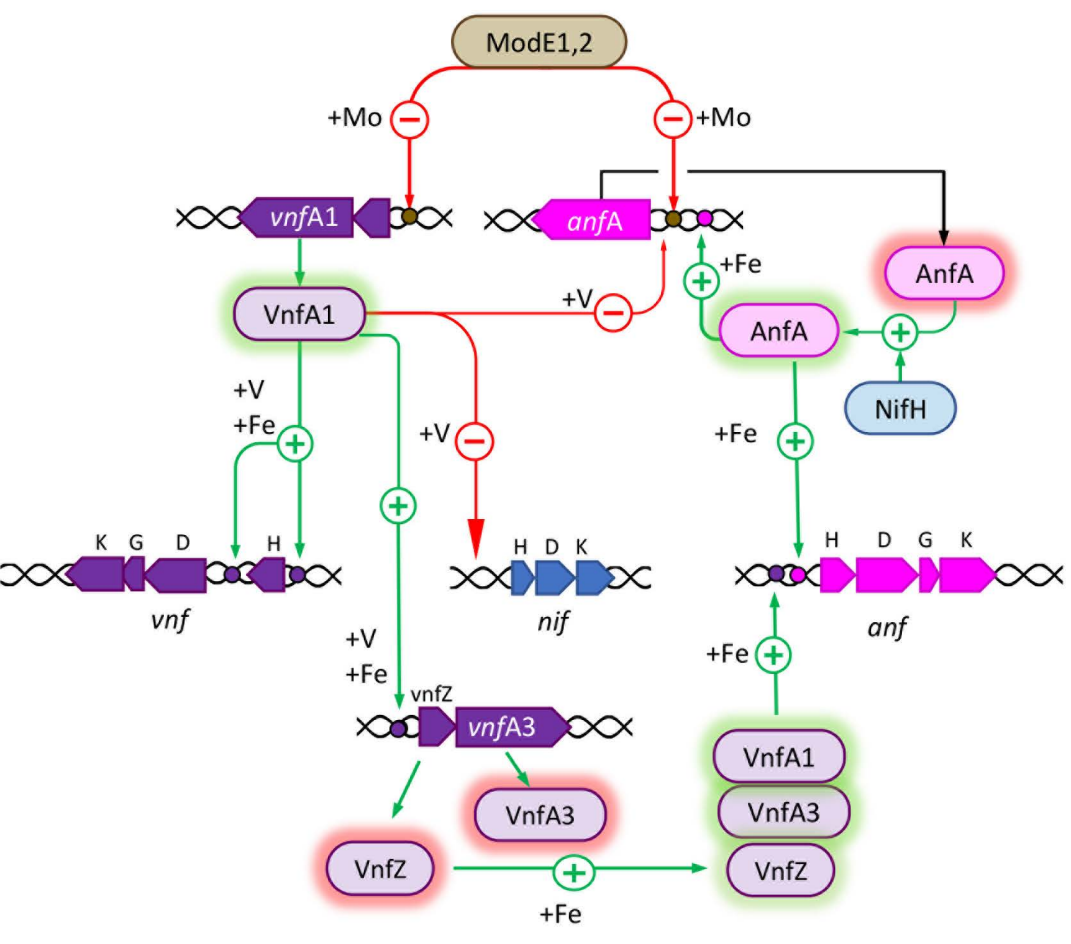
ModE1,2
+Mo
+Mo
vnfA1
anfA
AnfA
+Fe
VnfA1
+V
AnfA
NifH
+V
+Fe
+V
+Fe
K G D H
H D K
H D G K
vnf
nif
anf
+V
+Fe
vnfZ
vnfA3
+Fe
VnfA1
VnfA3
VnfA3
VnfZ
VnfZ
+Fe

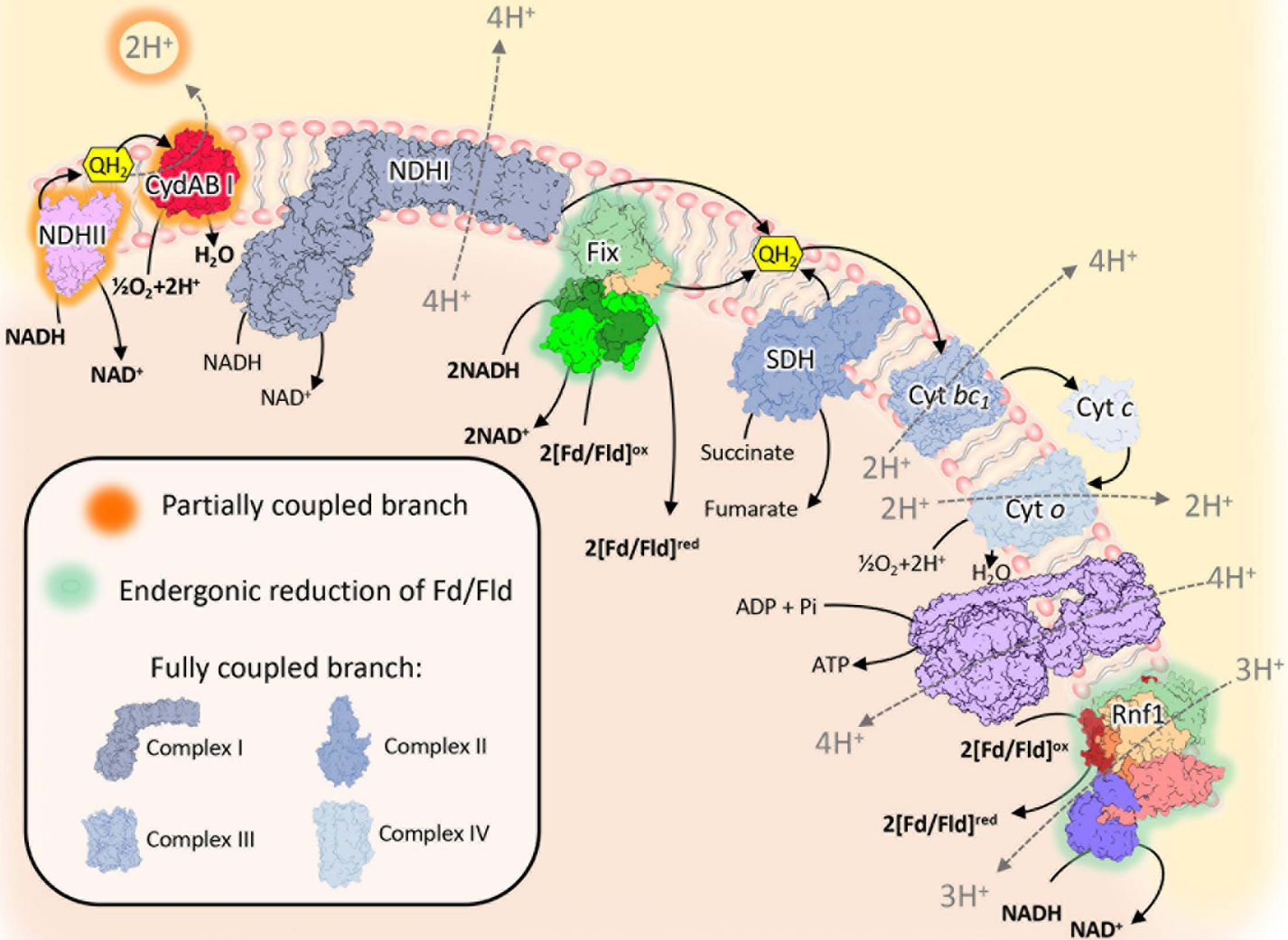
2H+
4H+
QH2
CydAB I
NDHII
NDHI
H2O
½O2+2H+
NADH
NAD+
NADH
NAD+
4H+
Fix
QH2
2NADH
2NAD+
2[Fd/Fld]ox
2[Fd/Fld]red
SDH
Succinate
Fumarate
4H+
Cyt bc1
Cyt c
2H+
2H+
Cyt o
2H+
½O2+2H+
H2O
4H+
ADP + Pi
ATP
3H+
4H+
Rnf1
2[Fd/Fld]ox
2[Fd/Fld]red
3H+
NADH
NAD+
Partially coupled branch
Endergonic reduction of Fd/Fld
Fully coupled branch:
Complex I
Complex II
Complex III
Complex IV

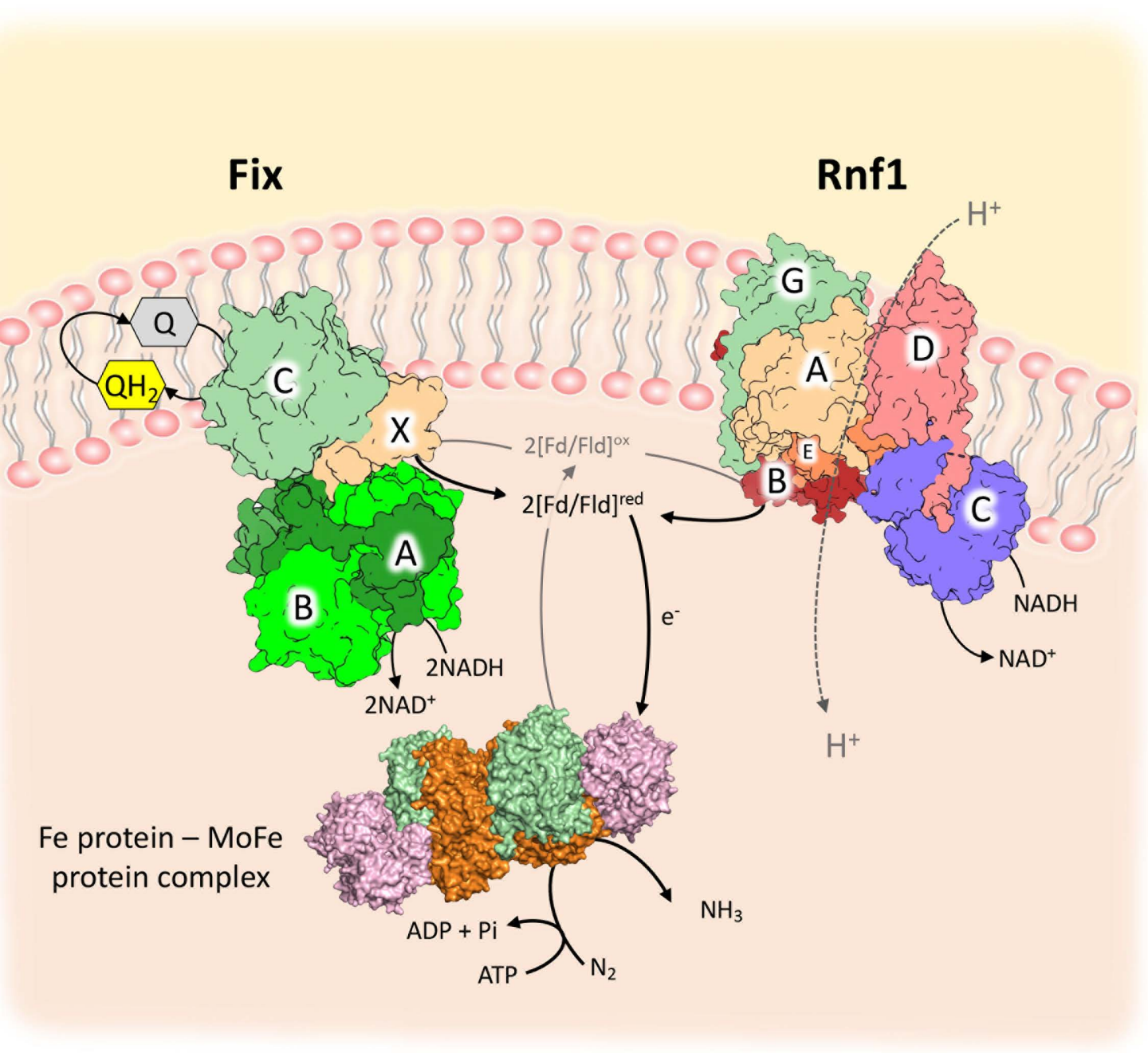
Fix
Rnf1
H+
G
A
D
E
B
C
Q
QH2
C
X
2[Fd/Fld]ox
2[Fd/Fld]red
A
B
e-
NADH
NAD+
2NADH
2NAD+
H+
Fe protein – MoFe protein complex
NH3
ADP + Pi
ATP
N2